POLITECNICO DI TORINO

Department of Mechanical, Aerospace and Automotive Engineering

Master's Degree in Automotive Engineering

Master's Degree Thesis

Development and Analysis of Power Supply Systems Based on Common Pressure Rail Architectures in Hybrid Excavators

Supervisors

Prof. Massimo RUNDO

Prof. Daniela Anna MISUL

PhD. Federico MIRETTI

Candidate

Alessio MAGNATI

Academic Year 2023/2024

Acknowledgements

I would like to express my sincere gratitude to Professor Massimo Rundo, my supervisor, for his invaluable support and guidance throughout this project. His expertise and advice have profoundly impacted my academic and professional growth.

I also extend my heartfelt thanks to Professor Daniela Anna Misul and PhD. Federico Miretti, my co-supervisors, for their valuable contributions and support. Their insights and suggestions were instrumental in refining this work.

Abstract

Construction machines, particularly excavators, contribute in a non negligible percentage to CO_2 emissions, which are considered one of the main causes of global warming. The excavators currently on the market have hydraulic architectures that are highly reliable from an operational standpoint but exhibit a low energy efficiency, as only a small percentage of fuel is converted into useful net work for the actuators. The causes of energy losses are distributed among various components of the excavator hydraulic circuit, but the greatest contribution can be attributed to hydraulic distributors. For this reason, in recent decades, new types of systems have been studied with the aim of reducing energy dissipation during the excavator's operating cycle, and among these, the Common Pressure Rail (CPR) architecture has proven to be very advantageous in terms of fuel consumption.

This thesis aimed to develop a model of a hybrid hydraulic excavator using the CPR system, with a primary focus on the design and optimization of its power supply. The study began by analyzing a Load Sensing hydraulic model of a 9-ton excavator, which was subsequently modified to obtain the innovative CPR architecture. To achieve system hybridization, gas accumulators were added and carefully sized. Furthermore, a control system was designed to mantain quasi-constant pressure levels within the accumulators, ensuring continuous operation while minimizing throttling losses. Subsequently, a CPR architecture based on a dual power supply system was studied, with the aim of investigating whether splitting the circuit could lead to further improvements in terms of fuel consumption and energy efficiency.

CPR architectures show significant limitations when operating at pressures very close to the system's maximum pressure; for this reason, two possible solutions were analyzed: the resizing of the accumulators and the introduction of a pressure intensifier.

In conclusion, well-designed CPR architectures demonstrate their viability as effective alternatives to conventional hydraulic systems in excavators, showing significant fuel savings, mainly due to their inherent energy efficiency and ability to recover energy that is typically wasted in traditional systems.

Sommario

Le macchine da costruzione, in particolare gli escavatori, contribuiscono in misura non trascurabile alle emissioni di CO2, considerate una delle principali cause del riscaldamento globale. Gli escavatori attualmente sul mercato presentano architetture idrauliche altamente affidabili dal punto di vista operativo ma con una bassa efficienza energetica, poiché solo una piccola percentuale del carburante iniziale viene convertita in lavoro utile per gli attuatori. Le cause delle perdite di energia sono distribuite tra i vari componenti del circuito idraulico dell'escavatore, ma il maggiore contributo può essere attribuito ai distributori idraulici. Per questo motivo, negli ultimi decenni sono stati studiati nuovi tipi di sistemi con l'obiettivo di ridurre la dissipazione di energia durante il ciclo operativo dell'escavatore, e tra questi, l'architettura Common Pressure Rail (CPR) si è dimostrata molto vantaggiosa in termini di consumo di carburante.

L'obiettivo di questa tesi è stato quello di sviluppare un modello di escavatore idraulico ibrido utilizzando il sistema CPR, con un focus principale sulla progettazione e ottimizzazione del suo sistema di alimentazione. Lo studio è iniziato analizzando un modello idraulico Load Sensing di un escavatore da 9 tonnellate, che è stato successivamente modificato per ottenere l'innovativa architettura CPR. Per rendere il sistema ibrido, sono stati aggiunti e dimensionati accuratamente degli accumulatori idraulici. Inoltre, è stato progettato un sistema di controllo per mantenere livelli di pressione quasi costanti all'interno degli accumulatori. Successivamente, è stata studiata un'architettura CPR basata su un sistema di alimentazione doppio, con l'obiettivo di capire se la suddivisione del circuito potesse portare a ulteriori miglioramenti.

Le architetture CPR mostrano limitazioni significative quando operano a pressioni molto vicine alla pressione massima del sistema; per questo motivo, sono state analizzate due possibili soluzioni: il ridimensionamento degli accumulatori e l'introduzione di un amplificatore di pressione.

In conclusione, le architetture CPR si dimostrano potenziali alternative ai sistemi idraulici convenzionali presenti negli escavatori, mostrando significativi risparmi di carburante, principalmente grazie alla loro efficienza energetica e capacità di recuperare energia che viene tipicamente dissipata nei circuiti idraulici tradizionali.

Contents

List of Tables

List of Figures

Acronyms

CPR
Common Pressure Rail

DCPR
Double Common Pressure Rail

ERTs
Energy Recovery Technologies

FD
Fixed Displacement

HE
Hydraulic Excavator

HP
High Pressure

ICE
Internal Combustion Engine

LC
Local Compensator

LP
Low Pressure

LS
Load Sensing

MCV

Main Control Valve

MP

Medium Pressure

OCV

Over Center Valve

OP

Operating Mode

PDCV

Proportional Directional Control Valve

SOC

State Of Charge

VD

Variable Displacement

Introduction

Given the worsening environmental situation, particularly concerning pollution and global warming, reducing the impact of human and industrial activities has become a central focus in political discourse, driving both legislative and industrial advancements. Regulations have increasingly emphasized the need to improve fuel efficiency and reduce emissions not only for light-duty vehicles but also for construction machinery. In the context of heavy machinery, hydraulic excavators are responsible for more than half of the total CO_2 emissions produced [1], a fact that is objectively concerning and has led many researchers to develop innovative solutions to make these machines more energy efficient. It is widely agreed within the technical community that the transmission efficiency of hydraulic actuation systems must be improved in order to reduce environmental impact, increase machine autonomy, and lower operational costs [2].

Numerous approaches have been proposed to address the challenges mentioned and enhance the efficiency of fluid power systems in multi-actuator off-road vehicles, typically with the aim of minimizing throttling losses. One strategy that has gained considerable attention in recent years is based on the Common Pressure Rails (CPRs) principle, according to which several actuators share common supply lines maintained at different pressure levels [3]. The concept was further refined with the introduction of the STEAM architecture, which incorporated accumulators into at least two of the pressure rails. The addition of these accumulators enabled energy storage within the system, allowing for advanced secondary control strategies for the cylinders. This enhancement not only improved overall system efficiency but also created opportunities for more sophisticated energy management and recovery [4].

The focus of this thesis was to develop an architecture based on the aforementioned CPR principle for a hybrid excavator and to evaluate its performance during digging and leveling cycles. The starting point was the analysis of a hydraulic circuit from a traditional 9-ton excavator based on the Load Sensing principle, which was subsequently modified to achieve the new hybrid architecture. Specifically, the design and analysis of the excavator's power supply system were conducted with a heightened focus on the precise sizing of the accumulators and the regulation

of pressure levels within them. Special attention was given to optimizing these elements to ensure efficient energy storage and consistent system performance. All the work was carried out in a simulation environment using Simcenter AMESim software, from the creation of the hydraulic circuit to the development of the accumulator recharging strategy based on a finite state machine. Two different types of CPR architecture were analyzed: one very similar in design to STEAM and a completely new one that utilizes a dual power supply system. The latter, as will be explained in the following chapters, allows for coupling of components that operate at similar pressures, with the advantage of further reducing throttling losses.

Not only the advantages of this new architecture were highlighted, but also the limitations that arise when the excavator operates at very high pressures, close to the system's limit. For this reason, two possible solutions were proposed: resizing the accumulators by increasing the pressures and using a pressure intensifier.

Chapter 1

A General Outlook on Hydraulic Excavators

An extensive review of the parts, subsystems, and operational dynamics of hydraulic excavators (HEs) is given in this chapter along with a thorough explanation of their fundamentals. The objective is to lay a strong basis of knowledge of the conventional components of hydraulic excavators, the ideas that regulate the energy flow in these devices theoretically, and the normal duty cycles that these machines go through when they operate.

A look is also provided at the possible forms of energy that can be recovered during different working cycles, highlighting the limitations of traditional hydraulic architectures.

In this chapter, a comprehensive view of the excavator will be presented, laying the groundwork for understanding why a hybrid structure is necessary to improve the energy efficiency and fuel consumption of these machines.

1.1 Excavator Layout and Subsystems

Excavators are powerful construction machines that feature a boom, arm, bucket, and cab mounted on a rotating superstructure positioned atop an undercarriage equipped with either tracks or wheels. Primarily used for digging, excavators are also versatile enough to handle a range of tasks, including lifting, carrying, and material handling in various applications across construction, mining, and other industries. An excavator is normally equipped with six hydraulic actuators, providing six degrees of freedom in its movements (see Figure 1.1). Two of these actuators control the machine's travel along the ground, while the remaining four manage the motion of the swing body, boom, arm, and bucket. This arrangement allows for precise and coordinated movement, enabling the machine to perform

complex tasks with flexibility and efficiency.

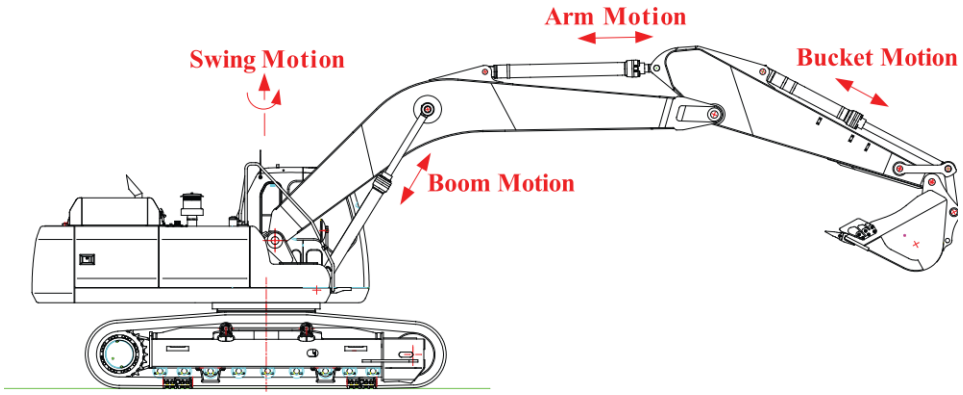

Figure 1.1: Excavator Degree Of Freedom [5]

Going into more detail, as shown in the 1.2, a traditional excavator typically includes one or more hydraulic pumps (2) powered by a diesel engine (1) to supplying pressurized flow to the system. The movement of the machine is managed in the cabin (12) by the operator, who uses two joysticks to precisely control a series of directional valves located in a block, commonly referred to as the main control valve (MCV) (3). This valve block allows for controlling the speed of the linear actuators (boom (6), arm(8), bucket (10)) and the hydraulic motors for the structure rotation (4) and the vehicle motion (11).

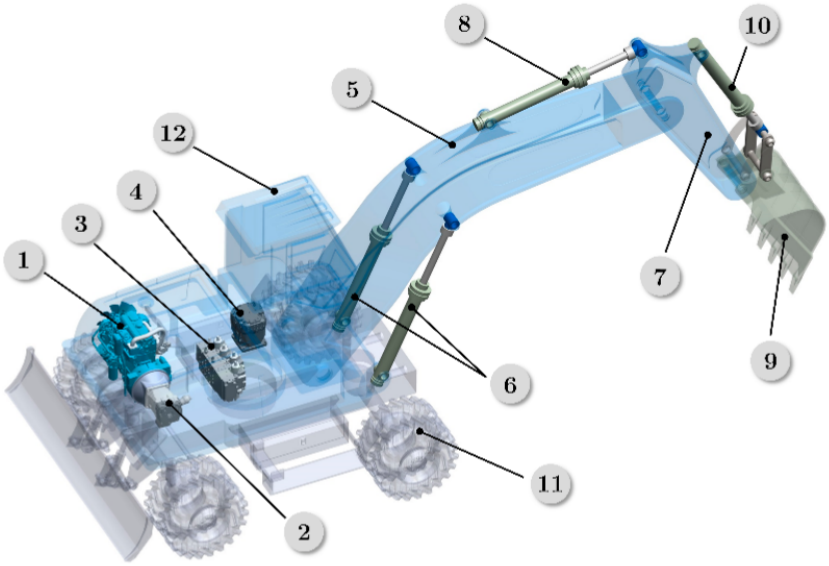

Figure 1.2: Layout of a traditional hydraulic excavator [4]

To study the energetic efficiency of the excavator, it is beneficial to categorize the various components into specific subsystems, such as the engine system, hydraulic system, and hydraulic actuator system, as illustrated in figure 1.3. This categorization facilitates a thorough examination of energy consumption characteristics, as losses can arise from multiple sources and it helps to pinpoint less efficient components and the primary factors contributing to energy losses.

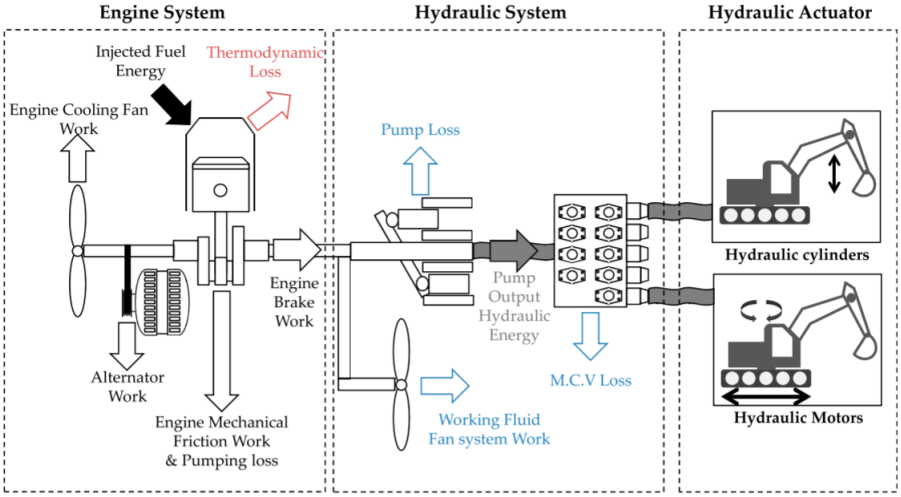

Figure 1.3: Hydraulic Excavator Subsystems [6]

The engine converts fuel energy through combustion into heat that is dissipated as losses and into mechanical energy which powers various engine components and is subsequently transferred to the hydraulic system. Within this process, mechanical energy is transferred to the main pump, where it is converted into hydraulic energy and then directed to the MCV. Mechanical friction, pressure losses, and flow losses occur in the pump, with these losses varying depending on the pump's operating conditions.

From this brief description, it can be understood that before fuel energy is converted into useful work for the actuators, it undergoes many dissipations. Some of these dissipations can be reduced by hybridizing the hydraulic system, which is the focus of analysis in the following chapters of this thesis.

1.2 Excavator Working Modes

The primary goal of any mobile hydraulic system is to enable the operator to easily and intuitively control all machine movements. To achieve this, the hydraulic system must interact not only with the operator but also with the surroundings

and the internal combustion engine (ICE). The operator provides input for the desired actuator movements, the objects and forces in the environment determine the system pressure, and the engine supplies the necessary power.

The hydraulic actuators' interaction with the surrounding environment is especially intricate and complex. The force and velocity coefficients of every actuator are not only entirely independent of one another, but also vary independently of one another depending on the operator's commands. Based on the interaction between external forces and the displacement inputs provided by the operator, both linear actuators and hydraulic motors can operate in four different conditions, as shown in the following Figures 1.4 and 1.5.

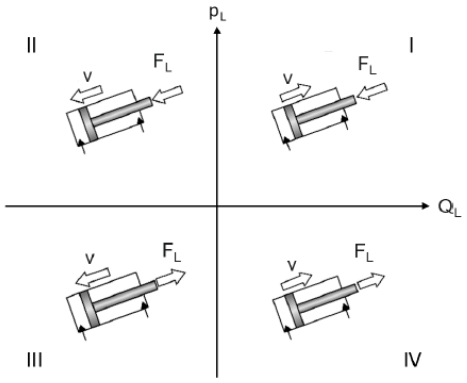

Figure 1.4: Linear Actutors Working Modes

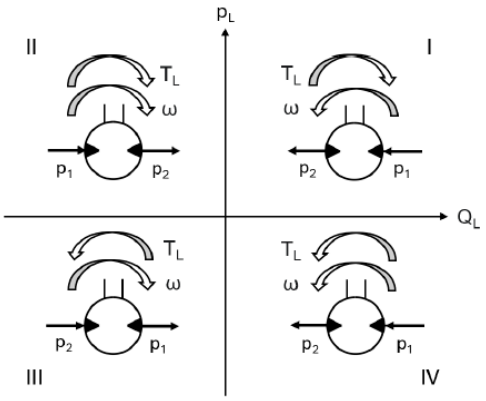

Figure 1.5: Hydraulic Motor Working Modes

In both the figures above, the horizontal x-axis represents the flow rate (Q_L) required by each actuator to achieve the speed input requested by the operator. As for the vertical y-axis, it shows the force required, or more precisely, the load pressure (p_L) experienced in the actuators as a direct consequence of the external environment. With regard to the linear actuators, the load acting on them arises from both the weight of the connected structure and the external forces encountered during digging and other tasks, whereas inertial forces produced during acceleration play a less critical role. Depending on the motion, each actuator faces either a resistive force that opposes its movement (Quadrants I and III) or a supportive force that assists its movement (Quadrants II and IV). Consequently, in Quadrants I and III, the actuator must be actively powered, whereas in Quadrants II and IV, the actuators can actually provide power to the system, exploiting the so called overruning loads.

Both the motor powering the turret and the travel motors also undergo four-quadrant operation. In fact, depending on the rotational movements, the hydrostatic

machine may experience either a resisting torque opposing its motion (Quadrants I and III), or an assisting torque helping its movement (Quadrants II and IV). Therefore, the hydrostatic machine works in Quadrants I and III in all the situation in which it needs to start the movement from standstill and so it requires an active power input; whereas it works in Quadrants II and IV when the turret is in motion and requires stopping, and so it acts as a pump delivering power to the system. Each point in the planes of the two Figures 1.4 and 1.5 represents a state of nearly stationary equilibrium, where the pump flow rate is proportional to the joystick displacement of the operator, the system pressure is dictated by the load, and the engine torque is equal to the pump torque [7].

1.3 Excavator Duty Cycles

Excavators are primarily used to dig, load, and unload soil or materials with a bucket, offering significant versatility as construction machines. To gather data for analyzing such machinery, it has been essential to define standard operations with preset actuator displacements, ensuring that the outcomes are both relevant and, crucially, comparable. The following Figure 1.7 shows the most common cycles found in the scientific literature; however, only the first (a) and the last (c) of these were used in the analysis of the new hybrid system based on the CPR principle.

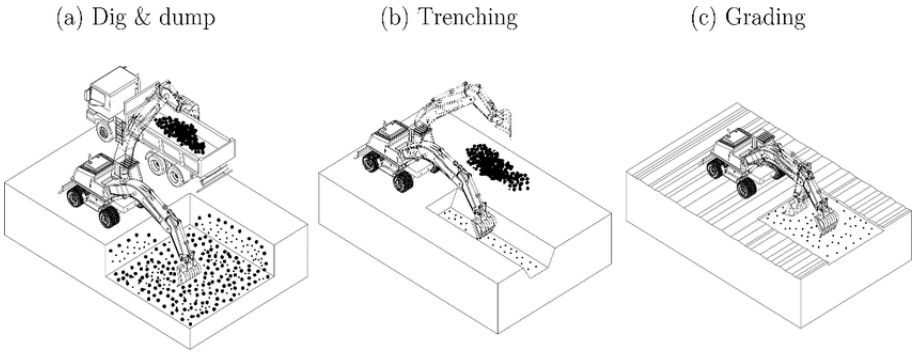

Figure 1.6: Escavator Duty Cycles [7]

During the dig and dump cycle, the gravel is excavated from a pit and loaded into a truck positioned roughly 90° relative to the excavator [7]. The air grading cycle, on the other hand, subjects the excavator to much lighter loads, but the movement of the front attachement structure is significantly faster and requires more precise control, as the goal is to level the ground [8]. Generally, the pressure level of the linear actuators is lowest during the levelling cycle. Both the cycle closely follow the Japanese JCMAS test cycle standard for excavators.

Due to the kinematic arrangement of the implement structure, the load force

acting on each actuator not only changes throughout a duty cycle but also varies depending on the specific actuator. This implies that each actuator has its own distinct power demand profile for each cycle [8].

1.4 Energy Recovery in Excavators

In this introductory phase, it is also necessary to explain the forms of energy available for recovery in an excavator to further emphasize how much is dissipated by a traditional hydraulic system and to understand how a hybrid architecture can be crucial for enabling energy regeneration. Specifically, the two forms are gravitational potential energy and kinetic mechanical energy: the former manifests with the lowering of the boom actuator, while the latter is associated with a sudden change in the angular velocity of the swing; both are linearly dependent on mass or inertia. Similarly, a change in height affects potential energy linearly, while a change in speed affects kinetic energy quadratically. As a result, changes in mass or height have a smaller impact compared to changes in speed.

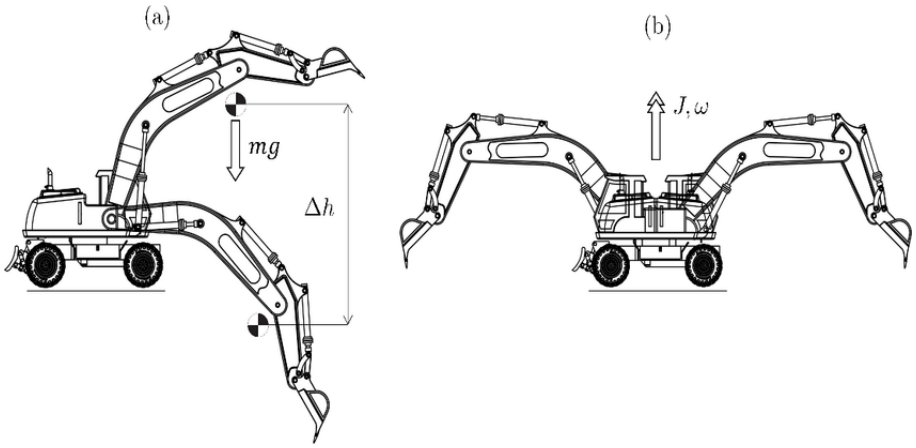

Figure 1.7: Escavator Energy Recovery [7]

Due to its significant mass and considerable height variations, the boom structure possesses the highest amount of recoverable potential energy. On the other hand, due to the low speed of the center of mass, its kinetic energy is negligible. The swing drive does not have potential energy, but because of its large rotational inertia, it generates kinetic energy as the superstructure is accelerated.

If the energy released during lowering and braking cannot be reused or stored immediately, it must be dissipated and exits the system as heat. In a standard valve-controlled machine, the recoverable energy is first converted into hydraulic power, represented by flow and pressure, and then throttled to tank pressure, generating heat and causing an unnecessary rise in oil temperature.

Chapter 2

Classification of Hydraulic Architectures for Excavators

Over the past six decades, a wide variety of mobile hydraulic system layouts have been created, each offering distinct advantages and drawbacks. To develop the next generation of highly efficient systems, it is crucial to have a deep understanding of the core principles behind these different architectures.

The following sections offer a comprehensive overview of the most commonly used hydraulic architectures in mobile machinery today, along with the most prominent circuits employed in modern equipment. Additionally, it highlights advanced hydraulic systems currently being explored and optimized by research institutions worldwide. These architectures aim to address key challenges such as energy efficiency, control precision, and reduced emissions, reflecting the evolving needs of the machinery industry.

Hydraulic circuits are essential in many industrial applications and can be broadly divided into two main categories based on their configuration and control mechanisms: valve-controlled systems and valve-less systems. The key characteristics of these two categories are outlined below.

- *Valve-controlled* hydraulic circuits are systems where hydraulic valves serve as key control elements. Flow throttling mainly takes place in the primary transmission lines, offering a precise method for executing control functions. This setup allows for controlled fluid flow, enabling fine-tuned adjustments in hydraulic machinery operations.

- *Valve-less* hydraulic circuits use designs that exclude throttling valves from the main transmission lines, relying instead on variable-flow hydraulic units as control elements. This method removes the need for conventional valves, providing an alternative approach for achieving control and regulating fluid

dynamics within the system.

2.1 Valve-Controlled Systems

Hydraulic systems utilizing valve control are a well-known and widely used category of hydraulic circuits, popular in the past for their precise control and regulation capabilities. In these systems, hydraulic valves play a crucial role, acting as the main control components within the primary transmission lines. However, a significant drawback arises during valve operation, as flow throttling is required to achieve the desired pressure, leading to notable power losses within the system.

These systems, when they do not include energy storage systems, can be defined as non-hybrid systems and further classified as mechanical-hydraulic and electro-hydraulic systems, whose main characteristics are summarized below.

- *Mechanical-hydraulic* systems operate solely through mechanical-hydraulic control mechanisms, without the involvement of electronics. Common examples include manually controlled valves in agricultural machinery or mechanical-hydraulic joysticks found in excavators. These systems are typically classified into open-center or closed-center types, depending on how proportional directional control valves (PDCVs) link the pump to the reservoir when the valves are in their neutral state.

- *Electro-hydraulic* systems utilize sophisticated control techniques, providing increased flexibility in machine configurations and enhancing energy efficiency. Many of these systems have evolved from mechanical-hydraulic designs, integrating electronics at different levels, such as electronic joysticks for controlling PDCVs or expanding the use of electro-hydraulic components throughout the system.

The following figure 2.1 presents a comprehensive classification of valve-controlled non-hybrid systems currently used in mobile machinery [9]. Generally, these systems are categorized as open center or closed center types, based on the design of the proportional directional control valves (PDCVs) and on how the pump is connected to the reservoir when the valves are in their neutral or centered position.

The next section will focus on one of the most common non-hybrid valve-controlled systems, Load-Sensing, which is categorized as a mechanical-hydraulic system featuring a closed-center variable pressure pump, as illustrated in Figure 2.1. In particular, this section will provide an overview of pre-compensated Load Sensing systems, since the hydraulic circuit of the excavator used as reference for the following analyses is based on it.

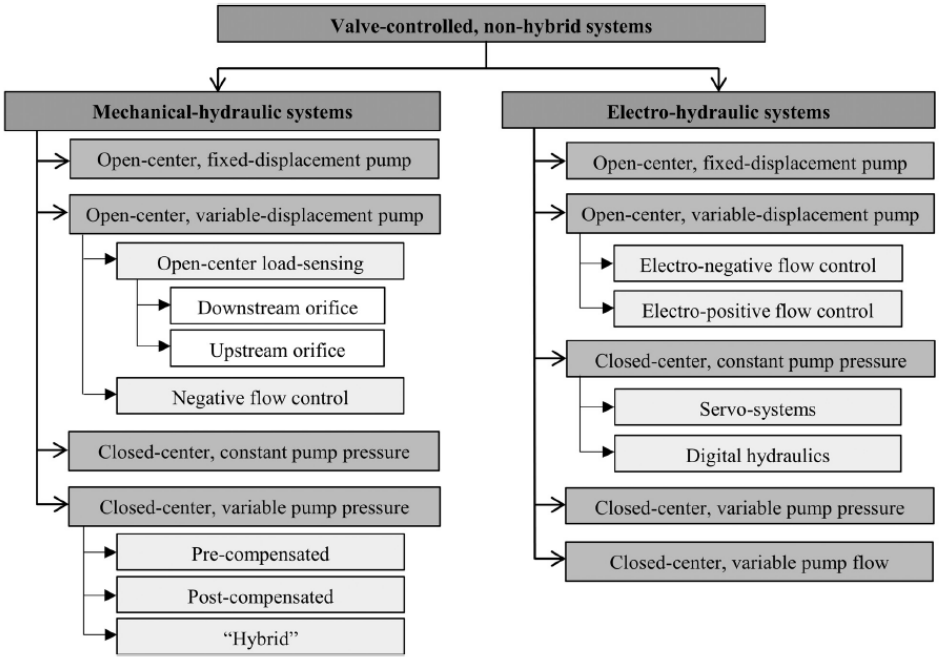

Figure 2.1: Classification of the working hydraulics for non hybrid, valve-controlled mobile machines [9]

2.1.1 Load-Sensing Hydraulic Systems

Load sensing has become a widely used approach in mobile machinery for hydraulic power transmission, replacing the older fixed-displacement pump systems, shown in figure 2.2, which provided constant flow regardless of the system's demands. The main issue with fixed-displacement pumps is their tendency to release excess flow to the tank through a pressure relief valve when load pressures are low, leading to significant heat loss across the valve. This results in a great decrease in efficiency, especially in applications with variable loads, such as excavators.

The core advantage of the Load Sensing (LS) system lies in its principle of delivering only the necessary flow to meet the actuator's pressure requirements. This minimizes pressure drops across the valve when supplying a single user, effectively reducing power losses. While the LS technique is efficient in controlling excess flow, its performance decreases when managing multiple actuators, as it can be seen in systems with a single pump serving multiple loads, such as excavators. In these cases, the LS system adjusts to provide the highest required pressure among all actuators. However, since different actuators have varying pressure demands, the pressure drop across the valve with the lowest demand becomes substantial, causing significant power losses. This issue recurs with other actuators requiring

lower pressure. As a result, the LS system is most efficient for the actuator with the highest pressure need, while inefficiencies and power losses occur for those requiring less pressure.

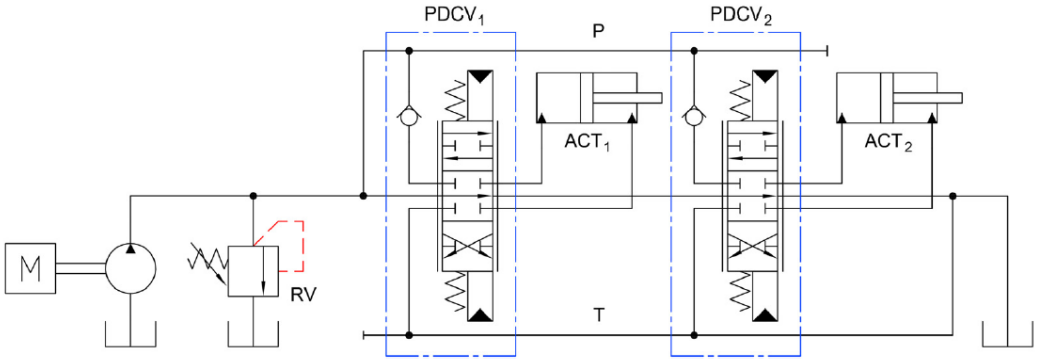

Figure 2.2: Fixed Displacement Pump System [9]

LS system is designed to minimize excess flow and throttling by utilizing a variable displacement pump that adjusts its output based on the actuators' needs through feedback mechanisms. This system aims to provide only the necessary flow, reducing waste. In addition to the variable displacement pump, the Load Sensing setup includes a compensator block and a load-sensing directional control valve; the compensator block, which is directly mounted on the pump, features both a differential pressure compensator and a high-pressure compensator. This block is essential for allowing the pump to supply the required flow to meet the Load Sensing system's pressure demands by adjusting the pump's swash plate.

Local compensators in the Load Sensing system can be configured in two main ways: either before the proportional valves, known as pre-compensated systems, or after the proportional valves, known as post-compensated systems. As mentioned before, only the first type of compensator will be examined in detail below, as it is present in the traditional excavator model used as a reference.

Pre-Compensated Load Sensing System An example of a Load Sensing circuit with pre-compensators used for controlling two linear actuators is shown in Figure 2.3. The operating mechanism works as follows: the actuator's load pressure is detected in the pilot line of the pressure-flow compensator, which is connected to the pump displacement cylinder's inlet. If higher pressure is needed, the compensator directs the swash plate to increase flow, raising the system pressure. Conversely, when the system pressure becomes too high, the high-pressure compensator signals the swash plate control piston to reduce the flow. The compensator block plays a crucial role in ensuring consistent velocity control

for all actuators. Afterward, the directional control valves regulate the flow to the actuators, and the local compensator maintains a constant pressure drop across the valve, regardless of load, to ensure precise control.

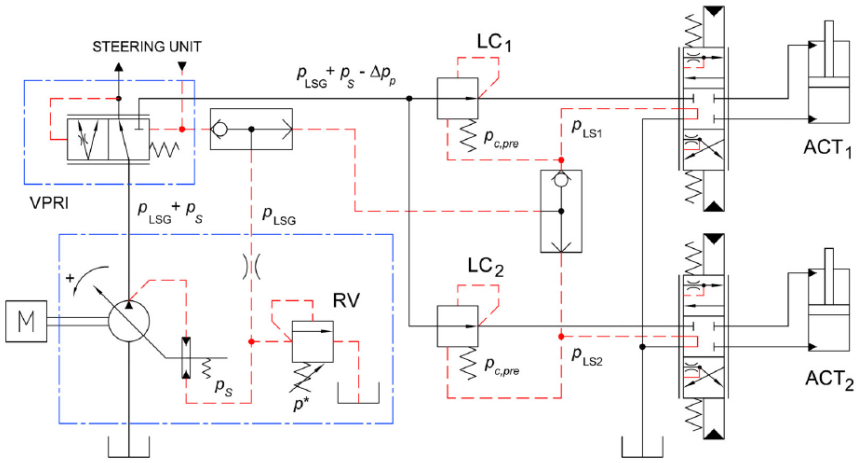

Figure 2.3: Simplified Scheme of a Pre-Compensated Load Sensing System [9]

In the described pre-compensated configuration, the pressure at each actuator's inlet port acts as the opening force on the local compensators (LCs), which are set to a pressure level of pc_{pre}. The LCs ensure a constant pressure drop across the metering edge of the directional control valves, making the actuator flow rates, and therefore their velocities, entirely dependent on the operator's input. The total load sensing pressure p_{LSG} is established by a series of shuttle valves arranged in a cascade, and this pressure is used to control the pump's displacement. The pump output is adjusted to maintain the delivery pressure at p_{LSG} plus a constant margin p_s, determined by setting the differential pressure limiter. When PDCVs are inactive, the load-sensing signal is connected to the reservoir, causing the pump displacement to be minimized, along with its delivery pressure. A pressure-relief valve, set at p^*, along with a fixed orifice in the power supply, limits the pump's delivery pressure to p^* plus p_s [9].

This setup eliminates interference between loads, ensuring that the flow rates to the actuators, and therefore their speeds, are determined entirely by the input provided to the distributor valve, which directly reflects the operator's commands.

Under flow saturation conditions, the pre-compensated layout struggles to function effectively without electronic control of the main spool's position. In such cases, the flow rates to the actuators decrease progressively, starting with the one experiencing the highest load, then decreasing based on the load. However, during normal operating conditions, this Load Sensing configuration should not significantly impact machine performance, aside from a potential delay in system

response.

2.2 Valve-less Systems

It is important to highlight that, while the energy efficiency of LS systems is generally higher than other valve-controlled systems, it remains suboptimal since the efficiency drops significantly in situations involving multiple actuators, as previously discussed. Actuators operating at lower pressures experience substantial dissipation across their local compensators, leading to considerable energy losses. A possible solution to improve efficiency is to eliminate the hydraulic control valve that causes constant pressure drops. This can be done introducing the Valve-less systems, in which flow demand is regulated without traditional valves. These systems typically exhibit reduced complexity, as they have fewer moving parts compared to valve-based designs, leading to lower maintenance needs and reduced overall costs. Additionally, the reduced mechanical components contribute to increased reliability and operational uptime. They also offer enhanced dynamic response, enabling faster reactions and better overall performance.

Valve-less systems can operate using either *flow control* or *pressure control* mechanisms, each with its own distinct features. The main difference lies in whether the system controls the fluid's flow rate or maintains a specific pressure. Flow-controlled systems manage how quickly fluid moves through the system, whereas pressure-controlled systems focus on sustaining a stable pressure level. Depending on the application's needs, one approach may be more appropriate than the other.

In *flow-controlled* systems, two primary strategies are commonly used. The first is displacement control, which employs a linear actuator with a variable displacement pump, often referred to as a hydrostatic actuator (HA) in the literature. The second strategy involves regulating the velocity of a fixed displacement pump, typically achieved by controlling the main power source. Consequently, the major architectures in this category are hybrid systems, including Electro-Hydrostatic Actuators (EHA) and Hybrid Hydraulic-Electric Architecture (HHEA) [10].

On the other hand, *pressure control* systems use mechanisms that adjust or regulate pressure based on predefined settings or feedback loops. These systems are particularly useful in applications where maintaining consistent pressure is essential, regardless of flow rate changes. Among various pressure-controlled systems, CPR architecture will be thoroughly examined in the upcoming sections, since it is the subject of study in this thesis.

2.2.1 Common Pressure Rail Architectures

The CPR or multi-pressure system is a new approach in hydraulic systems aimed at enhancing energy efficiency and reducing throttling losses, ultimately leading to smaller pumps and diesel engines. In LS systems, throttling losses occur caused by local compensators that require a constant pressure differential between the pump and actuator, which results in significant power losses. These inefficiencies become more pronounced when multiple actuators with varying pressure demands operate simultaneously. In mobile hydraulic systems, the diesel engine is the primary power source, sized to meet the peak power requirements of the LS system, because power demands often exceed the average power during different load cycles. The main contributors to efficiency loss in the power transmission system are throttling and diesel engine inefficiencies, with additional minor losses occurring in other hydraulic components [11].

The multi-pressure system addresses these issues by introducing multiple pressure sources, allowing for more precise pressure matching to meet the varying demands of each actuator. This system reduces throttling losses by connecting actuator chambers to pressure sources through on/off valves, providing discrete pressure levels based on the load's requirements. The setup, shown in Figure 2.4, ensures that the cylinder chambers are supplied with the appropriate pressure levels, minimizing pressure drops across the valves and enhancing overall system efficiency.

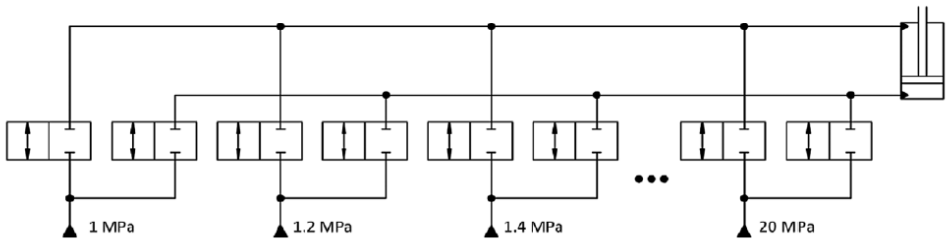

Figure 2.4: CPR Concept Architecture

It is possible to implement two different types of CPR: single-pressure or multi-pressure, with the key concepts summarized below.

- The *Single-Pressure Rail* architecture operates with a uniform pressure level throughout the system, typically featuring two pressure rails, high and tank pressure. Control in these systems can be achieved either continuously or discretely. Discrete control, which is more common in the literature, typically involves the use of multi-chamber actuators, multi-pressure amplifiers, and digital hydraulic transformers.

- Multi-Pressure Rail architectures allow for multiple pressure levels across different sections of the system, offering more precise and individualized pressure control tailored to the specific needs of each component. This setup provides greater flexibility, as different parts of the hydraulic system can operate at optimal pressures suited to their requirements.

The next paragraph will specifically investigate the STEAM architecture, which is a hybrid variable multi-pressure rail system; the key concepts will be presented and later used as reference points for designing the CPR architecture developed in this thesis.

STEAM Architecture As previously discussed, a highly efficient mobile hydraulic system must achieve three key objectives: minimizing idle losses, eliminating throttling, and effectively utilizing the potential and kinetic energy of the actuators.

The STEAM framework, first introduced by Vukovic, Sgro, and Murrenhoff in their research [7] conducted at the Institute for Fluid Power Drives and Systems (IFAS) at Aachen University in Germany, offers a promising approach to meeting these goals. STEAM, which stands for "energy-efficient hydraulic implementation in mobile machinery" (from its German abbreviation), represents an optimized architecture for mobile hydraulics, as illustrated in Figure 2.5.

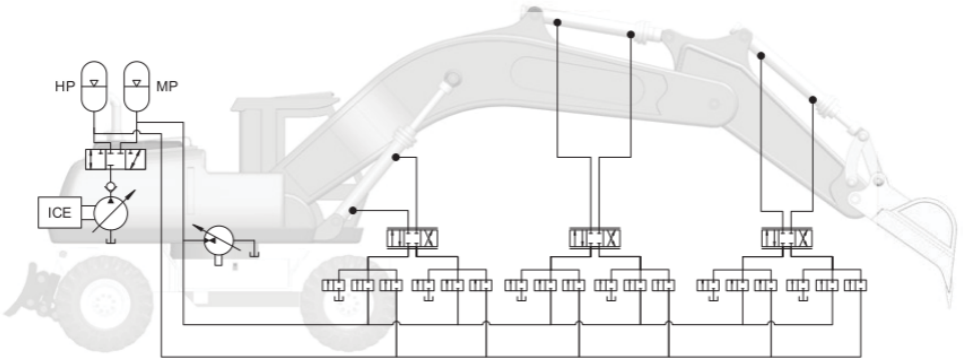

Figure 2.5: Steam Possible Implementation [8]

The key characteristics of the STEAM system can be summarized as follows: it incorporates two distinct pressure levels, operates the engine at reduced speeds, and uses accumulators to supply peak power. Furthermore, throttling minimization and energy recovery are achieved by introducing several new operational modes that allow different methods of connecting an actuator to the system's three pressure levels: high, medium, and tank pressure.

The pressure rails, along with their respective accumulators, handle peak power demands, enabling the engine to operate more efficiently at lower speeds, typically in the 1200 rpm range. To reduce throttling losses when supplying flow to linear actuators, a series of switching valves allows both pressure rails and the tank line to be individually connected to the piston and rod chambers of each cylinder. This configuration creates a system with nine artificial supply pressures, visible in the figure 2.6, which can be selectively used based on current load pressure to minimize throttling losses and recover energy. To control actuator movement, various valve topologies can be employed, from basic 4/3 proportional valves, to more complex systems such as digital hydraulic valves, independent metering, or single-edge meter-out control with pressure compensators.

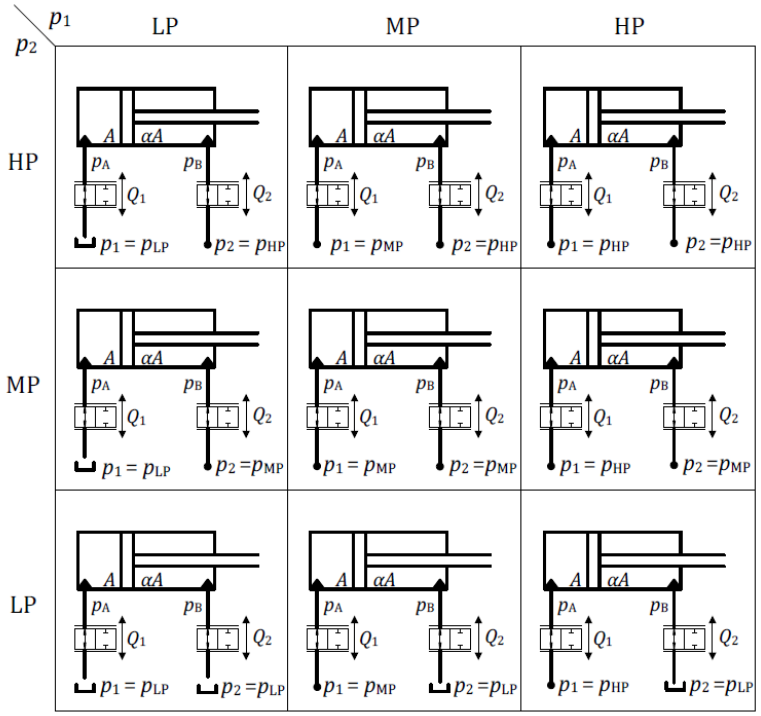

Figure 2.6: STEAM Artificial Supply Discrete Pressures [12]

The combinations shown in the figure above, referred to as operating modes, fall into five main categories: standard, regeneration, recuperation, assistive and resistive float.

In standard mode, the cylinders require an energy supply from the pressure rails. In regenerative mode, both sides of the cylinder are connected to the same pressure rail, thus requiring a lower flow rate from the pump. Recuperation mode allows the cylinder to act as a pump, supplying fluid back to the pressure rail. In assistive float

mode, no energy is needed from the system, and it is used when energy recovery isn't possible due to insufficient load. Finally, resistive float mode is employed when an actuator needs to passively dampen the forces exerted by another active actuator, such as when the boom float function is used during hammer operations. A graphical depiction of these operating modes, based on the combination of high pressure (HP) and medium pressure (MP) in the cylinder chambers, is illustrated in figure 2.7.

The figure 2.7 illustrates the different combinations of operating pressures to clarify how the operating modes are influenced by the positions of operating points within the p/Q plane. It is evident that certain modes may overlap, such as regeneration with recuperation, or recuperation with standard use. Conversely, some combinations do not represent any operational mode, as they do not manifest under real-world conditions.

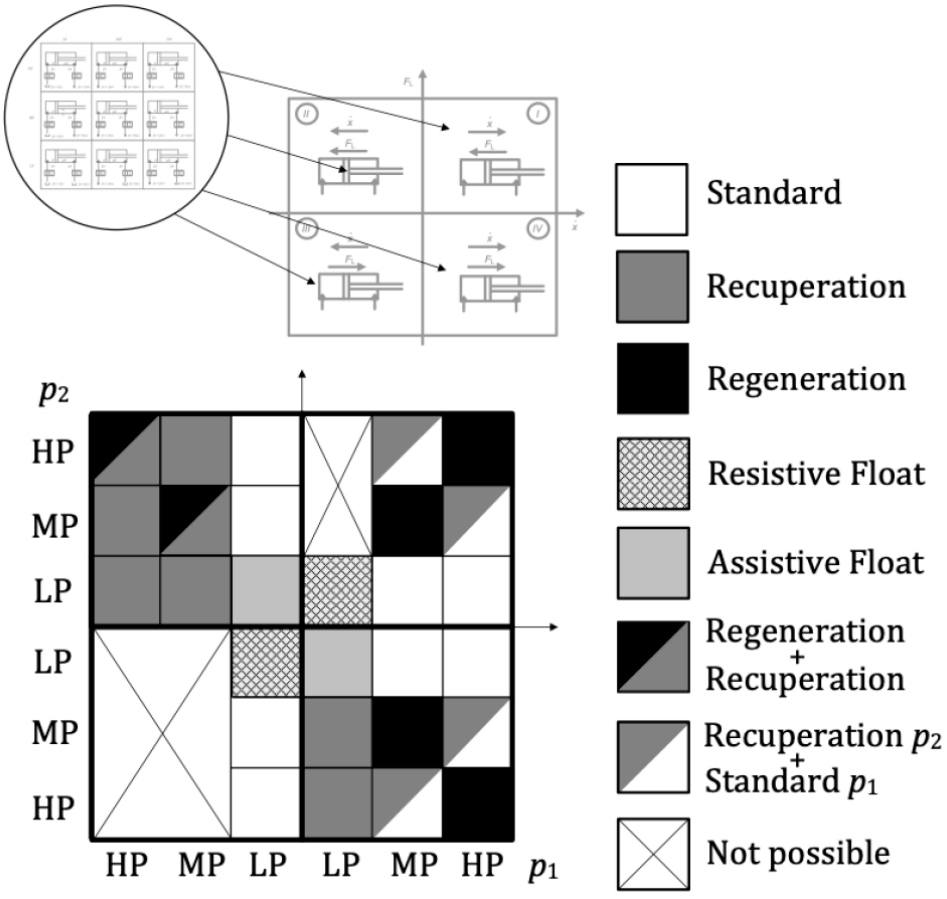

Figure 2.7: STEAM Operating Modes

As previously mentioned, the key efficiency benefit of the STEAM architecture lies in the optimized operation of the engine and pump. Since these components are only utilized to charge the accumulators, they are decoupled from the real-time power demands of the actuators and can operate in a digital mode. When the accumulator's state of charge (SOC) decreases, the engine and pump run at full load to recharge them. Once the accumulators reach full capacity, the engine and pump switch to idle. This approach ensures that the components never operate under part-load conditions, significantly reducing energy losses.

Another advantage of the STEAM system is its ability to prevent pressure peaks at the actuator end-stops. In typical excavator operations, operators often drive actuators to their end-stops to fully empty the bucket during digging. In standard flow-impressed systems, such as load sensing, this movement causes a rapid spike in supply pressure, reaching the system's pressure relief setting, which results in unnecessary pressure peaks and throttling losses, particularly when other actuators are operating simultaneously. In contrast, a constant pressure system avoids this issue by supplying pressure rather than flow, thereby mitigating pressure surges [12].

2.3 Energy Recovery and Hybrid Systems

The systems in both categories described in the previous sections can incorporate hybrid technology, integrating an additional energy source in conjunction with the combustion engine of the machine.

As noted previously in section 1.4, excavator tasks are often cyclic, alternating between phases that require energy input and those where gravitational force aids in movement, allowing for displacements powered by previously accumulated potential energy. Several studies, like [13], have already examined the magnitude of recoverable energy, leading to the development of new technologies designed to capture and store excess energy from the environment, known as Energy Recovery Technologies (ERTs) in the literature.

The components of an excavator most suitable for energy recovery are the boom and swing, which is why ERTs have been specifically designed to target these functions. ERTs are commonly categorized based on the type of energy storage, which can be electric, hydraulic, or mechanical. The combination of different energy forms improves overall performance and flexibility, making hybrid systems an attractive option for certain applications. Therefore, selecting the appropriate energy storage method and control strategy is crucial among the various opportunities available for energy recovery. Additionally, the cost of implementing these technologies is a significant consideration, especially in the context of their industrial applications, where economic feasibility plays a vital role in determining

their adoption.

Depending on the specific needs of various industrial and technological contexts, either of the mentioned systems can be employed, each offering its own set of advantages and disadvantages. The Ragone plot, shown in the figure 2.8, assists in selecting the appropriate energy storage method by comparing various storage devices based on their energy and power densities. Energy density refers to the amount of energy stored per kilogram, while power density indicates how rapidly this energy can be stored or released. When designing a hybrid system for excavators, the objective isn't to supply energy to the actuators over extended periods without engine assistance, as this is neither practical nor achievable. A simple calculation underscores this point. Batteries, although having one of the highest energy densities after diesel and hydrogen fuels, would require around 4 tons of batteries to provide an 18-ton excavator with 50 kW of power for an eight-hour workday [7]. This clearly demonstrates the impracticality of relying solely on batteries for such applications, making diesel engines the only feasible solution currently.

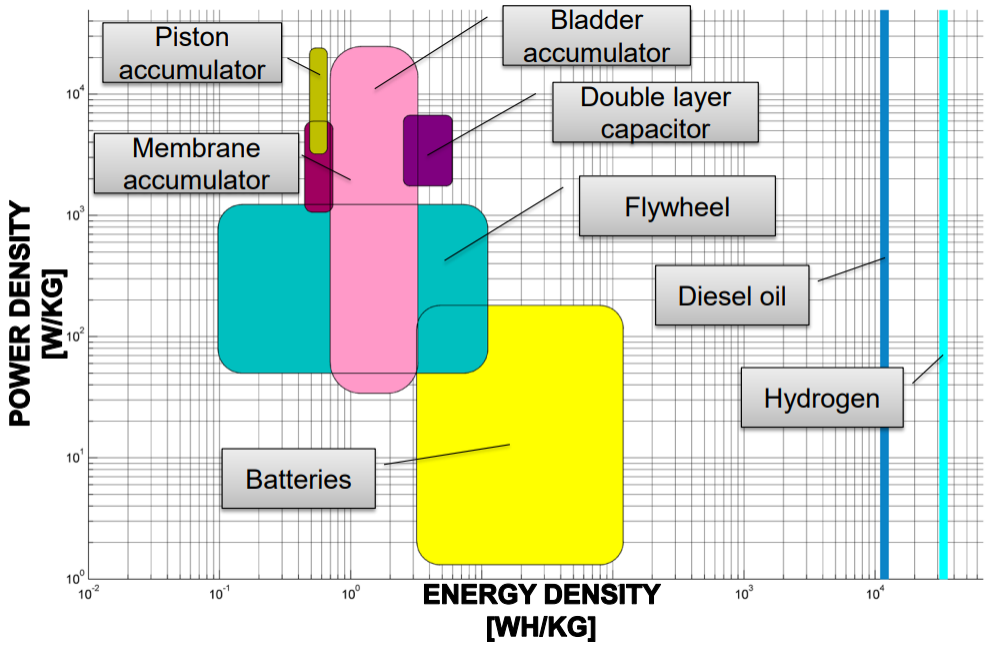

Figure 2.8: Ragone Plot of different ERTs [14]

For hybrid excavators, power density becomes the critical factor in selecting the appropriate energy storage device, since its primary function is to smooth engine output, storing a relatively small amount of energy but handling large power flows. Batteries, because of their high internal resistance and relatively low power density, are not well-suited for such tasks, as the electrochemical reactions within batteries require a slow and steady process for optimal performance. For example,

to provide 100 kW of power an additional ton of batteries would be required, which is impractical for mobile machinery [7].

In addition to power density, the robustness and lifespan of the storage device are crucial considerations. Hydraulic accumulators excel in this regard, boasting a high abuse tolerance and a long operational lifespan of up to three million cycles between charge and discharge [7]. Moreover, unlike electric batteries, which may exhibit significant capacity fade over time, hydraulic accumulators generally maintain their performance throughout their lifespan, aside from minor reductions in pre-charge pressure that can be easily rectified.

In addition to the technical attributes of each energy storage technology, cost is an important factor to consider. While providing exact figures can be challenging, it is generally accepted that hydraulic accumulators are among the most affordable options, thanks to their simplicity and widespread use.

Chapter 3

Traditional Load Sensing Excavator: Description of the Original Model

This chapter focuses on the analysis of the traditional hydraulic excavator model, based on a Load Sensing architecture, used as the baseline circuit, which will then undergo modifications to achieve the hybrid CPR architecture discussed in this thesis, and will be analyzed in the following chapter. Using the AMESim simulation software, this hydraulic circuit model was developed to represent a commercially available Komatsu PC75R 9-ton excavator [15]. Mechanical relationships between the actuators and the environment were incorporated using the "2D Mechanical Library" in AMESim, accounting for machine inertia and real-world dynamics. Simplifications were introduced, such as setting the Internal Combustion Engine (ICE) to a constant speed regardless of torque demands, and removing of the hydraulic modules related to the blade and tracks of the excavator, which are negligible in the specific duty cycles under study.

The complete excavator circuit was developed and studied at the Polytechnic University of Turin by PhD Gabriele Altare, PhD Damiano Padovani, and Professor Nicola Nervegna [9]. A theoretical and experimental validation process was conducted to ensure the digital model closely mirrors the actual machine, helping to ensure that simulation results are meaningful and accurate.

3.1 Load Sensing Machine Layout

The 9-ton crawler excavator, a mid-size mobile machine, is depicted as a 3D model in Figure 3.1. The hydraulic circuit of the excavator used for all tests, developed

in the AMESim environment, is illustrated in Figure 3.2. As mentioned earlier, this model is based on doctoral research [15], and several modifications have been made to simplify the system. However, these simplifications were carried out with special care to avoid deviating too much from the results of the detailed model. The goal was to strike a balance between reducing complexity and preserving accuracy, ensuring that the simplified model could still provide useful results for analyzing the performance of the excavator's hydraulic system without compromising the validity of the data.

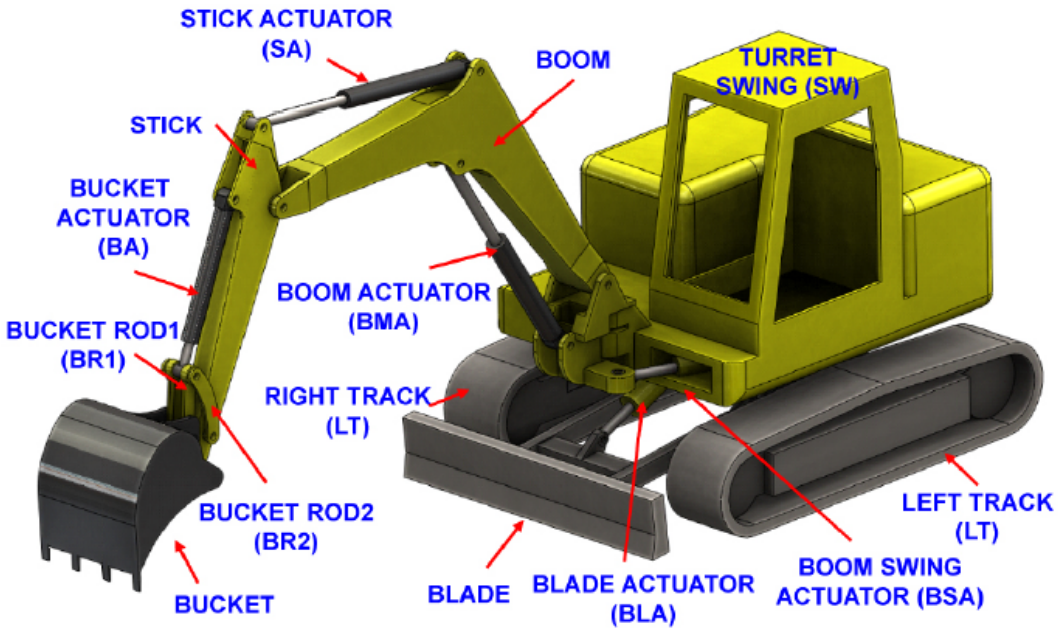

Figure 3.1: 3D model of the Komatsu PC75R [16]

This simplified hydraulic circuit was carefully designed to meet the high standards required for hydraulic system modeling in engineering. It serves as a foundational tool for conducting in-depth performance analyses, accurately reflecting the dynamics and operational characteristics of the excavator's hydraulic system under various scenarios and load conditions. The modifications made from the original thesis model were essential for optimizing simulation efficiency while maintaining real-world hydraulic behavior and response accuracy.

It is important to note that the diesel engine powering the commercial hydraulic excavator is not included in the AMESim model, which is simulated by an ideal prime mover to simplify the analysis and concentrate on the hydraulic circuit. In the actual vehicle, this engine provides a maximum output of 55 kW and can reach a peak speed of 2300 rpm.

Since all studies are performed with the excavator at rest, meaning the travel motors are inactive, a further simplification was made by removing the tracks motors and their associated hydraulic circuits (see Figure 3.3).

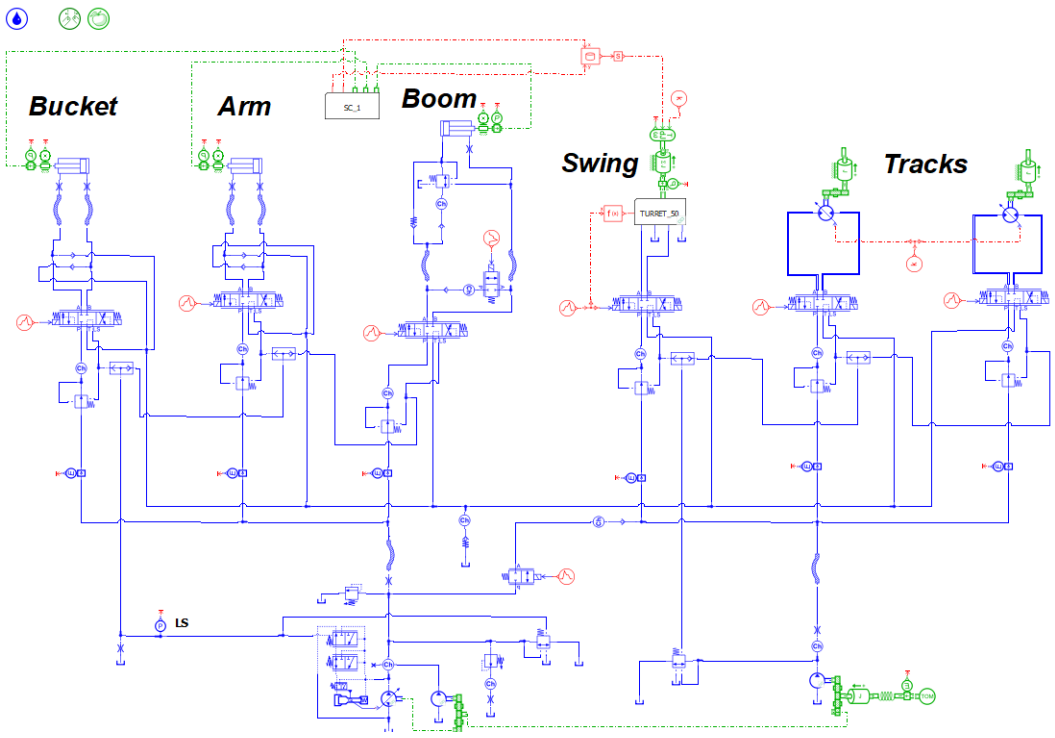

Figure 3.2: Simplified AMESim model of LS hydraulic excavator

In the AMESim model, the ideal prime mover is connected to three hydraulic pumps: one with variable displacement (*VD pump*) and two with fixed displacements. The variable displacement pump and one fixed displacement pump, which serves to provide flow when the pump is at zero displacement, supply hydraulic fluid to the boom, arm, and bucket actuators, while the other fixed displacement pump (*FD pump*) provides fluid to the turret rotation motor and the travel motors for the left and right tracks. The speed of the actuators is controlled through the displacement of the LS type distributors. Additionally, an over-center valve (OCV) is installed on the boom actuator to ensure the boom remains in a fixed position without any safety issues.

The model, obviously, includes also local pre-compensators and an on-off valve that can be opened when additional flow from the FD pump is required, mainly to ensure proper performance of the boom, also referred to as boom boost. The Arm Kinematic and Turret blocks contain the model of the actuators kinematic, which will be explained in the following sections.

As stated in the introduction to this chapter, this final model was used to develop the CPR hybrid architecture model and served as a comparative reference for studies on fuel efficiency and system losses.

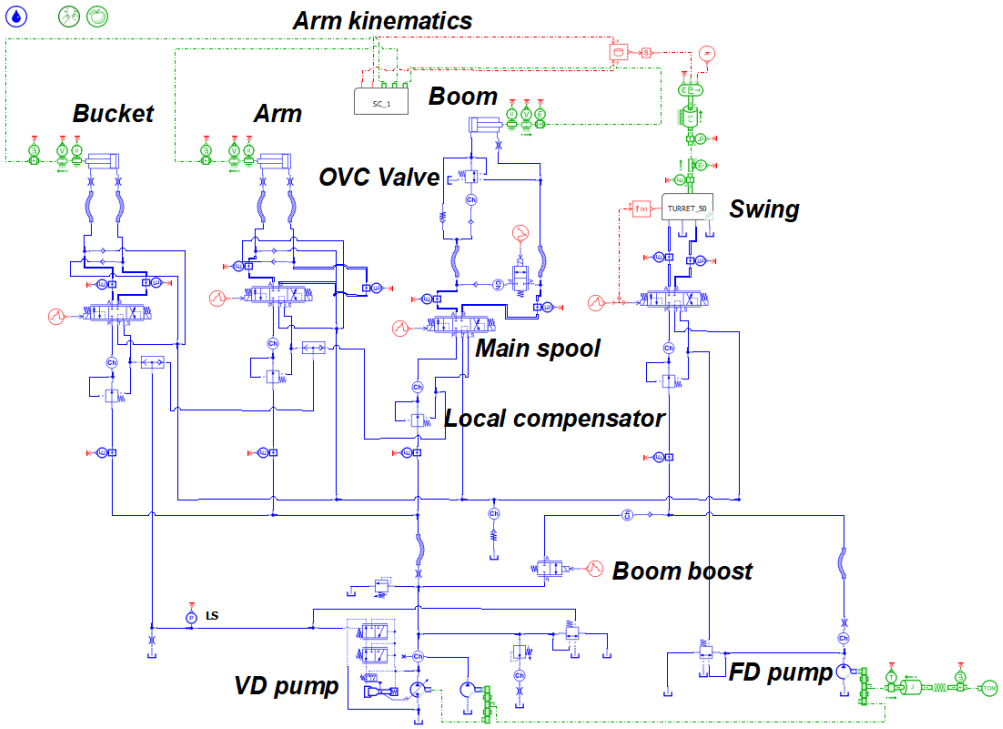

Figure 3.3: Simplified AMESim model of LS hydraulic excavator without tracks motors

3.2 LS-HE Baseline Model Power Supply System

The following paragraphs in this section will delve into the subsystems that make up the traditional LS excavator's supply power system, highlighting the key characteristics of each component.

Engine Subsystem The prime mover for the excavator model in this study is a turbocharged diesel combustion engine, known for its fuel efficiency and torque suitability for such applications. The chosen engine has six cylinders, a displacement of 2.9 liters, a maximum speed of 2300 rpm, and a maximum power output of 55 kW. The engine behavior was characterized using data from experimental tests, which provided a detailed engine map (shown in Figure 3.4) that highlights maximum torque at different speeds and indicates zones of constant efficiency.

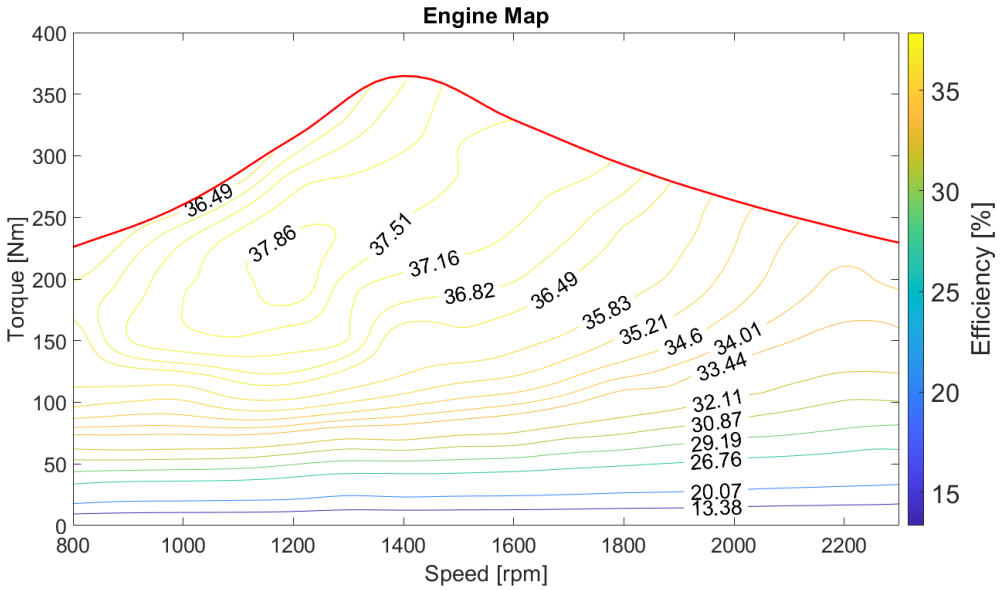

Figure 3.4: Diesel ICE Efficiency Map

In the traditional HE model, the engine's rotational speed is maintained at a constant 2300 rpm throughout the work cycle to ensure adequate hydraulic flow. To enhance accuracy in fuel consumption calculations and reduce simulation times, the engine model was simplified, through a look-up table which was used to evaluate fuel consumption based on speed-torque combinations derived from the experimental data. The choice to implement an interpolation table for fuel consumption data (shown in Figure 3.5) rather than relying on the ICE model from the AMESim library (illustrated in Figure 3.6) was primarily driven by the need to enhance simulation efficiency and accuracy.

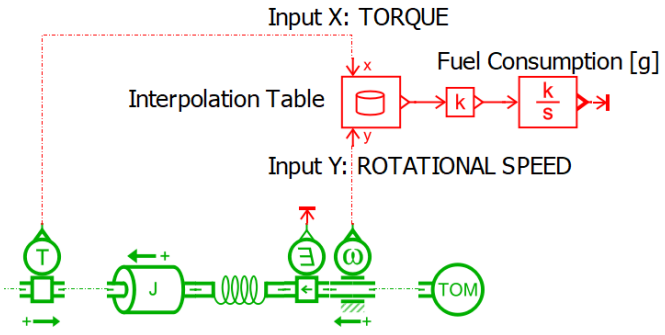

Figure 3.5: ICE model with Look-Up Table

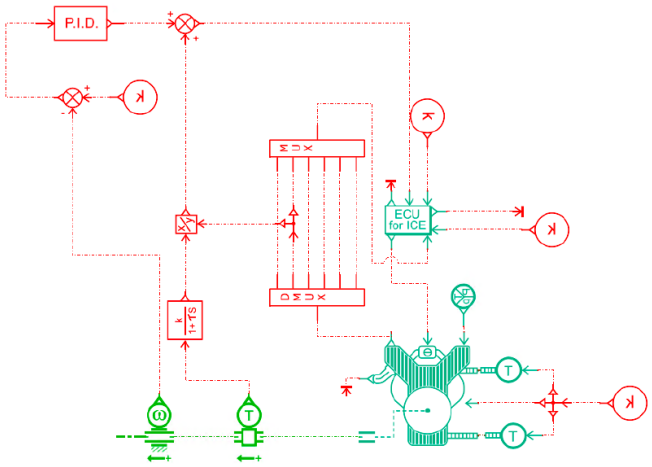

Figure 3.6: ICE model with AMESim Library

In the final implementation (depicted in Figure 3.5), a simplified prime mover element was selected instead of the detailed ICE component. This element runs continuously at 2300 rpm, utilizing the rotational speed together with torque sensor outputs as input for the fuel consumption map. The software interpolates values from the table to provide fuel consumption in grams per hour, which is then converted to grams per second and integrated over time to calculate the total fuel consumed. The 2-D fuel consumption map, represented in Figure 3.7, allows for precise fuel usage estimation.

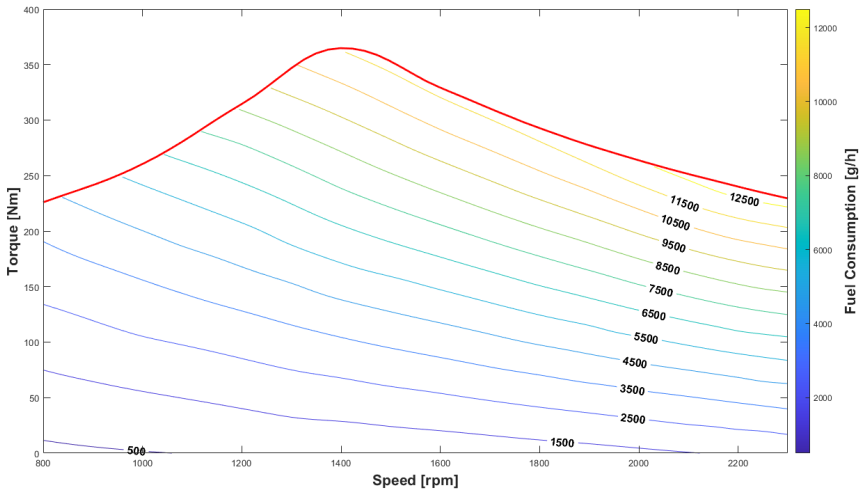

Figure 3.7: Diesel ICE 2D Fuel Consumption Map

Flow Generation Unit Subsystem As mentioned, the reference hydraulic system model utilizes three pumps: a variable displacement axial piston pump (65 cc/rev) and a fixed displacement pump (10.6 cc/rev) supplying the boom, arm, and bucket, along with a fixed displacement gear pump (27 cc/rev) for the turret swing motor. The flow generation unit detail can be seen in figure 3.8.

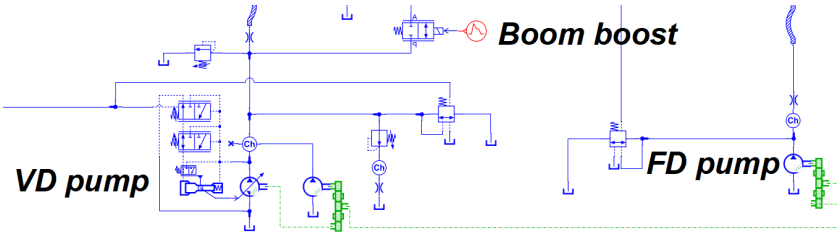

Figure 3.8: Flow Generation Unit Detail

In the commercial excavator setup, the two pumps for the linear actuators are replaced by a single VD pump rated at 75 cc/rev. This choice reflects that, at minimum displacement, the 75 cc/rev pump can deliver a flow rate of 10.6 cc/rev. However, since the AMESim simulation environment does not support a fixed minimum flow rate for variable displacement pumps, a dual-pump configuration was implemented. The fixed displacement pump, as said before, consistently provides the necessary minimum flow, while the variable displacement pump adjusts from zero to its maximum capacity to meet additional flow requirements.

The VD pump is controlled by a hydraulic piston actuator model featuring a torque limiter, which adjusts the pump's displacement to maintain a balanced flow rate and pressure difference at the pump ports, effectively managing the theoretical torque. A pre-loaded spring counteracts regulated pressure, keeping the system minimally pressurized.

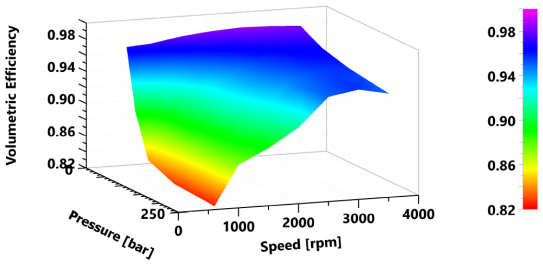

Figure 3.9: FD Volumetric Efficiency

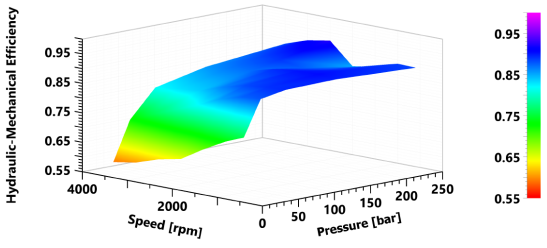

Figure 3.10: FD Hydraulic-Mechanical Efficiency

Efficiency data for the pumps were incorporated into the AMESim model, with volumetric and hydraulic-mechanical efficiencies for the swing motor pump

illustrated in Figures 3.9 and 3.10, respectively. Figures 3.11 and 3.12 present the efficiency maps for both the variable displacement pump and the fixed displacement pump supplying the linear actuators, which are identical.

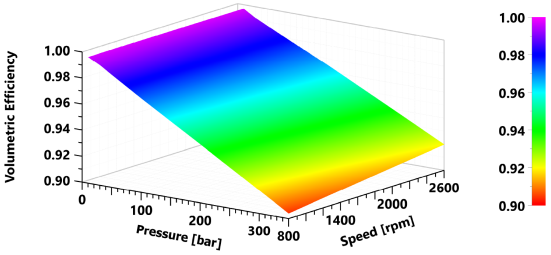

Figure 3.11: VD Volumetric Efficiency

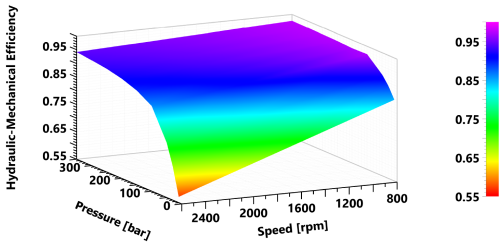

Figure 3.12: VD Hydraulic-Mechanical Efficiency

To accurately represent hydraulic losses in the real circuit, flow restrictors were integrated to account for pressure drops, ensuring that hydraulic losses in the AMESim model matched those of the commercial excavator. Flexible hoses were also included to accommodate volume variations due to pressure fluctuations.

3.3 Hydraulic Circuit Subsystem

In modeling the hydraulic circuit subsystem, illustrated in the figure 3.13, simplifications were implemented to balance fidelity with computational efficiency. The excavator's conduits were initially modeled using the "Hydraulic Resistance" library to accurately account for pressure drops, especially at high flow rates. Flexible hoses were included to represent volume variations due to pressure changes. The PDCVs and LS system were modeled using local pressure compensators and ideal shuttle valves, enabling optimal pressure delivery to the hydraulic control of the variable displacement pump. The hydraulic proportional valve with an LS port from the dedicated AMESim library was also utilized.

The local pressure compensator in the AMESim model maintains a constant pressure drop across each upstream orifice, set to 10 bar in this case. The compensator features two hydraulic ports, two control ports, and a normally open position. In Figure 3.13, the compensators are shown upstream of each actuator's hydraulic proportional valve, with dashed lines indicating hydraulic pilot ports used solely for hydraulic control with no volumetric flow rate. The valve's fractional opening is calculated as an internal variable, limited to a maximum value when fully open.

The hydraulic proportional valve model includes an LS port that supplies pressure for actuator control in LS systems. Four flow paths connect the pump

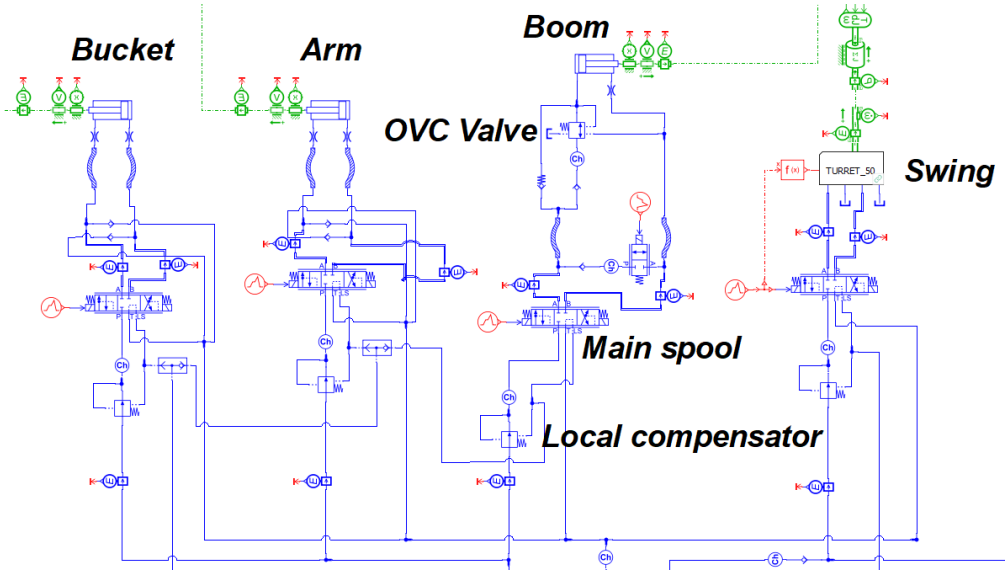

Figure 3.13: Detail of Hydraulic Circuit

and tank to the actuator chambers, with specified flow rates (in L/min) and corresponding pressure drops (in bar) for fully open conditions, based on real component characteristics. The proportional opening signal, ranging from 0 to 1 mA, is provided externally.

Additionally, the boom circuit incorporates an over-center valve (OCV) for managing overrunning loads during descent and when stopping at intermediate positions. The OCV generates back pressure on the actuator's exhaust port based on pressure readings from both actuator ports, allowing it to remain stationary in intermediate positions. These normally closed poppet valves prevent fluid leakage, ensuring the actuator's position is maintained under load indefinitely while also limiting maximum pressure in the actuator chambers.

3.4 Turret Subsystem

The turret rotation of the excavator is driven by a hydraulic circuit comprising a hydraulic motor, parking brake valves, anti-cavitation valves, a relief valve, a planetary gear, and a slewing ring. Figure 3.14 illustrates the corresponding AMESim model.

The planetary gear system transmits power to the output shaft, incorporating a torque multiplier with a gear ratio of 200.88, which enhances the torque output. For modeling purposes, the turret is approximated as a rotating inertia. The Arm Kinematic block outputs the coordinates of the hydraulic excavator arm, which are

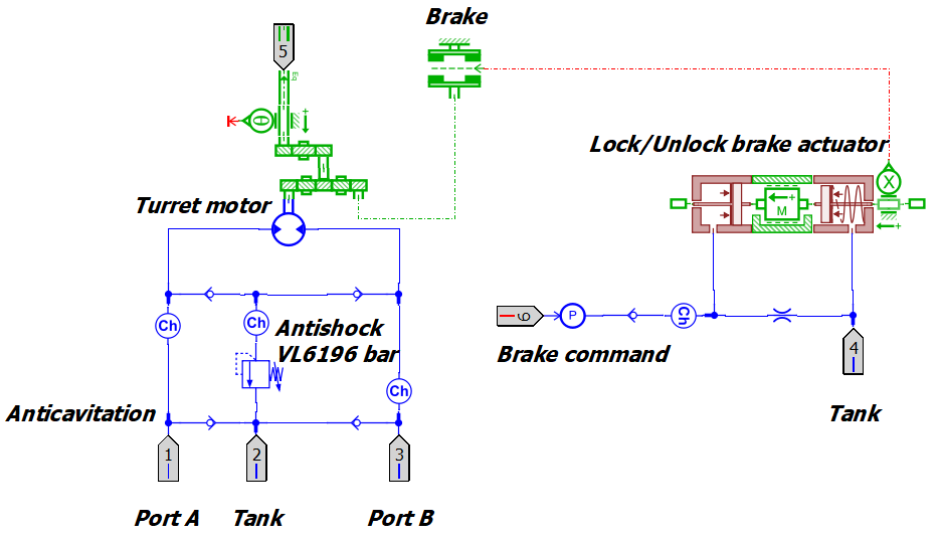

Figure 3.14: Turret Amesim Model

used in an interpolation table to determine how inertia varies based on the arm's position. This variation is then combined with the equivalent inertia of the turret housing to provide a total inertia value as an input to the hydraulic motor.

To develop the control system, it was crucial to assess how the effective inertia at a given arm position, system acceleration, and torque applied to the turret shaft could be modeled. The initial rotational inertia, was calculated for the fully extended position of the excavator arm, yielding a value of 15536 $kg \cdot m^2$. Friction effects during turret rotation were modeled as viscous torque, characterized by a viscous friction coefficient of 340 Nm/rpm, ensuring that these dynamics are appropriately represented in the simulation.

3.5 Excavator Arm Subsystem

The mechanics and kinematics of the actuator subsystem, along with the interaction between the excavator system and the environment, have been modeled using the Planar Mechanical Library of AMESim [16]. This library allows for the representation of rigid bodies and joints with two or three degrees of freedom operating in a plane. Additionally, it enables the implementation of a soil model to compute resistive forces during digging and to calculate the volume and weight of the excavated soil.

To create the mechanical model of the excavator arm, the coordinates and dimensions of various components were defined using a CAD program. The final AMESim implementation of the excavator arm is illustrated in Figure 3.15, which

is integrated within the Arm Kinematic or SC block of the simplified AMESim excavator circuit in Figure 3.3.

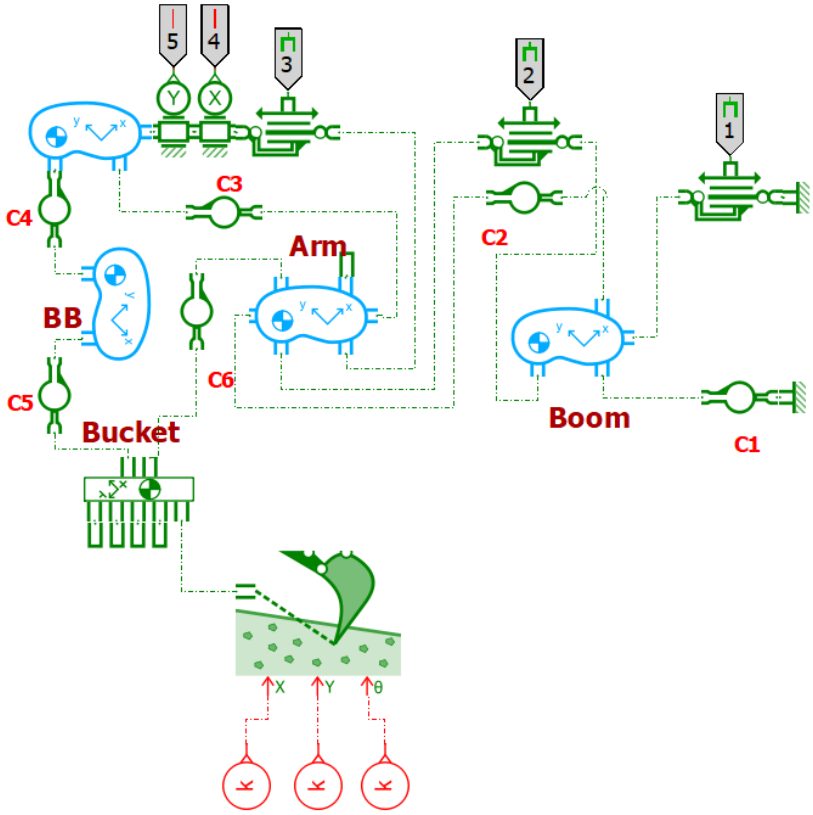

Figure 3.15: Arm Kinematic Model

In the excavator arm model (Figure 3.15), tags (1, 2, 3) are connected to each actuator—specifically the boom, arm, and bucket actuators (see Figure 3.3). These tags link to translational actuator components that output position, speed, and acceleration based on the input force, thus integrating the hydraulic and mechanical-kinetic aspects of the model.

The soil submodel, located at the bottom of Figure 3.3, is significant for simulating the excavator's interaction with the ground. It includes three signal ports representing the X, Y and the inclination of the soil, respectively. A fourth port serves as a standard 2D port representing the tool blade's tip. By inputting the soil coordinates and angle of inclination, the submodel outputs torque and force in the X and Y directions, utilizing the position, velocity, and acceleration of the tool blade's tip obtained from port 4. Additionally, the excavator arm model features two more tags (4 and 5) that provide the X and Y positions of the bucket, which are crucial for computing variations in the moment of inertia.

3.6 Duty Cycles used for Simulation Tests

As mentioned in chapter1.3, to evaluate the performance of the LS architecture and to compare it with CPR architectures, that will be explained in the next chapters, two specific duty cycles were selected for testing the machine, offering several key advantages.

This approach enhances the realism of the assessment, as different cycles can replicate a wider range of real-world operating conditions, such as varying loads and movement speeds. This enables the analysis of the excavator's performance in different scenarios, ranging from light to heavy loads. Furthermore, utilizing multiple cycles provides a more thorough performance evaluation, with each cycle customized to test specific aspects of excavator capabilities, ultimately helping in design optimization for improved equipment efficiency. The reference cycles used in this study were defined according to the Japanese standard JCMAS H020:2007.

The following sections will offer an in-depth overview of actuator movements and hydraulic swing motor, both of which are crucial elements in the standardized tests used to assess the performance of excavator models.

The next chapter will present and analyze the pump's pressure and flow rate data, as these factors are essential for accurately sizing the accumulators and establishing the reference pressures for the CPR system rails.

3.6.1 Dig and Dump Cycle

The dig and dump cycle is a core operational sequence for excavators, which involves excavation and material discharge. In this reference cycle, the excavator begins in a properly positioned stance relative to the excavation site, with its arm fully extended. The cycle starts with the digging phase, where the bucket penetrates the ground, applying force to excavate and lift the material. Once the material has been excavated, it is raised by the boom lifting motion. This is followed by the turret rotation, which moves the arm toward the discharge point, where the material is released. Afterward, the arm returns to its initial position, allowing for potential simulations with repeated cycles. This process is designed to optimize excavator efficiency in excavation and material handling, while maintaining safety and accuracy in construction tasks.

In the AMESim simulation environment, the dig and dump cycle was implemented starting with the excavator arm fully extended (see Figure 3.16). The first step involves the bucket digging into the ground (see Figure 3.17), followed by the lifting of the arm. The turret rotates approximately 110°, positioning the arm over the dumping area (see Figure 3.18). Once the material is dumped, the turret rotates back to its original position (see Figure 3.19).

For completeness, the reference velocities for each actuator during the entire

Figure 3.16: Air Grading

Figure 3.17: VD Hydraulic-Mechanical Efficiency

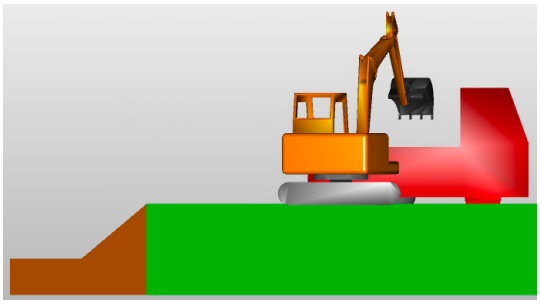

Figure 3.18: Air Grading

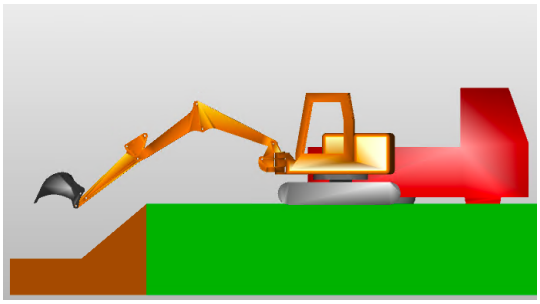

Figure 3.19: VD Hydraulic-Mechanical Efficiency

dig and dump cycle are also provided in the Figures from 3.20 to 3.23 . It is important to note that the velocity profiles represent signals proportional to the joysticks commands in the excavator's cabin, establishing a direct link between the operator's inputs and the movements of the actuators.

This cycle was initially developed in thesis number [15], by controlling the opening and closing of the proportional distributors for each actuator through piece-wise functions. In order to compare this architecture with the CPR-based ones, it was necessary to create a control logic based on the input of actuator speeds. The logic simulates operator input via the joysticks located in the excavator's cabin. The velocity profiles, shown in the following figures, were obtained using step approximations based on the outputs from the speed sensors positioned on each actuator in the AMESim environment 3.13.

The control of the actuators in the traditional excavator was developed using open-loop logic, which is further explored in the thesis [17].

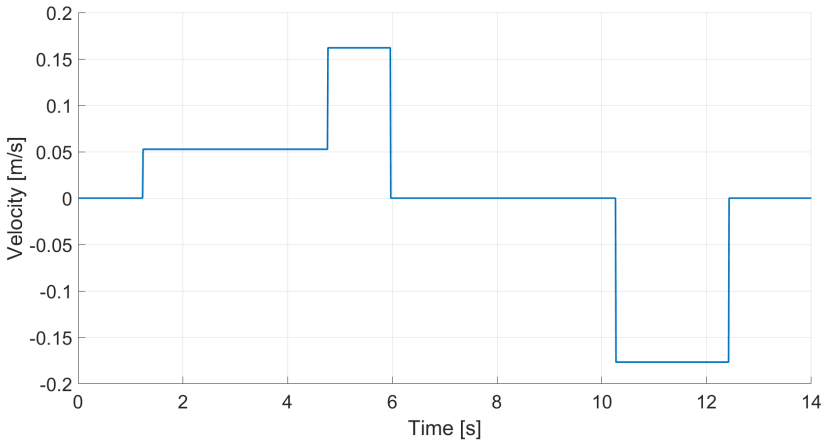

Figure 3.20: Boom reference velocity, Dig and Dump cycle

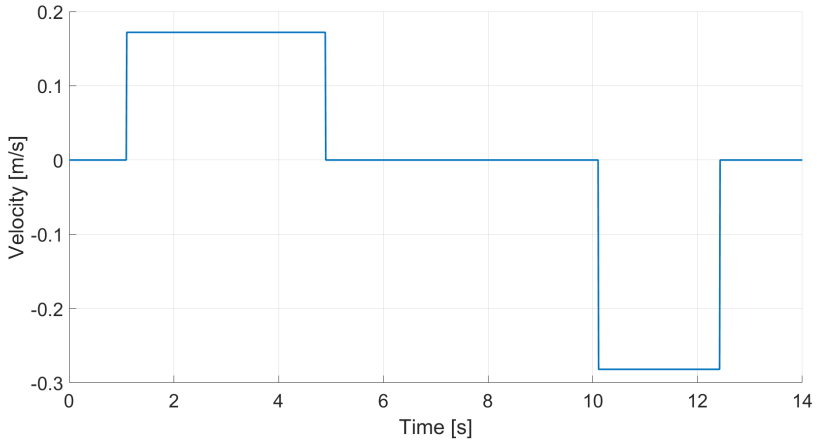

Figure 3.21: Arm reference velocity, Dig and Dump cycle

3.6.2 Air Grading

The air grading cycle, which typically begins with the excavator positioned in the target area, with the arm extended and the bucket in contact with the surface (see figure 3.24, can be broken down into two main phases. The first phase, leveling, involves pulling the bucket backward along the ground while maintaining a constant angle to smooth out irregularities and level the terrain. During this phase, the excavator's arm is used to control the leveling depth and angle (see Figure 3.25). The second phase occurs once a leveling pass is complete and involves returning the arm and bucket to their starting position (see Figure 3.25) .

This cycle simulates a different mode of operation compared to the dig and dump

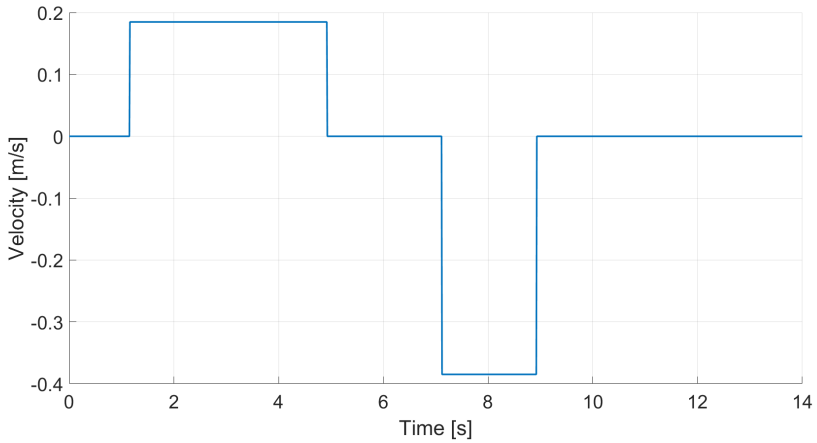

Figure 3.22: Bucket reference velocity, Dig and Dump cycle

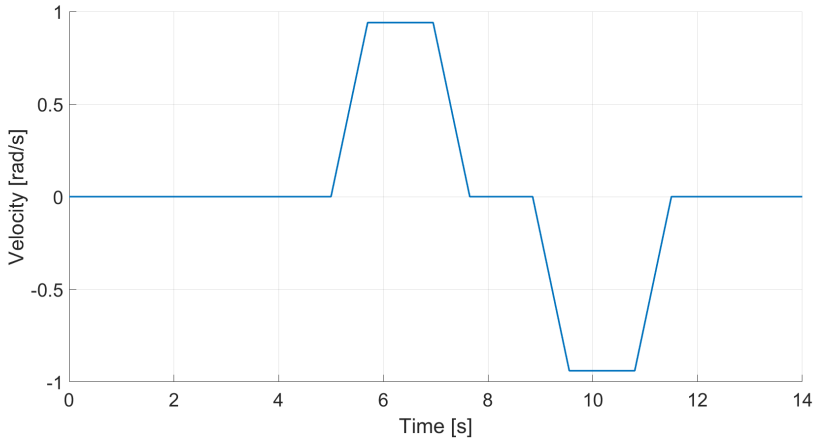

Figure 3.23: Swing reference angular velocity, Dig and Dump cycle

cycle, and testing different architectures with the air grading cycle was deemed important for a more comprehensive performance evaluation. This approach helps determine whether the potential benefits observed in one cycle extend to other applications, ensuring that any architectural advantages are not limited to specific tasks.

As previously specified, it is crucial to define the speeds of the actuators, which in this case were derived by analyzing the mechanics and kinematics of the excavator's arm from a theoretical perspective, before implementing piece-wise functions directly within the AMESim environment. To execute this cycle, only the movements of the boom and arm actuators are required, as it is performed with the turret stationary and the bucket fixed in a position that allows for leveling

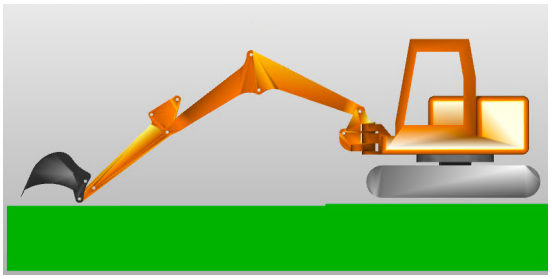

Figure 3.24: Air Grading Starting and Final Position

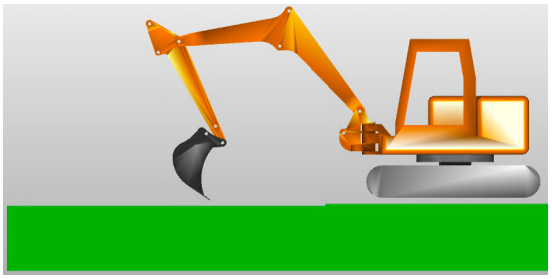

Figure 3.25: Air Grading Intermediate Position During Levelling

the ground.

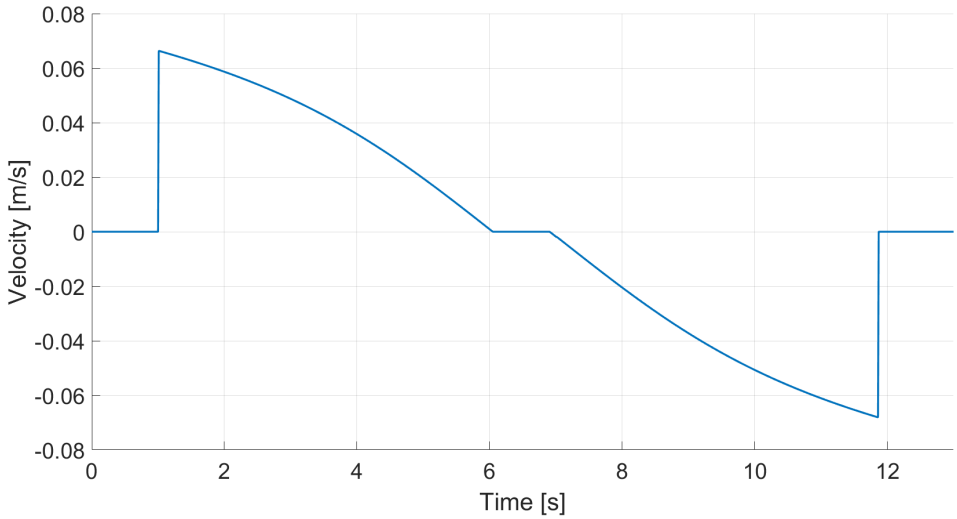

Figure 3.26: Boom reference velocity, Air Grading cycle

The logic and explanation behind how these speed inputs, shown in Figures 3.26 and 3.27, were determined can be found in the following thesis [17]. It is important to highlight that a temporal pause was introduced between the forward and return movements of the excavator arm, along with a gradual increase in the speed of the arm's actuator. This adjustment was made to ensure smoother overall motion, rather than maintaining a linear variation of the arm's inclination angle and a constant rod movement speed. Additionally, the precision of the control system is crucial for the successful execution of this cycle, as it allows for precise adjustments to the arm's inclination and speed, both of which are essential for maintaining the correct depth and uniformity during the leveling process.

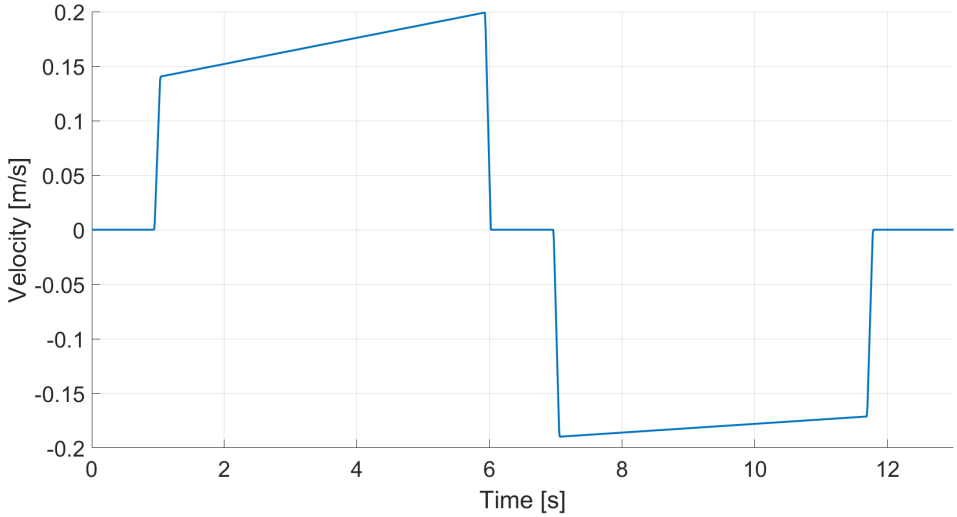

Figure 3.27: Arm reference velocity, Air Grading cycle

Chapter 4

CPR Architecture: Design and Analysis of the Hybrid Excavator Power Supply System

In this chapter, the CPR hybrid hydraulic excavator model implemented in AMESim will be introduced. This model was developed and designed based on the STEAM architecture concept outlined in Chapter 2. Building upon the traditional excavator model, the mechanical modeling of the actuators (see Section 3.5) and turret motor (see Section 3.4) remained unchanged, with the assumption that the new hydraulic architecture could meet the same operational demands as the conventional system. However, to improve efficiency, modifications were made by integrating energy recovery and hydraulic storage components, and adjusting the hydraulic layout to enable and facilitate energy recovery. For consistency, the same engine model was retained (see Section 3.2), with a focus on its more efficient use.

As discussed in the previous chapter, the foundation for the new hydraulic circuit design was the simplified LS model of the 9-ton Comatose PC75R excavator, illustrated in Figure 3.3. Key characteristics of the excavator, including mass, actuators, and hydraulic motor for swing rotation, were kept unchanged.

The main modification focused on the power supply system feeding the various actuators, aiming to improve fuel efficiency and enable energy recovery. In this chapter, it will be explored the innovative flow generation group in detail, with particular emphasis on the sizing of key components, such as the bladder accumulators. Additionally, a finite state machine based control logic will be presented, which ensures that the desired pressure values are maintained in the rails.

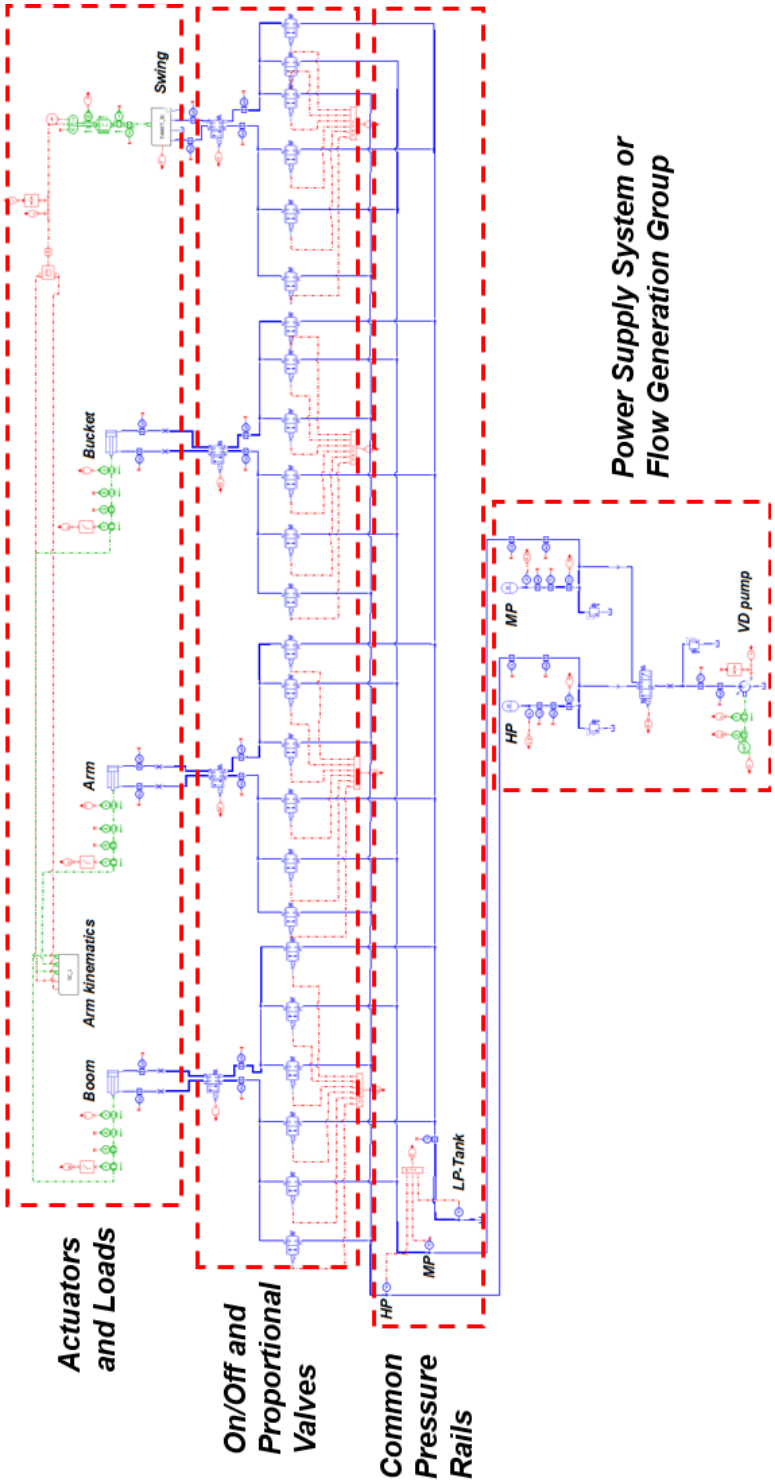

Figure 4.1: Hybrid Hydraulic CPR Architecture

4.1 Machine Layout

As previously mentioned, this study is based on data from a commercial excavator used to develop the traditional excavator model. The subject of this study is a 9-ton excavator, with the primary differences between the two models being the structure of the hydraulic subsystem. The LS system is a reliable and well-established approach, offering precise load control with pressure-independent speed characteristics and improved energy efficiency compared to other valve-controlled systems. However, it can result in high energy consumption when actuators require significantly different pressures, and it lacks the capability to recover energy from external sources (see section 2.1.1).

To address these limitations, the CPR architecture has been considered as a more efficient alternative to the LS system, allowing each actuator to access the most appropriate pressure line based on its load, reducing losses in proportional valves. Moreover, it can recover energy from external sources and store it in accumulators, making it a promising solution for enhanced energy efficiency.

The complete hybrid hydraulic excavator model is shown in Figure 4.1, rotated 90° for a clearer view of the entire circuit, with the various subsystems highlighted. As previously noted, the modeling of the actuators, the arm kinematics and the turret motor remain unchanged with respect to the traditional excavator and will not be repeated here. Instead, the following sections will focus on the development and sizing of the power supply system of the CPR model and on the modifications done to make the ICE more fuel efficient.

4.2 Power Supply System Design

A key consideration in designing the flow generation group of the hybrid CPR excavator was the selection and sizing of the hydraulic accumulators, as well as determining the optimal engine speed. This process involves analyzing the average power demand of the internal combustion engine during the dig and dump duty cycle, which represents the most complete and realistic cycle to verify the proper functioning of the machine and its fuel consumption. The idea is to select a range of operating pressures that fluctuate within the bladder accumulator, effectively damping the engine's torque fluctuations (see Figure 4.2). This allows the engine to supply only the average power required for the cycle, rather than the peak power demanded at any given moment (see Figure 4.3).

The objective, as will be further detailed in the following sections, is to identify the optimal operating pressure values for the system, particularly the pressures in the lines shared by all actuators. Once these values are determined, engine downspeeding will be applied to ensure operation within the areas of maximum

energy efficiency of the ICE map (illustrated in the map shown in the Figure 3.4).

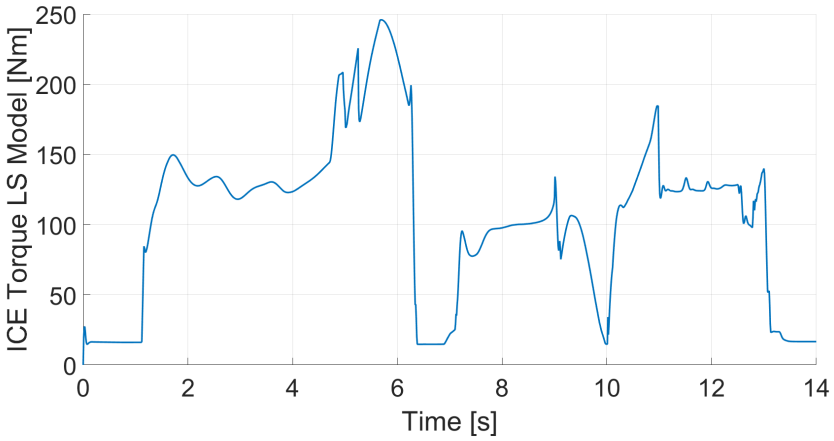

Figure 4.2: Torque ICE LS Model, Dig and Dump Cycle

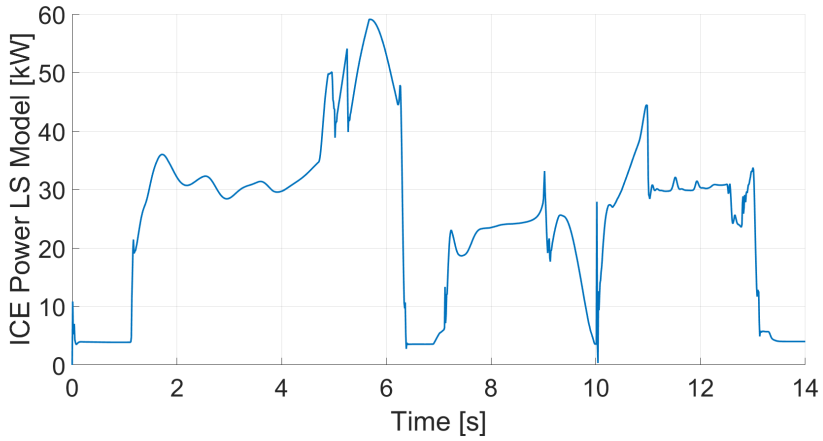

Figure 4.3: Power ICE LS Model, Dig and Dump Cycle

4.2.1 Pressure Levels and Accumulator Sizing

As introduced in Chapter 2, the CPR architecture enables each linear actuator to connect to any of the available pressure rails in the system whose values are maintained at specific levels thanks to the presence of two bladder accumulators (see figure 4.1). In the following study case, there are three pressure rails available: a high-pressure rail (HP in the Figure 4.1) for handling heavy external loads, a medium-pressure line (MP in the Figure 4.1) for standard load conditions, and

a low-pressure line, represented by the tank pressure (LP in the Figure 4.1). By controlling and managing the on/off and proportional valves (see Figure 4.1), whose design is explained in detail in the thesis [18] and will be summarized in this section, it is possible to provide nine different pressure combinations for each actuator (see Figure 4.4). This enables the actuators to select the pressure combination that best matches the actual load demand, significantly reducing throttling losses. The naming convention lists the pressure level connected to the piston side first, followed by the pressure level connected to the rod side. For example, HP/MP denotes high pressure on the piston side and medium pressure on the rod side. In Table 4.1, all the available pressure combinations for the actuators are listed. It is important to note that combinations involving low pressures (LP/LP), such as tank pressures, are not considered in this analysis, as they would result in a null force, which is not usable for either resisting or overrunning loads.

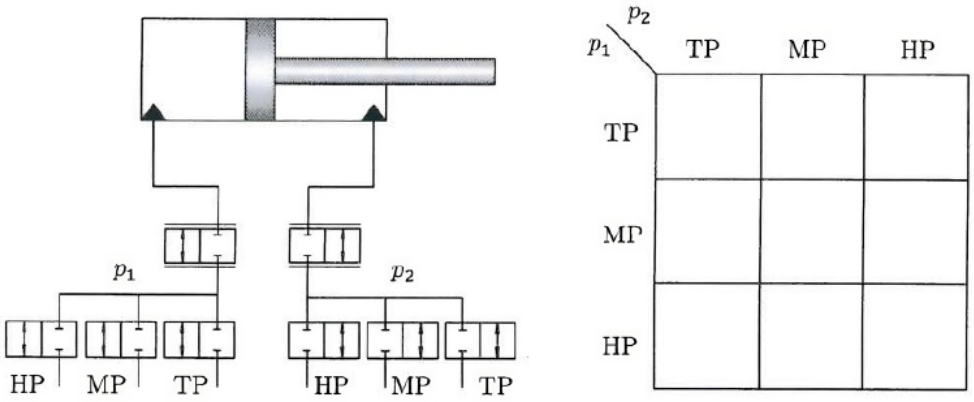

Figure 4.4: Linear Actuator Operating Modes [7]

Combination Index	Small Chamber	Big Chamber
1	HP	LP
2	MP	LP
3	HP	MP
4	MP	MP
5	LP	MP
6	HP	HP
7	MP	HP
8	LP	HP

Table 4.1: Combination of Small and Big Chambers

Figure 4.5 illustrates the concept setup in the hybrid CPR architecture, which includes a force sensor, two electric joysticks, and a controller responsible for mode selection and valve activation. In real-world excavator applications, this setup is typically replaced by two pressure transducers connected to each actuator chamber, eliminating the need for a force sensor. Proportional valves regulate actuator velocity, and as load pressure and joystick inputs change, the controller identifies the operating point and switches modes to minimize throttling, as said before. The Q_L/p_L graph in the Figure 4.5 illustrates how the control system selects the closest curve, or operating mode, based on the excavator's operating points (determined by external load and operator input), represented by the black dots, in order to minimize throttling losses.

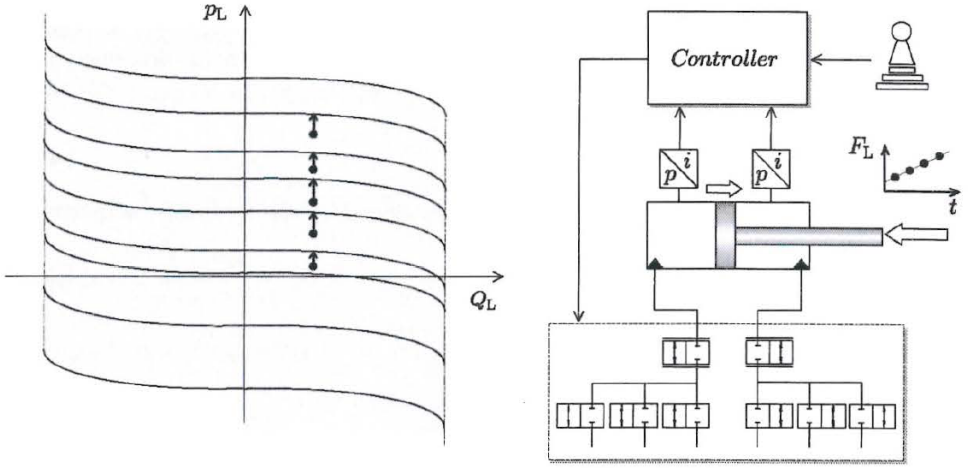

Figure 4.5: Concept Model CPR [7]

The core idea behind this actuator control logic is to identify three constant pressure values that can provide the actuators with eight distinct and ideally equidistant operating modes (OP), each of which corresponds to an ideal resultant force on the actuator. If these forces were equidistant from one another, as shown in Figure 4.6, throttling losses would be significantly reduced, leading to more efficient system operation.

However, achieving this ideal scenario is not feasible due to several factors, including the actuator area ratio, the limited capacity of the accumulators, and particularly the fixed minimum pressure losses associated with the opening and closing of on/off valves, as well as the regulation of proportional distributors.

As a result of these considerations, the real operating modes are not equidistant from each other, leading to greater pressure dissipation. Therefore, the valve block control system must select the curves that are closest to the working points, based on their position on the Q_L/p_L plane, in order to maximize the efficiency of the

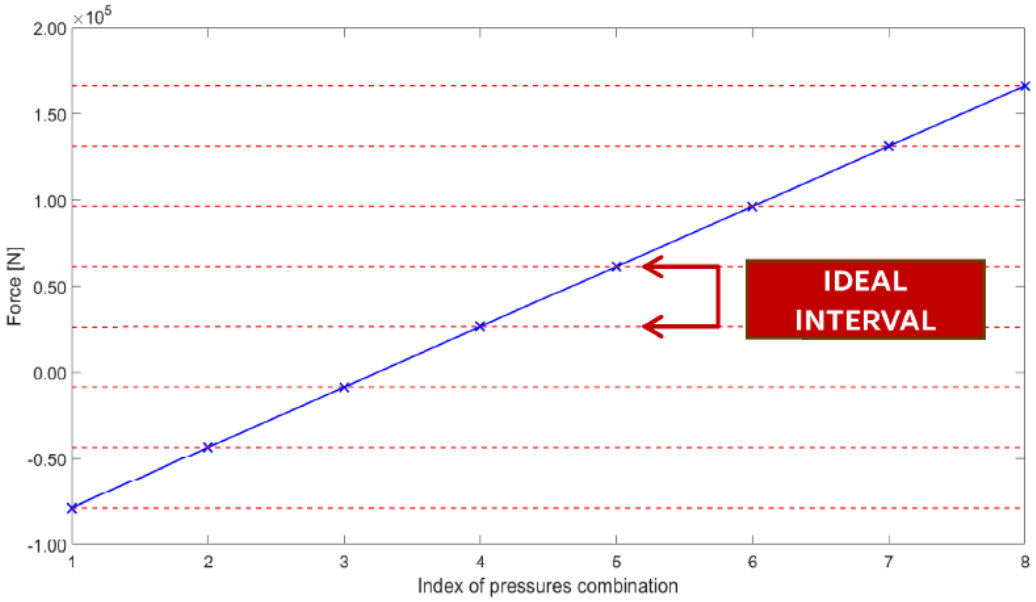

Figure 4.6: Ideal Operating Modes

system (see Figure 4.7). Lines passing through Quadrants I and III supply power to the actuator, enabling active operation. In contrast, lines through quadrants II and IV facilitate energy recovery from the actuator, contributing to energy conservation by storing excess energy in accumulators when possible. This design enhances operational efficiency by utilizing available energy rather than wasting it. The positioning of the operating mode lines is influenced by factors such as high-pressure (HP), medium-pressure (MP), and tank pressure (LP) levels, as well as the piston area ratio (α), that is the ratio between the rod side and piston side area of the linear actuator. Ideally, measurement data should be thoroughly analyzed to strategically position the lines, enabling efficient system operation and minimizing throttling losses [7]. This ensures the system operates effectively under varying load conditions, striking a balance between energy efficiency and the required output [7].

Accumulators Pressures Choice As a starting point for the analysis, the model presented in the previous chapter was considered during the dig and dump cycle (see Chapter 3). The following figure 4.8 illustrates the pressure values downstream of the LS proportional distributors (see Figure 3.13) for all actuators, as well as the discharge of the variable displacement pump. In this figure, two pressure working range areas can be identified: a high range with values fluctuating between 170 and 190 bar, and a medium range with values ranging from 60 to

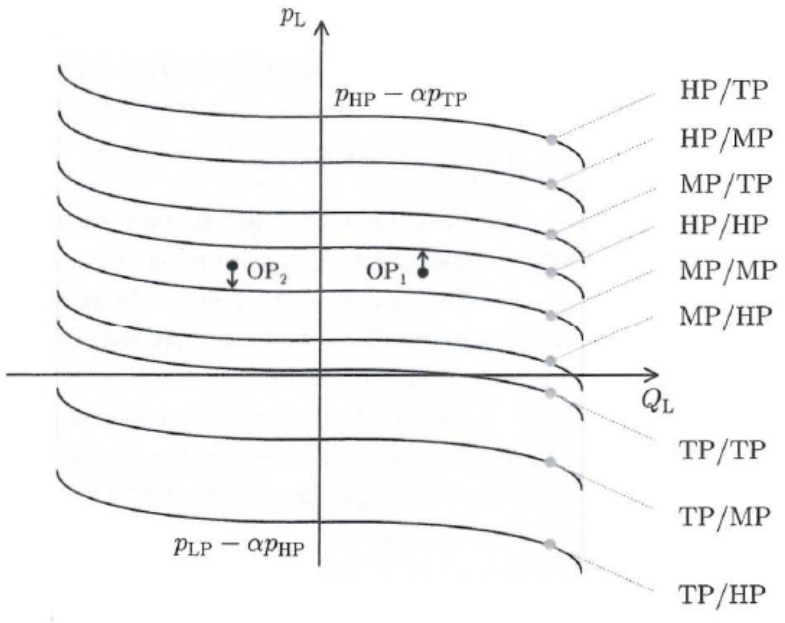

Figure 4.7: Region of operation of OP in linear actuator [7]

90 bar. It is important to note that the observed pressure spikes are caused by the end of stroke of the actuators and should not be regarded as reliable values; therefore, they have been ignored.

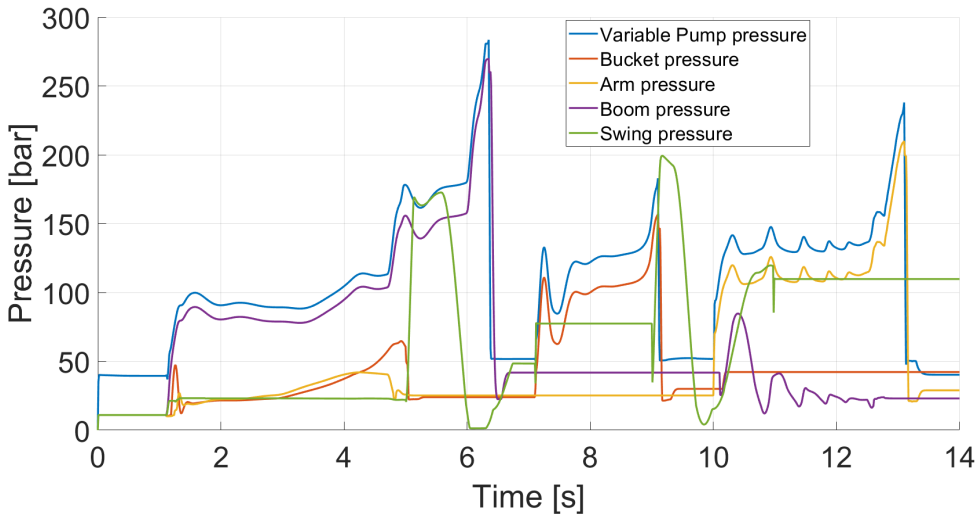

Figure 4.8: Pressure Levels in LS architecture

Once these two pressure ranges were identified, an algorithm was developed, as

detailed in the Appendix 6.3, to determine the ideal pressure values for the high and medium rails that should be available to all actuators at every moment of the desired duty cycle. The logic employed was as previously described, aiming to identify pressure combinations within the two ranges that minimize the distance between each operating mode. Specifically, for each combination of low, medium, and high pressure, the maximum force (using the HP/LP combination) and the minimum force (using the LP/HP combination) were first calculated. Following this, the so-called ideal range between the operating points was established, enabling the achievement of the optimal configuration illustrated in the figure 4.6. Using iterative cycles, the ideal range of each pressure combination was compared with the actual ranges, storing all the differences between them, specifically the root mean square errors, in a matrix. The best combination corresponds to the minimum error.

This algorithm was applied to each linear actuator, and the resulting plots can be found in the following figures, from 4.9 to 4.11.

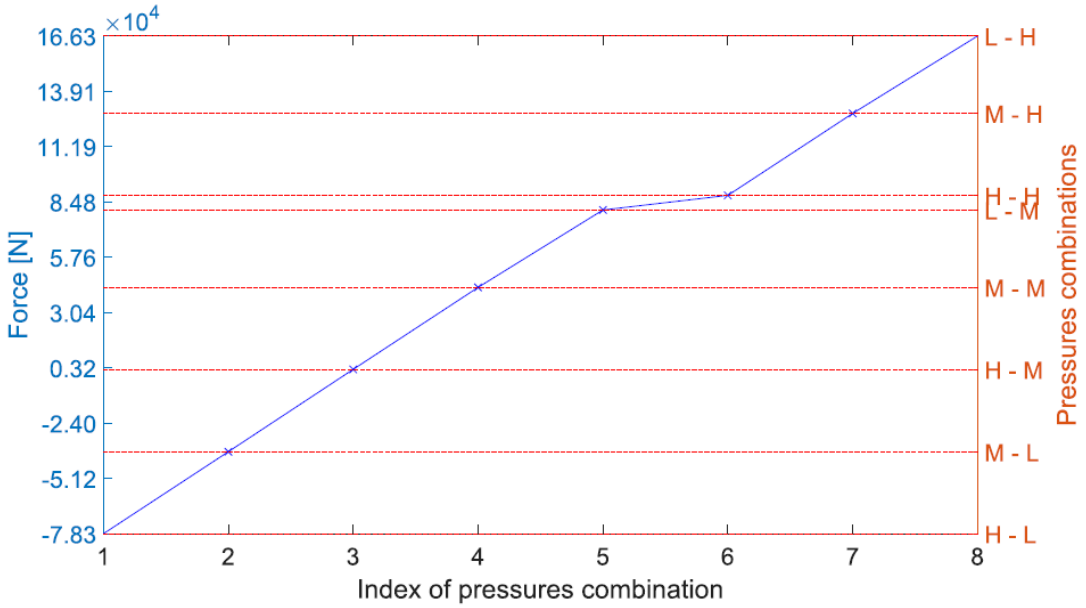

Figure 4.9: Boom Ideal Operating Modes

Of course, each actuator has different ideal pressures since the conditions vary significantly based on the sizes of their two areas. To address this issue, an average was calculated from the various values, resulting in a final high-pressure value of 175 bar and a medium-pressure value of 85 bar. These are the two values that should ideally be guaranteed in the common rails for all actuators, which is impossible to achieve due to the limitations of the accumulators, which obviously cannot have an

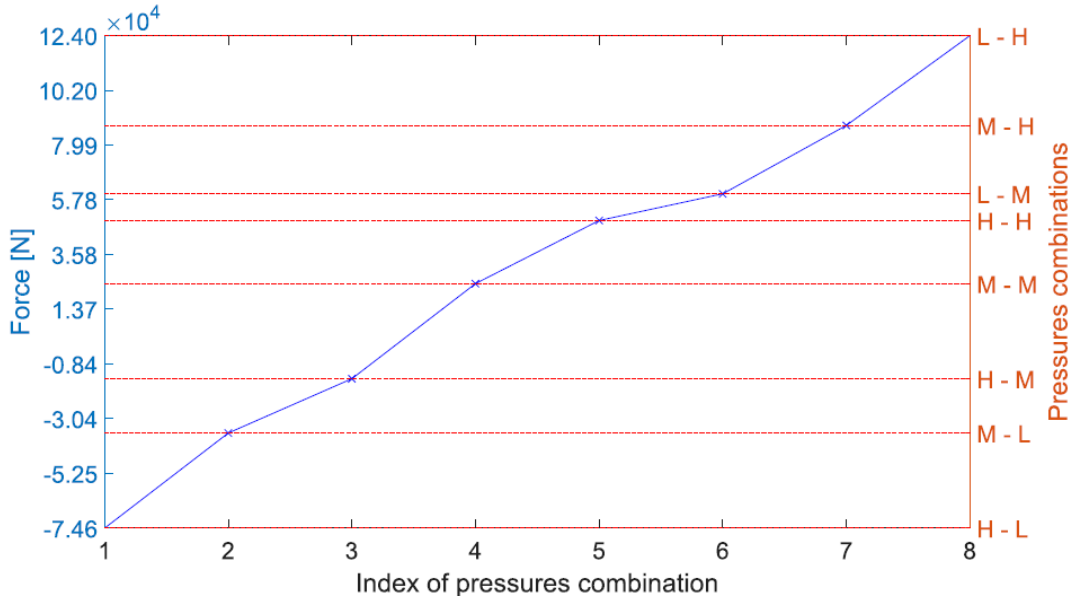

Figure 4.10: Arm Ideal Operating Modes

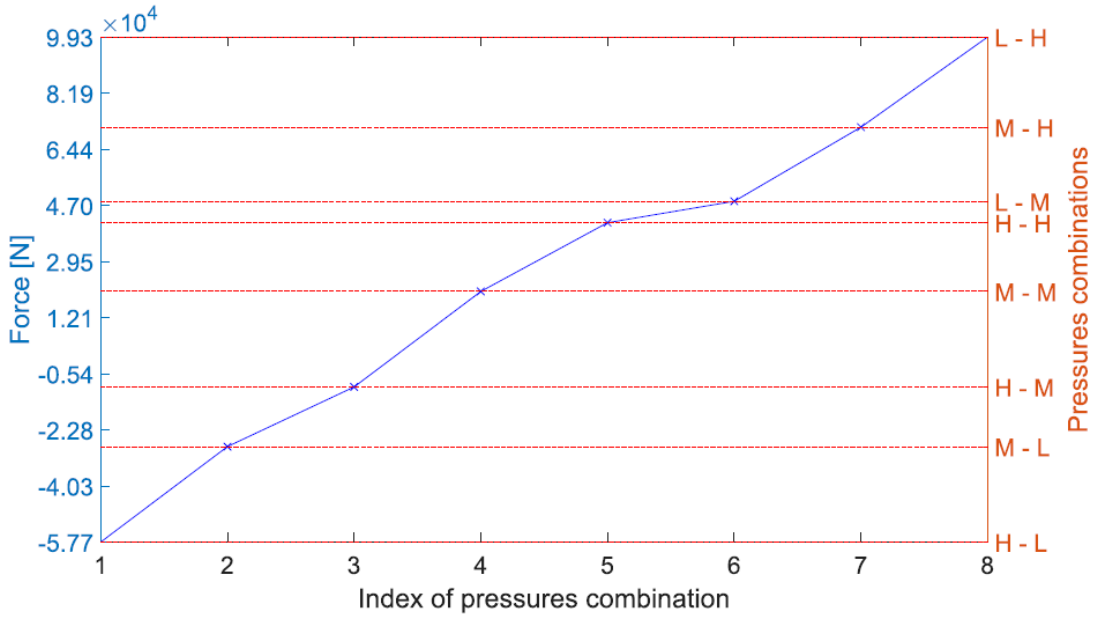

Figure 4.11: Bucket Ideal Operating Modes

infinite volume.

Accumulators Sizing The two pressure values found represent the maximum working pressures (p_2) to be ensured within the accumulators of the high and medium pressure rails, in order to avoid excessive and unnecessary throttling losses. Providing a single value for the accumulator pressure is not entirely accurate, as the pressure continuously fluctuates. When an accumulator begins to release oil, the pressurized bladder expands, leading to a decrease in pressure. The size of the accumulator (V_0) and the pre-charge pressure (p_0) determine the bladder's "stiffness" and how the pressure varies as oil is released. A larger accumulator will result in smaller pressure fluctuations, but if the average flow demand exceeds the flow supplied by the pump, even a larger accumulator will eventually deplete its oil reserves.

The volume of oil entering and exiting the accumulator (ΔV) is dictated by the operating cycle and remains independent of the accumulator's size. However, the sizing of the accumulator determines how its pressure will vary over the course of the duty cycle. The relationship between the exchanged oil volume (ΔV), accumulator size (V_0), pre-charge pressure (p_0), and working pressures (p_2 and p_1) is described in Equation 4.1. The isentropic coefficient k is used to characterize the thermodynamic changes in the system's state.

$$\Delta V = V_0 \left[\left(\frac{p_0}{p_1} \right)^{\frac{1}{\kappa}} - \left(\frac{p_0}{p_2} \right)^{\frac{1}{\kappa}} \right] \tag{4.1}$$

Rearranging the equation results in the relationship 4.2, which outlines a design procedure for determining the required accumulator size and pre-charge pressure. This is applicable in cycles where the maximum oil volume requirement is (ΔV), the maximum pressure is p_2, and the allowable pressure drop is p_1. By employing this approach, it is possible to calculate the appropriate dimensions (V_0) and pre-charge pressure (p_0) needed to meet the system's demands while ensuring that the performance parameters remain within the specified limits throughout the cycle [7].

$$p_0^{\frac{1}{k}} V_0 = \frac{\Delta V}{\left[\left(\frac{1}{p_1} \right)^{\frac{1}{k}} - \left(\frac{1}{p_2} \right)^{\frac{1}{k}} \right]} \tag{4.2}$$

The equation 4.3 indicates that increasing the pre-charge pressure results in a smaller accumulator size. Therefore, it is advisable to select the highest feasible pre-charge pressure, and a common practice is to set p_0 at 0.9 times the minimum working pressure p_1.

In the analyses conducted with the CPR model during the specific dig and dump cycle, as discussed later, the primary objective was to minimize the excavator's fuel consumption as much as possible. The best results were obtained by using pre-charge pressure values that were intermediate between the minimum ($0.9p_1$) and the maximum ($p_2/4$) allowed: p_{0HP} has been set to 90 bar and p_{0MP} to 40 bar.

$$V_0 = \frac{\Delta V}{(p_0)^{\frac{1}{k}} \left[\left(\frac{1}{p_1}\right)^{\frac{1}{k}} - \left(\frac{1}{p_2}\right)^{\frac{1}{k}} \right]} \tag{4.3}$$

To apply the equation 4.3, it's essential to determine the volume of oil that ideally leaves the two accumulators during the work cycle. Starting from an analysis of the total flow reaching all actuators (see Figure 4.12) during the dig and dump cycle of the traditional excavator (see Chapter 3), the approach was to define the average flow rate and then calculate the integral of the area above this average flow (see Figure 4.13). This value represents the net volume of oil exiting the accumulators during a cycle. Since it is not possible, in this case, to differentiate between the contributions of flow at high pressure and medium pressure, the ΔV value obtained was divided in half, with the assumption that half of the oil exits from the high pressure accumulator and the other half from the medium pressure accumulator.

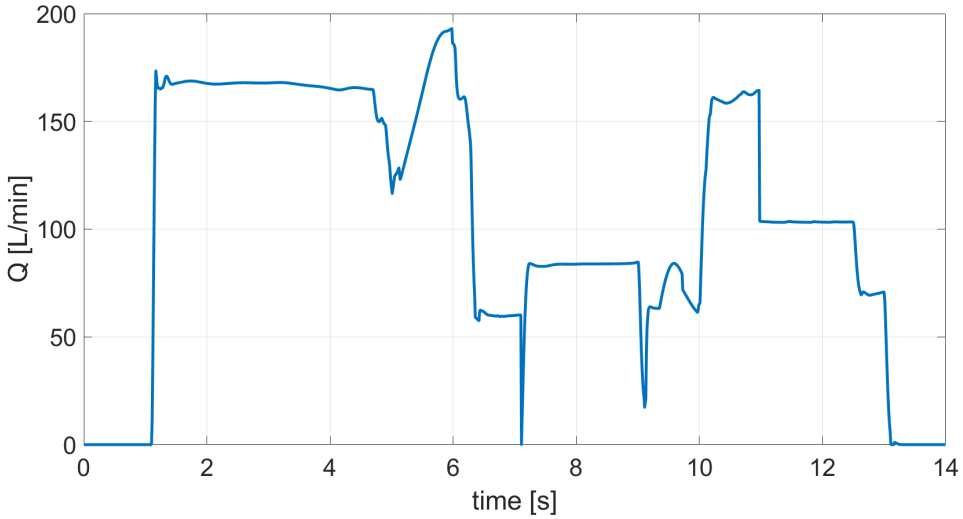

Figure 4.12: Flow Rate Requirements during Dig and Dump for LS Excavator

So, by integrating the positive area between the flow rate curves and the average supply lines (represented in Figure 4.13), the net volume of oil leaving each accumulator can be determined, that is about 3 L each. The allowable pressure fluctuations for MP and HP are set to 25 bar and 35 bar respectively, as shown in equation 4.4 and 4.5.

$$60\,\text{bar} = p_{\text{MP},1} < p_{\text{MP}} < p_{\text{MP},2} = 85\,\text{bar} \tag{4.4}$$

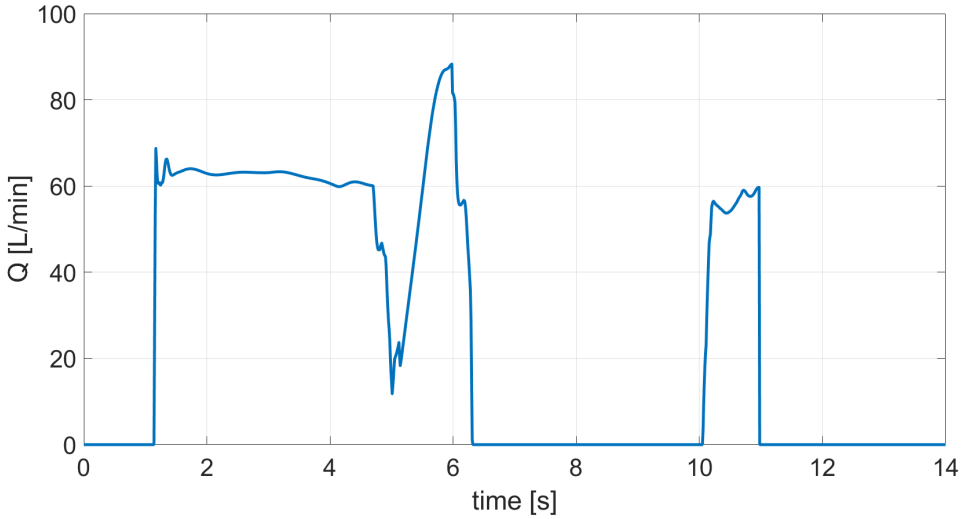

Figure 4.13: Flow Rate over the Average supply line during Dig and Dump for LS Excavator

$$140\,\text{bar} = p_{\text{HP},1} < p_{\text{HP}} < p_{\text{HP},2} = 175\,\text{bar} \tag{4.5}$$

Using Equation 4.3, the required accumulator sizes can be determined:

$$V_{\text{MP},0} = 27.6\,l \tag{4.6}$$

$$V_{\text{HP},0} = 17.4\,l \tag{4.7}$$

Due to the parallel installation implemented in the model, as illustrated in Figure 4.1, there is only one pump available to charge both accumulators. Consequently, during periods when both accumulators are supplying flow to the actuators but only one is being charged, the pressure level in the other accumulator could fluctuate more than desired. This presents a significant drawback of the single-pump system, which can only be mitigated by using larger accumulators. To address this issue, one 30 liter bladder accumulators were installed for each pressure level, resulting in a total capacity of 60 liters. The final values for the sizing of the accumulators can be observed in the tables 4.2 and 4.3.

In terms of pump sizing, it was opted to retain the same displacement as the original variable displacement pump used in the LS architecture, which is 75 cc/rev. This choice facilitates engine downspeeding, allowing for a reduction in the average flow rate supplied while maintaining adequate power system supply. The two accumulators present in the system ensure that the power peaks required by the actuators are adequately met.

Parameter	Value
Max Pressure (p_2)	175 bar
Min Pressure (p_1)	140 bar
Gas Pre-Charge Pressure (p_0)	90 bar
Nominal Volume (V_0)	30 L

Table 4.2: Parameters and Values for HP accumulator

Parameter	Value
Max Pressure (p_2)	85 bar
Min Pressure (p_1)	60 bar
Gas Pre-Charge Pressure (p_0)	40 bar
Nominal Volume (V_0)	30 L

Table 4.3: Parameters and Values for MP accumulator

4.3 FSM for Accumulator Charging Controller

In the accompanying figure 4.14, the detailed composition of the CPR circuit's supply system is illustrated. As previously mentioned, the system is powered by a single pump. To optimize system efficiency and fully utilize the energy stored in the accumulators, a dedicated control logic for the pump displacement was developed. The pump operates exclusively at its maximum displacement, but only when necessary, ensuring that energy is conserved and the pump's operation remains efficient. This approach reduces unnecessary pump activity, enhancing fuel efficiency and ensuring that the pump delivers the required flow when needed.

In the figure 4.14, it can be observed that each accumulator is equipped with two types of sensors: a pressure sensor (*signals X1 and X2*) and a flow sensor (*signal 5 and 6*). The pressure sensor continuously monitors the accumulator's internal pressure, while the flow sensor tracks the amount of oil entering and exiting the accumulator. This dual-sensor setup allows for precise control and monitoring of the accumulators' behavior, ensuring that the system operates within the desired pressure ranges and flow rates. These sensors provide crucial data for the accumulator charging controller to make informed decisions about when to charge or discharge the accumulators, thus optimizing the system's efficiency.

Initially, the accumulator recharge strategy determined when and which accumulator to charge based solely on the signals from the pressure sensors and the previously established minimum pressure limits (see the tables 4.2 and 4.3). The pump was required to remain idle until the lower pressure threshold in the accumulator was reached. Once the pressure inside the accumulator dropped below

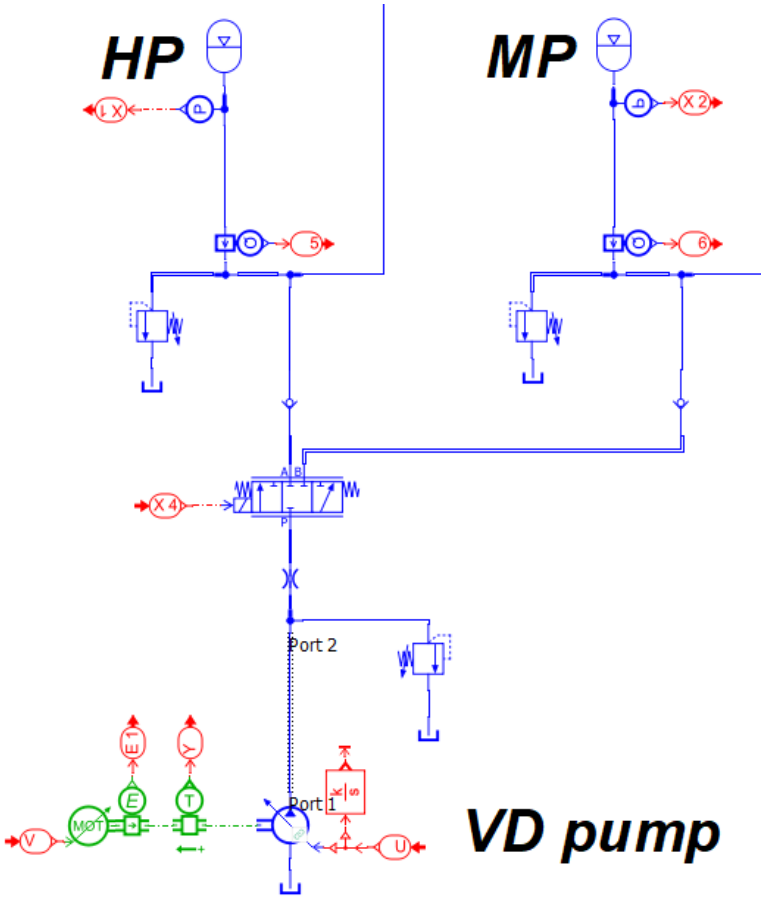

Figure 4.14: Flow Generation Group Detail

this threshold, the pump would activate and begin supplying flow to restore the accumulator's pressure. The pump continued to operate until the maximum pressure limit inside the accumulator was reached, at which point it would stop supplying flow to avoid over-pressurizing the system. This on-off control strategy, driven by pressure thresholds, ensured that the pump only operated when necessary, but it works well only for duty cycles with low average power demands [7].

During cycles like dig and dump, which have high average power demands, the limitations of the threshold-based approach become evident. The main issue is that the pump remains idle for extended periods. While oil is being discharged from the accumulators, the pump only activates once a lower pressure threshold is reached, which may be too late, resulting in the accumulator running dry. Ideally, the pump should engage as soon as flow is required to maintain a consistent pressure level. To address this, it's possible to leverage the current HP and MP flow demands, as calculated by the actuator power management controller [18], to initiate charging

before the lower threshold is reached.

In this specific case, the speed inputs, which directly correlate with the flow rate demands for the actuators, are predetermined and can therefore be integrated as inputs into the pump control system. By utilizing these known speed inputs, the pump control system can anticipate the required flow rates and adjust its operation more efficiently. This predictive control approach allows the system to maintain the required pressure levels in the accumulators, reducing the need for reactive adjustments and minimizing energy losses caused by unnecessary pump operation or delays in meeting flow demands.

To implement this control strategy, the AMESim State Chart tool was utilized, which facilitates the development of finite state machines (FSMs). The FSM approach allows for a structured method to manage different operating states of the pump based on the flow rate demands and accumulator pressure levels.

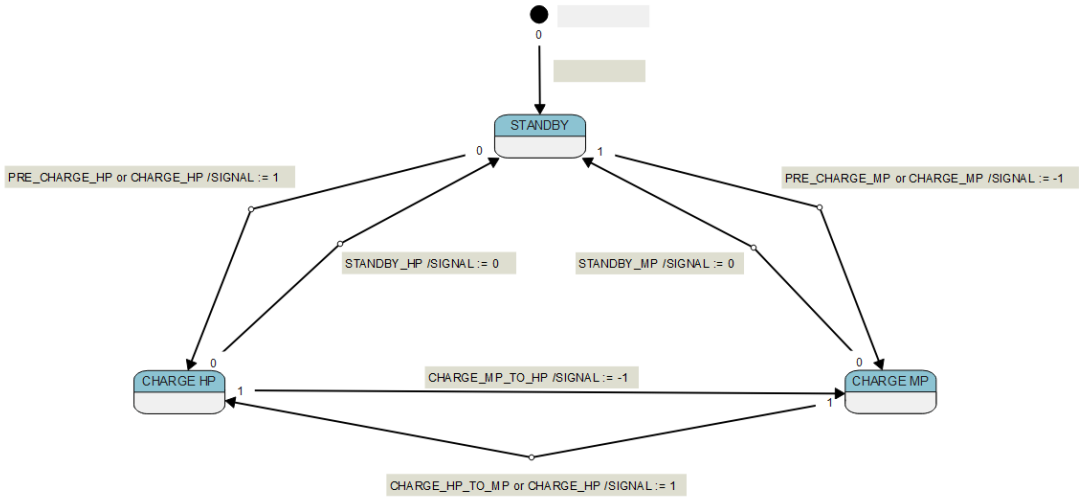

Figure 4.15: Finite State Machine for Accumulator Charging Control

In the general schematic (as shown in the figure 4.15), different states are defined according to specific conditions, such as:

- **Standby** : The pump remains idle when accumulator pressures are above the lower threshold, and no immediate flow demand exists.
- **Pump Charging HP Accumulator**: when the pressure in the HP accumulator drops below its lower threshold, the pump transitions to this state and begins charging the HP accumulator.
- **Pump Charging MP Accumulator**: if the MP accumulator's pressure falls below its threshold, the pump will prioritize charging the MP accumulator

unless the HP accumulator also needs charging.

It's very important to underline that high pressure takes precedence over medium pressure, meaning that the HP pressure level must remain above its lower threshold before the MP accumulator can be charged. Preventing the complete discharge of the high pressure rail is vital for the overall performance and reliability of hydraulic systems, allowing adequate system operation in the case of high external loads.

Before describing in detail the events that trigger the transitions between the different states of the FSM, it is important to outline the inputs and outputs of the control block, as shown in the figures 4.16 and 4.17. As previously mentioned, the MP and HP values are derived from pressure sensors installed on the accumulators (signals X1 and X2 in figure 3.13), while the flow values Q_{MP} and Q_{HP} originate from flow sensors (signals 5 and 6 in figure 3.13). The SPEED input receives signals representing actuator speeds, which convert into flow rate values necessary to trigger a state change when the user's demand surpasses a specific threshold, thereby anticipating the discharge of the accumulator. Input TIME gathers data on the cycle duration and is utilized solely in the initial phase to enter the FSM, initiating the transition to the initial standby state. The INT input indicates the permissible fluctuation range established by the control system, aimed at maintaining pressure close to its maximum value and for this reason has been set to 1 bar.

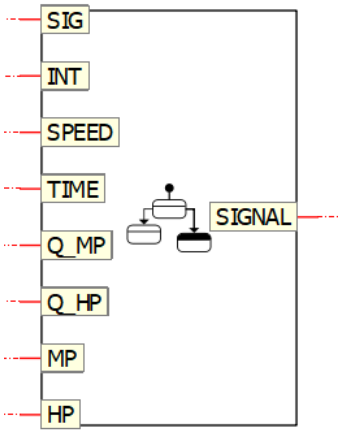

Figure 4.16: FSM Control Block

Input variables	
HP	Real
MP	Real
Q_HP	Real
Q_MP	Real
TIME	Real
SPEED	Real
INT	Real
SIG	Real

Figure 4.17: FSM Control Input

The output signal is sent to both the distribution valve (shown in figure 4.18) and the pump, and it takes on the following signals:

- Signal equals to -1 when the charge request comes from the MP accumulator.
- Signal equals to 0 when the pressure levels are inside the allowed ranges.

- Signal equals to 1 when the charge request comes from the HP accumulator.

It is crucial to emphasize that the absolute value of this signal is sent to the pump, indicating that the displacement can either be 0 (idle state) or 1 (fully open). In addition, the valve shown in the figure 4.18 was created using the AMESim Valve Builder tool, with its characteristic values set to a nominal flow rate of 200 L/min and a nominal pressure drop of 2 bar.

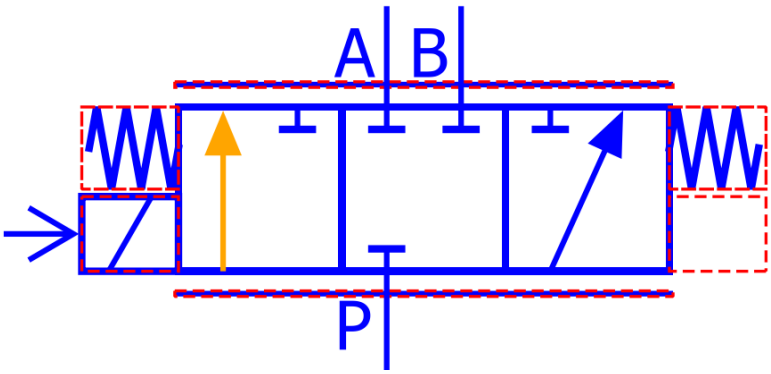

Figure 4.18: Charging Distribution Valve from AMESim Valve Builder

Events	
PRE_CHARGE_HP	TIME>0 and SPEED <= 0 and HP <= HP_MIN
CHARGE_HP	Q_HP>10 and HP < HP_MAX-2*INT and MP > MP_MIN
PRE_CHARGE_MP	TIME>0 and SPEED<=0 and MP <=MP_MIN and HP > HP_MIN and SIG <= 0.5
CHARGE_MP	Q_MP>10 and MP < MP_MAX-2*INT and HP >= HP_MAX-2*INT and SIG <= 0.5
STANDBY_HP	HP >= HP_MAX
STANDBY_MP	MP >= MP_MAX
CHARGE_HP_TO_MP	HP <= HP_MIN
CHARGE_MP_TO_HP	MP <=MP_MIN and HP > HP_MIN

Figure 4.19: FSM Charging Control Triggering Events

Each of the events shown in figure 4.19 plays a vital role in managing the charging and operation of the hydraulic system, ensuring that the accumulators maintain the necessary pressure levels for efficient actuator performance while avoiding conditions that could lead to system failures. The events are designed to respond dynamically to changes in pressure, flow demands, and actuator speed, facilitating efficient energy usage and reliable operation, and are described as flows:

- **PRE CHARGE HP:** This event occurs when the excavator is stationary and prior to the start of the work cycle, with the initial pressure value of

the accumulator falling below the minimum allowable level. This condition enables the restoration of the maximum pressure before the actual duty cycle begins.

- **CHARGE HP:** This event initiates the charging of the HP accumulator when there is a significant demand for high pressure (flow rate exceeds 10), the HP accumulator is below a specific maximum threshold interval, and the medium pressure is above its minimum level. This ensures that while charging the HP accumulator, the system maintains adequate medium pressure supply.

- **PRE CHARGE MP:** This event is similar to that of the HP accumulator but does not take precedence over it.

- **CHARGE MP:** This event triggers the charging of MP accumulator when there's a significant demand for medium pressure, the medium pressure is below its maximum threshold, HP accumulator is at or above its maximum threshold (ensuring safety). This ensures efficient charging while maintaining system stability.

- **STANDBY HP:** This event indicates that HP accumulator has reached or exceeded its maximum pressure threshold. The system will switch to standby mode, preventing any further charging of the HP accumulator to avoid over pressure conditions.

- **STANDBY MP:** Similar to STANDBY HP, this event is triggered when the medium-pressure accumulator reaches or exceeds its maximum pressure threshold, prompting the system to go into standby mode for the medium-pressure accumulator.

- **CHARGE HP TO MP:** This event indicates a transition state where the system can switch from charging the MP accumulator to focusing on the HP accumulator. It occurs when the HP accumulator drops to its minimum threshold, indicating the need for additional charging to prevent system operation issues.

- **CHARGE MP TO HP:** This event allows for the transition from charging the HP accumulator to focusing on the MP accumulator when the MP is at its minimum threshold, and the HP accumulator is above its minimum. This ensures that both accumulators can be managed effectively based on their pressure levels.

4.4 Single CPR analysis during Dig and Dump Cycle

The simulation of the Dig and Dump operational cycle (1.3) began with both accumulators at their ideal pressures: 175 bar for the high-pressure accumulator and 85 bar for the medium-pressure accumulator. Figures from 4.20 to 4.22 illustrate the pressure trends within the accumulators and the signal from the FSM recharge control. In the first five seconds, the actuators only require medium pressure, which means the accumulator alone cannot meet the total flow demand. Consequently, the pump activates to recharge the medium pressure. Once the system requires high pressure, HP accumulator takes priority in the recharge control and is supplied by the pump. The first pressure peak in the MP accumulator results from the flow recovery enabled by the HP/MP pressure combinations in the actuators.

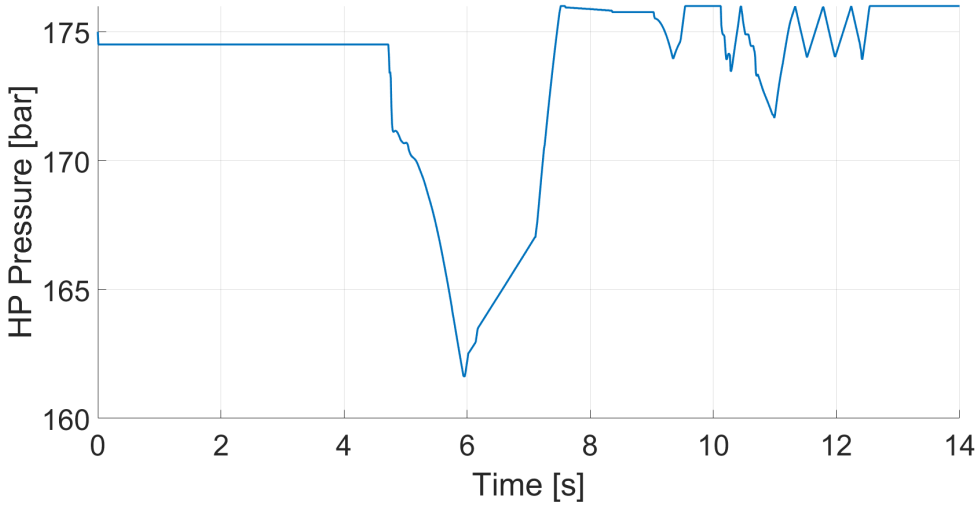

Figure 4.20: Pressure oscillations during Dig and Dump cycle - HP Accumulator

The actual energy regeneration utilizing the external load occurs in two distinct phases: first, between 7 and 8 seconds, when kinetic energy recovery from the turret allows for the recharging of the HP accumulator and second, in the final phase of the cycle, when MP accumulator is recharged through the potential energy generated by the lowering of the boom. In the figure 4.23, it is possible to see the return flow, between 6 and 8 seconds, towards the high-pressure accumulator, thanks to the exploitation of the turret's inertia. This allows the actuator controller to select the MP/HP pressure combination, generating a higher pressure flow compared to the initial flow leaving the medium-pressure accumulator. In the thesis [18], more detailed information can be found regarding the functioning of the swing control

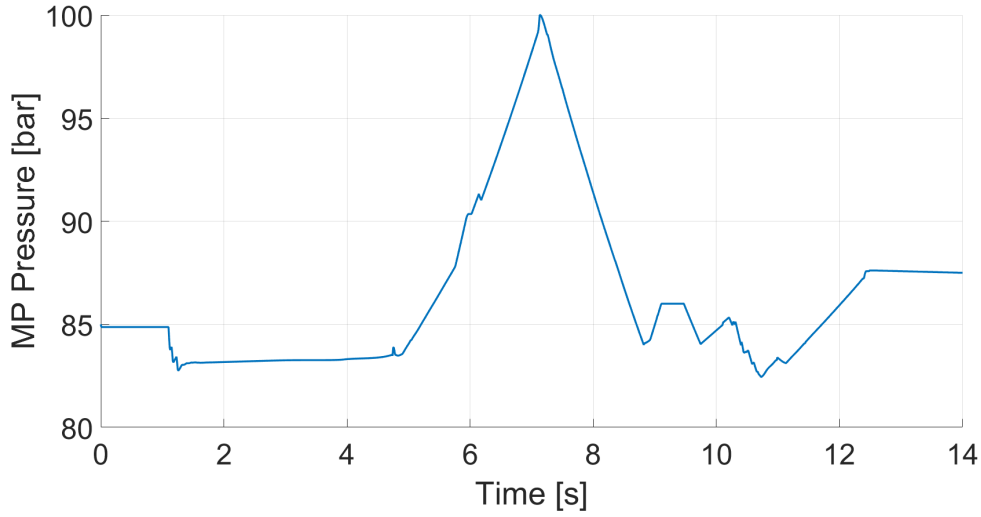

Figure 4.21: Pressure oscillations during Dig and Dump cycle - MP Accumulator

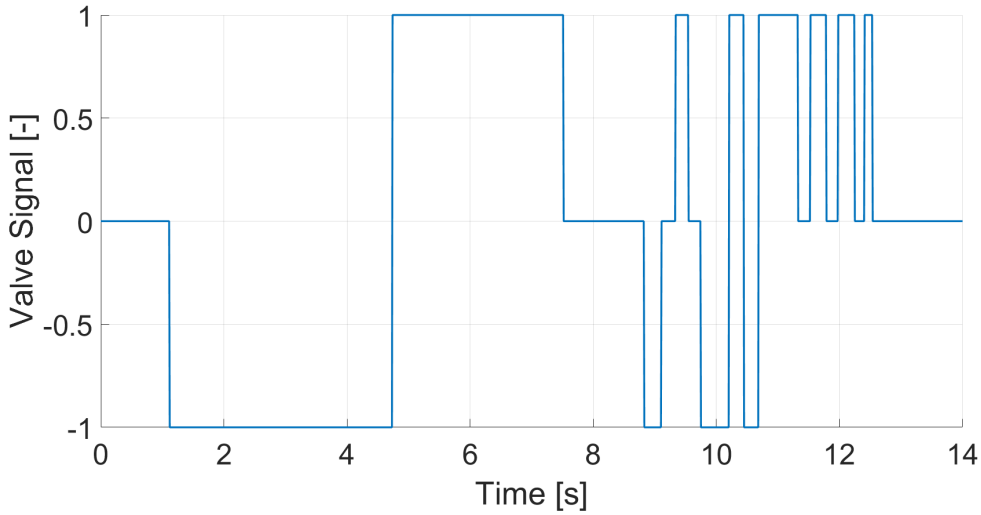

Figure 4.22: Charging Distribution Valve Signal during Dig and Dump cycle

system.

The flow rate of the pump (see 4.24) is, of course, proportional to the angular velocity of the engine (see 4.25), which follows the equation 4.8. This formula allows the model to adjust the engine speed dynamically as the torque demand changes, ensuring a more accurate simulation of the engine's performance. It mirrors real engine behavior where, for instance, during periods of higher load (HP), the engine speed would decrease proportionally to the increased torque demand. Conversely,

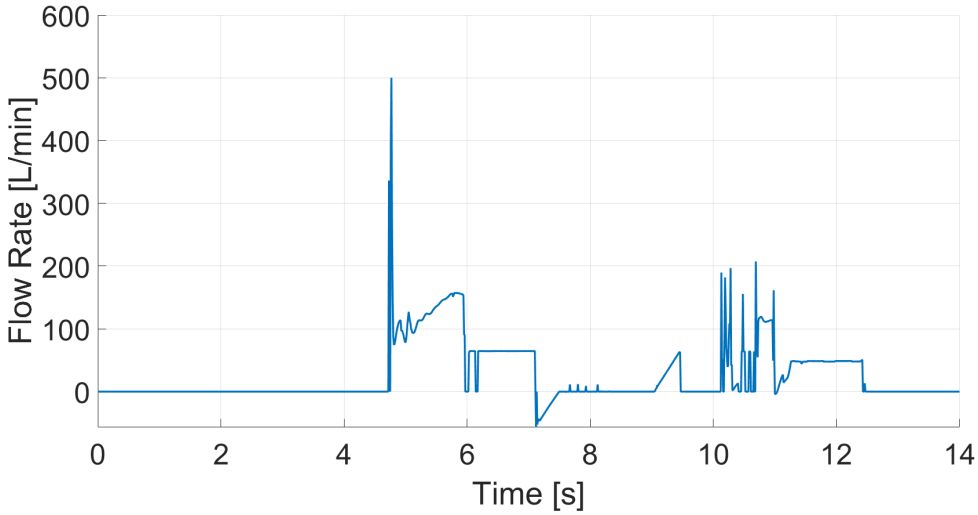

Figure 4.23: Flow Rate Regeneration to MP from HP Accumulator

during lighter load conditions (MP), the engine would operate at higher speeds. By implementing this equation, the model captures the non-linear relationship between torque and speed, providing a more realistic and functional representation of the engine's operation in a wide range of load scenarios.

$$\omega = \omega_0 + \left(\frac{\omega_1 - \omega_0}{\mathrm{T}_1}\right) \cdot \mathrm{T} \tag{4.8}$$

To clarify the relationship 4.8 between engine speed and load torque, here's a breakdown of the terms involved in the formula:

- w_0 represents the shaft speed at zero load torque. In other words, this is the engine's maximum speed when there is no torque applied (i.e., no load).
- w_1 stands for the shaft speed at a specific load torque, denoted as Torque1. It reflects the engine speed when a particular load (or torque) is applied, serving as a reference point in the model.
- w is the actual shaft speed being computed by the model at a given moment, when a certain torque (denoted simply as Torque in 4.8) is applied.

By using accumulators in the hydraulic system, it was observed that running the engine at maximum speed was not necessary to meet the required flow rate. Instead, the system was able to provide the necessary power and flow at a lower engine speed, that is 1200 rpm. This downspeeding, combined with the reduction in the average power supplied by the engine (see figure 4.26) and the lowering of

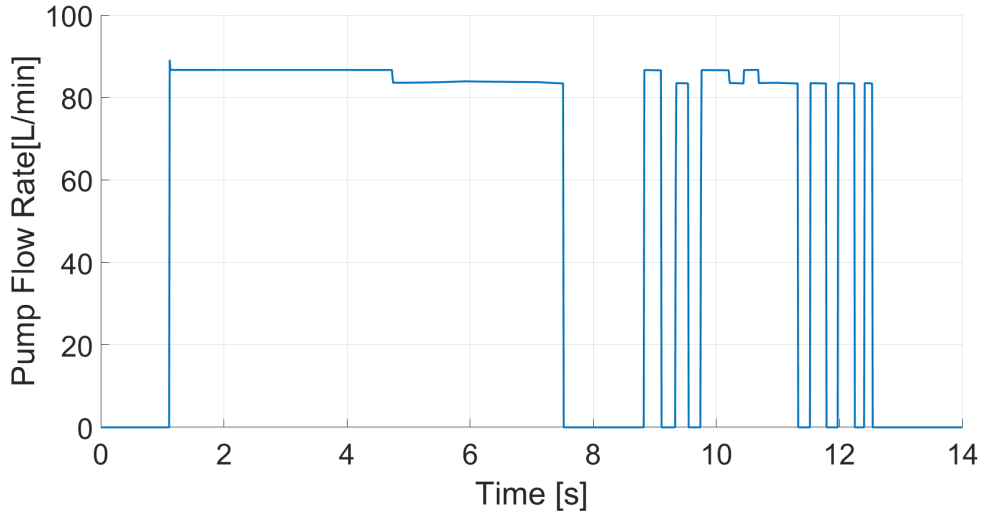

Figure 4.24: Single CPR Pump Flow Rate during Dig and Dump

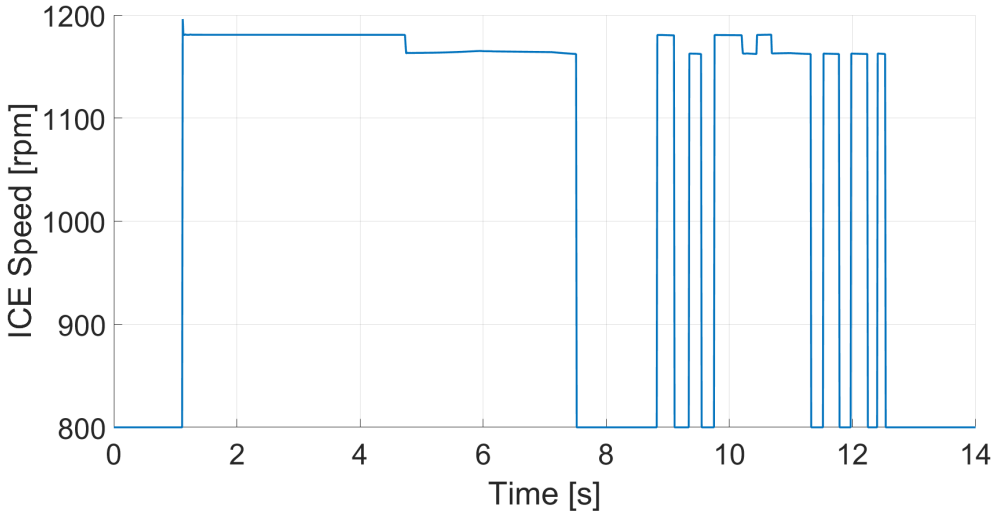

Figure 4.25: Single CPR ICE Speed during Dig and Dump

engine speed at 800 rpm, when the pump is in an idle state (i.e., not supplying the system), allows the ICE to operate in more efficient regions of its performance map (see figure 4.27), which in turn helped to reduce fuel consumption.

An important final consideration regarding the accumulator recharge strategy is to observe how the pressure trends within the accumulators change when multiple cycles are performed consecutively. In the Figures 4.28 and 4.29 are illustrated the pressure trends after four Dig and Dump cycles, clearly indicating that the

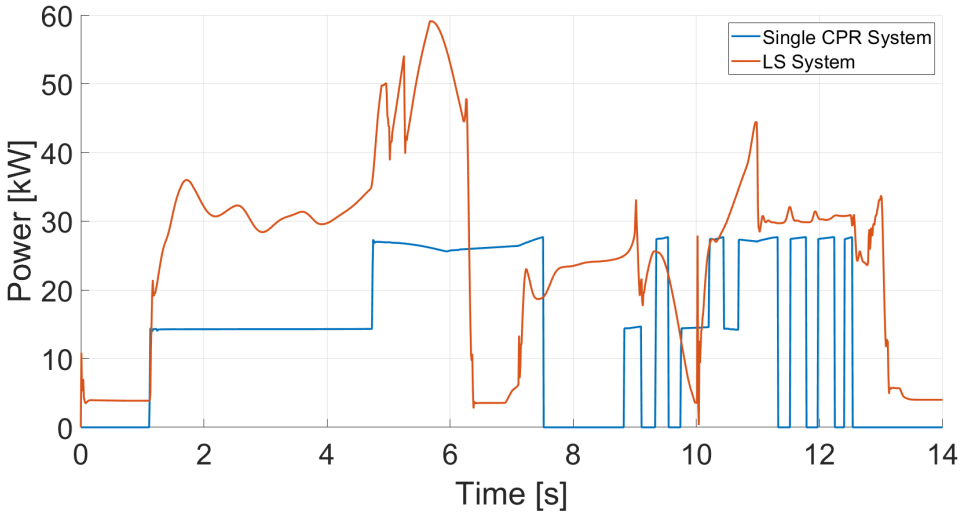

Figure 4.26: Single CPR vs LS System, ICE Power during Dig and Dump

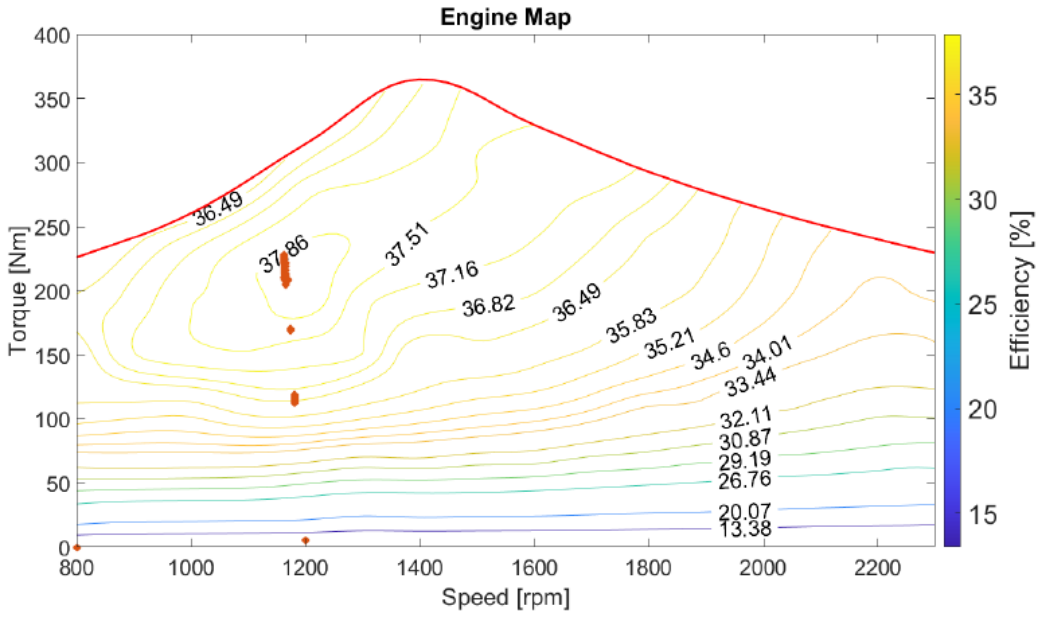

Figure 4.27: Single CPR ICE Map during Dig and Dump

pump's supply begins later from the second cycle onward compared to the first cycle. Notably, if the accumulators' contribution at the end of each cycle exceeds the initial value, it helps conserve energy in the subsequent cycle.

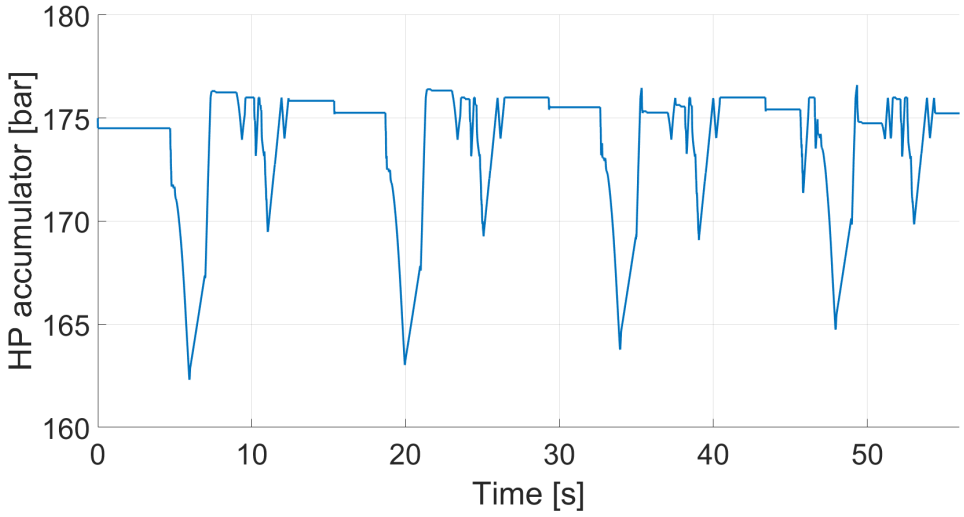

Figure 4.28: Pressure oscillations during 4 Dig and Dump cycles - HP Accumulator

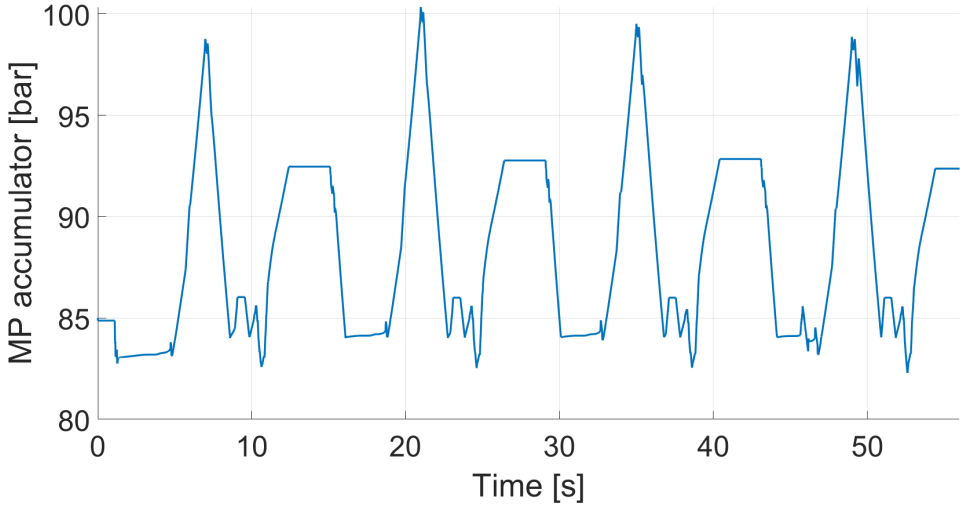

Figure 4.29: Pressure oscillations during 4 Dig and Dump cycles - MP Accumulator

4.5 Single CPR analysis during Air Grading Cycle

The air grading cycle, as mentioned earlier (see Chapter 1.3), requires lower loads compared to the Dig and Dump cycle, but it demands higher actuator speeds in certain moments. In the following figures 4.30 and 4.31, which illustrate the pressure

fluctuations within the accumulators during the leveling cycle, the intervention of the FSM recharge control is clearly evident, as the oscillation around the two ideal pressure values for both accumulators is prominently visible. As noted, the external loads are relatively low; indeed, the charge distributor signals (see figure 4.32) show that the pump primarily supplies the MP accumulator.

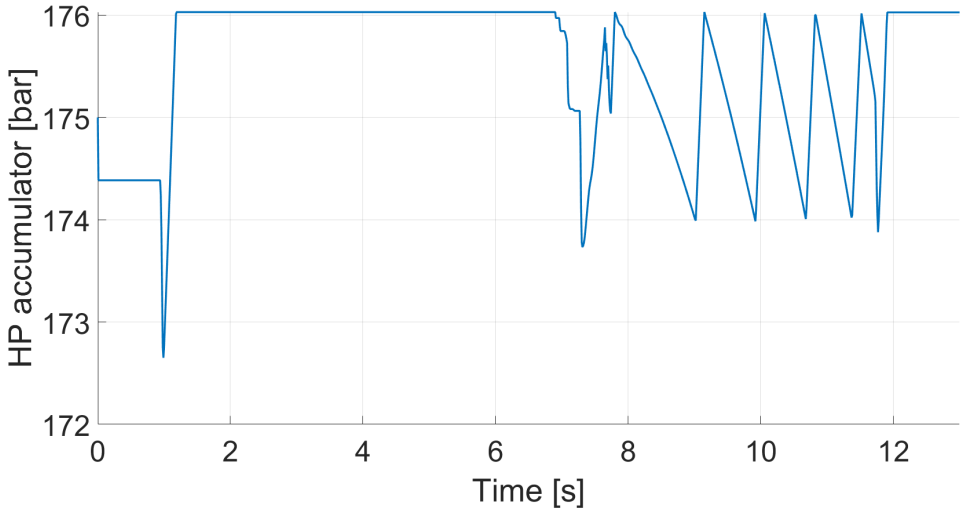

Figure 4.30: Pressure oscillations during Air Grading cycle - HP Accumulator

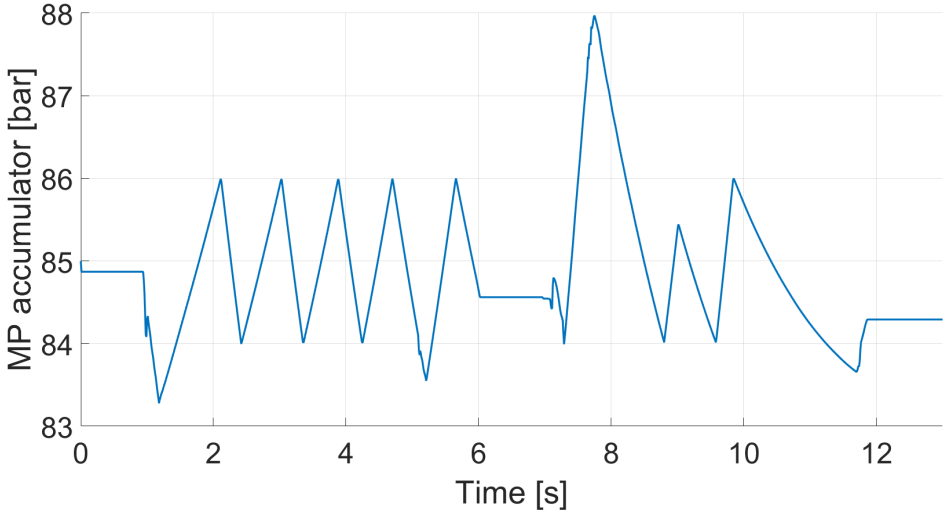

Figure 4.31: Pressure oscillations during Air Grading cycle - MP Accumulator

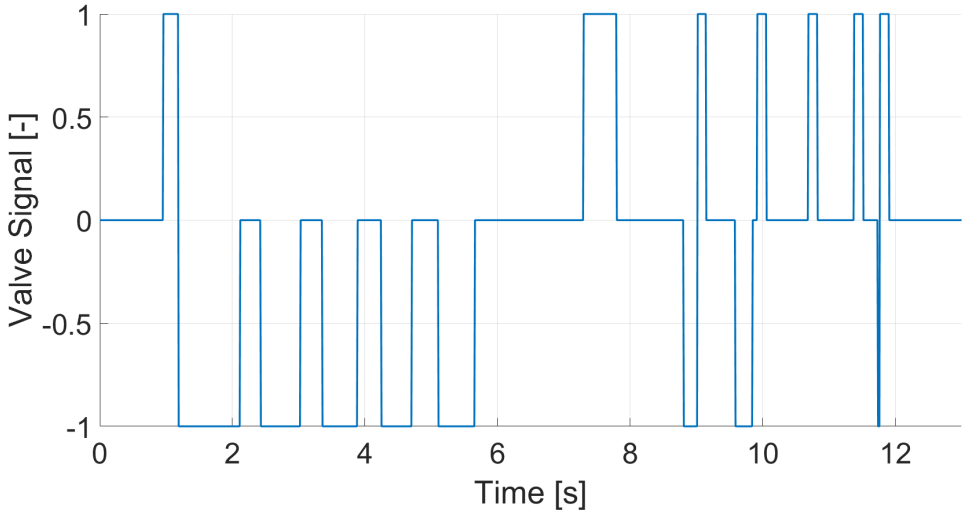

Figure 4.32: Charging Valve Switching Signal, Air Grading Cycle

Chapter 5

Double CPR Architectures: Concept, Development and Analysis of the Hydraulic Model

The CPR configuration powered by a single pump is derived from the study and prototype called STEAM [7]. This architecture, classified as a single CPR, demonstrates significant improvements in hydraulic efficiency and fuel consumption, as analyzed in thesis [17]. However, for excavators larger than the machine studied in this project (see Chapter 3), relying solely on a single pump, even one with a larger displacement, and utilizing only two accumulators may not be sufficient. For example, the STEAM prototype vehicle, which has a declared weight of 16 tons, employs a high displacement pump with a maximum flow rate of 400 L/min and is equipped with four 32 liter accumulators (see [7]).

A patent proposal by CNHi presents a new type of potential architecture based on a common pressure rail, where the power supply system is duplicated to feed two actuators each.

Initially, the idea was to pair actuators operating at different pressures, with the aim of sizing the accumulators to maximize energy recovery through the kinetic energy of the turret during braking and the potential energy of the boom during arm descent. However, this approach proves less effective when applied to a non-specific cycle, as sizing would need to be tailored to predetermined velocity inputs.

Consequently, the final strategy was to couple actuators operating at similar pressures. In this specific case, this involves pairing the boom with the swing and the arm with the bucket. This configuration allows for the utilization of four

accumulators operating at four different pressure levels, with the boom/swing pair handling significantly higher loads compared to the arm/bucket pair. Theoretically, this arrangement should further enhance the overall efficiency of the system by selecting pressure values that closely match external loads, thereby minimizing throttling losses even more than in the single CPR configuration.

5.1 Machine Layout

The figure displays the complete layout of the double CPR architecture. The two separate supply systems, powered by the same motor used in the single CPR configuration and the Load Sensing (LS) architecture, are clearly distinguishable. The components utilized, such as the valve block, actuators, tubes, and various throttles, are identical to those studied in the previous chapters.

The primary difference lies in the supply system, which is divided to allow for more precise sizing of the components, ultimately enhancing the overall efficiency of the system. This separation facilitates better optimization of pressure levels and flow rates for the paired actuators, thereby reducing throttling losses and improving energy recovery. By employing four accumulators operating at different pressure levels for the two actuator pairs, this architecture aims to achieve superior performance compared to the single CPR configuration.

5.2 Flow Generation Groups

In sizing the two different supply systems, significant attention was paid to the following limits:

- The volume of the accumulators in the double configuration cannot exceed the total volume of those used in the single CPR model. Given the machine's space limitations and the fact that double the number of accumulators is employed, it is essential to consider this constraint to conduct simulations that closely reflect real-world conditions.
- The high pressure lines of both power supply systems must have values such that, in the event that the engine needs to supply both pumps, the required torque does not exceed the maximum allowed based on a speed of 1200 rpm.
- The control logic used to recharge the two supply systems remains consistent with what was described in the previous chapter 4.
- Two identical variable displacement pumps, each with a capacity of 40 cc/rev, were used to ensure an adequate average flow rate for both pairs of actuators.

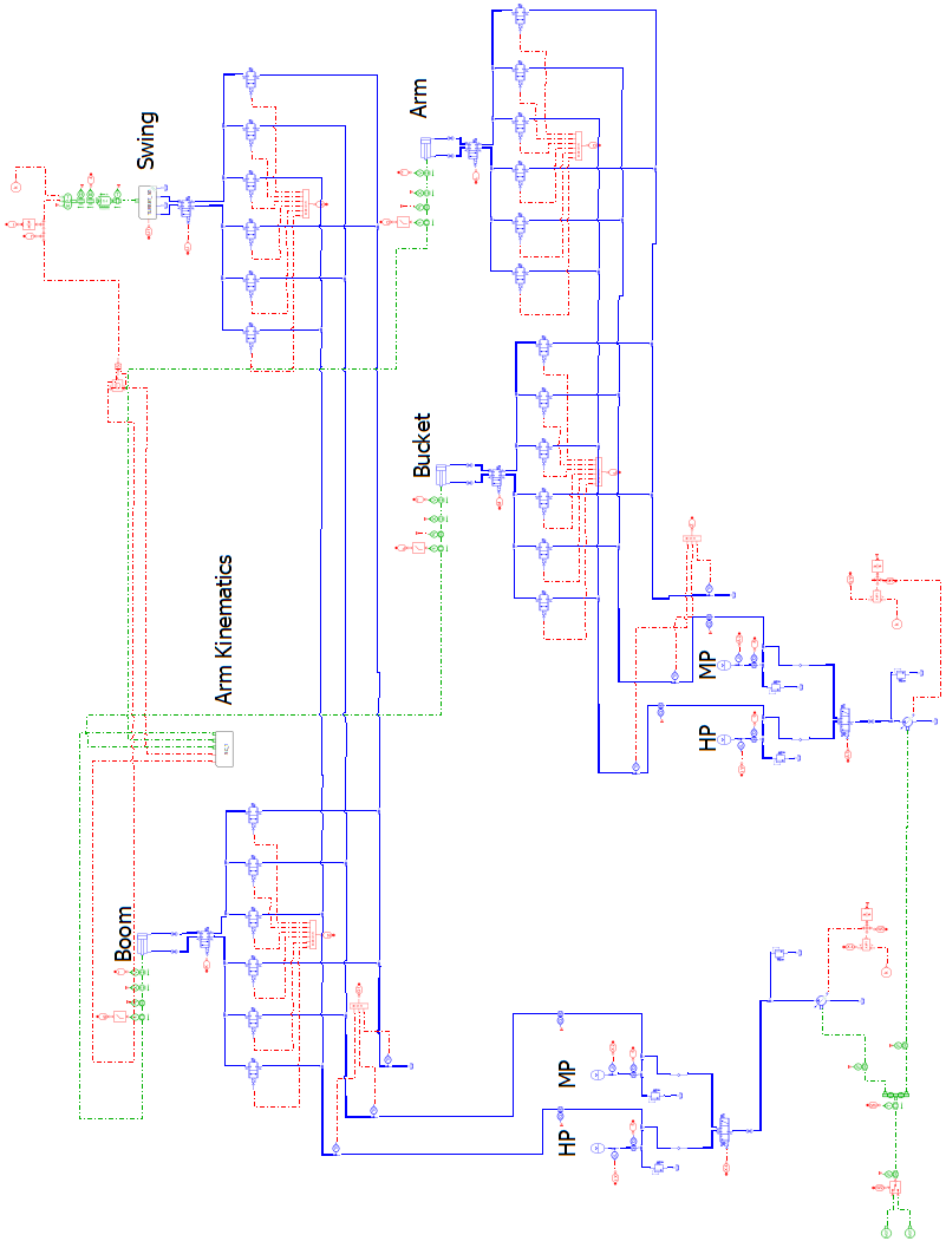

Figure 5.1: Double CPR Layout

5.2.1 Boom+Swing Power Supply System Sizing

In the previous chapter, the dimensioning and determination of the ideal pressure for the accumulators focused only on the three linear actuators boom, arm and

HP Parameter	Value
Max Pressure (p_2)	170 bar
Min Pressure (p_1)	130 bar
Pre-Charge pressure (p_0)	117 bar
Nominal Volume (V_0)	15 l

MP Parameter	Value
Max Pressure (p_2)	100 bar
Min Pressure (p_1)	80 bar
Pre-Charge pressure (p_0)	70 bar
Nominal Volume (V_0)	15 l

Table 5.1: DCPR: Boom/Swing Accumulators Sizing Values

HP Parameter	Value
Max Pressure (p_2)	78 bar
Min Pressure (p_1)	60 bar
Pre-Charge pressure (p_0)	50 bar
Nominal Volume (V_0)	15 l

MP Parameter	Value
Max Pressure (p_2)	15 bar
Min Pressure (p_1)	10 bar
Pre-Charge pressure (p_0)	9 bar
Nominal Volume (V_0)	15 l

Table 5.2: DCPR: Arm/Bucket Accumulators Sizing Values

bucket. After confirming the proper functioning of the single CPR system within the established duty cycles, no further adjustments were made to account for the hydraulic swing motor, as the system was deemed highly efficient. However, in the double CPR system, it becomes essential to also analyze the behavior of the swing motor. Identifying the correct starting pressure values for the accumulators is crucial, as this can facilitate energy recovery by harnessing the system's inertia.

Focusing on the swing motor, in particular, allows for better exploitation of kinetic energy during deceleration, which can be stored and reused later. By carefully selecting the high and medium pressures for the two CPR rails, overall system efficiency can be further enhanced by reducing throttling losses and optimizing energy recovery. In the double CPR configuration, the swing motor plays a pivotal role, as its energy demand and recovery potential must align closely with the selected accumulator pressures.

Before delving into the details of the dimensioning, it is important to briefly explain the physics behind the operation of a hydraulic motor, or more accurately a hydrostatic machine. For an ideal motor, the governing relationships are as follows 5.1. The torque generated at the shaft T_{th} is directly proportional to the motor displacement V and the pressure drop across the two ports Δp. The rotational speed w of the shaft, on the other hand, is directly proportional to the theoretical flow rate Q_{th} passing through the motor and inversely proportional to the displacement.

$$\begin{cases} T_{th} = V \cdot \delta p \\ Q_{th} = V \cdot \omega \end{cases} \tag{5.1}$$

Since the hydraulic motor operates in all four quadrants of the load pressure/flow rate plane during tests (see Figure 5.2), it is more accurately referred to as a hydrostatic machine. The lines passing through Quadrants I and III correspond to active power supply to the hydrostatic machine, indicating that net positive power is being generated and the machine behaves as a hydraulic motor. Conversely, lines passing through Quadrants II and IV allow for kinetic energy recovery. In this configuration, the machine generates net negative power and behaves as a hydraulic pump (see Table 5.3), and it is precisely these quadrants that must be optimally utilized when pairing the boom and swing. So, the generated pressurized fluid can be fed back into the system, contributing to energy conservation and efficient operation by storing excess energy in accumulators when available.

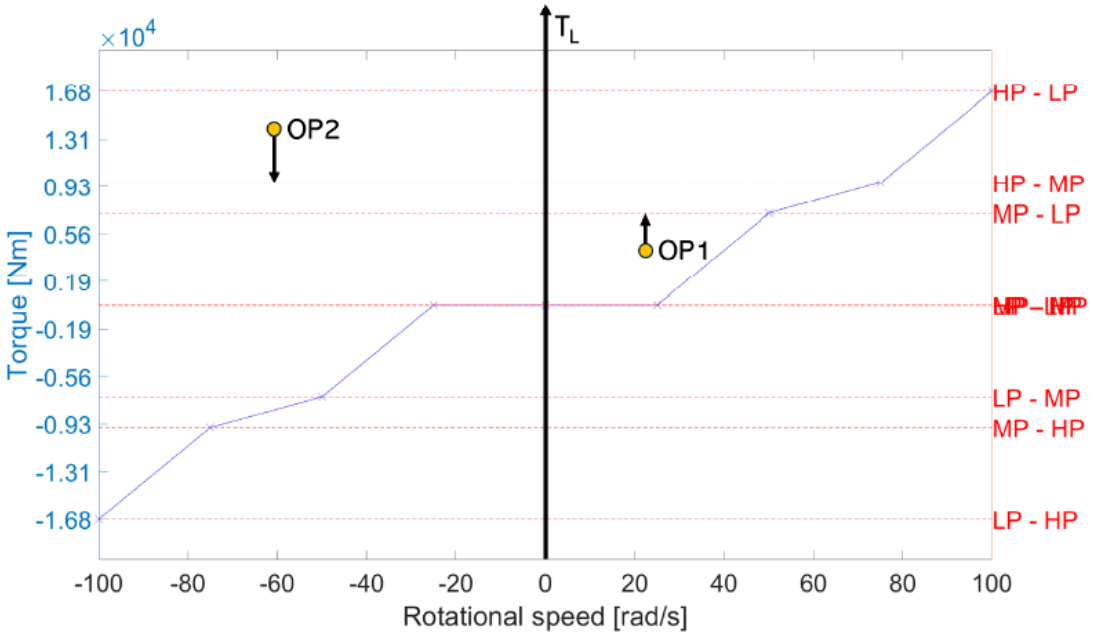

Figure 5.2: Operative Modes Ideal Swing

Inputs	$\omega > 0$	$\omega < 0$
$\delta p > 0$	Pumping mode	Motoring mode
$\delta p < 0$	Motoring mode	Pumping mode

Table 5.3: Modes based on inputs and rotational direction

To maximize the efficiency of operating points within the quadrants where energy regeneration can occur, the objective is to maintain the medium pressure as high as possible. This approach, combined with the turret's inertia, can generate

an energy surplus that facilitates the recharging of the high pressure accumulator. The ideal values identified are presented in the table 5.1 and demonstrate a suitable choice for the boom's operating modes, which ideally remain sufficiently distinct from one another, as illustrated in the figure 5.3.

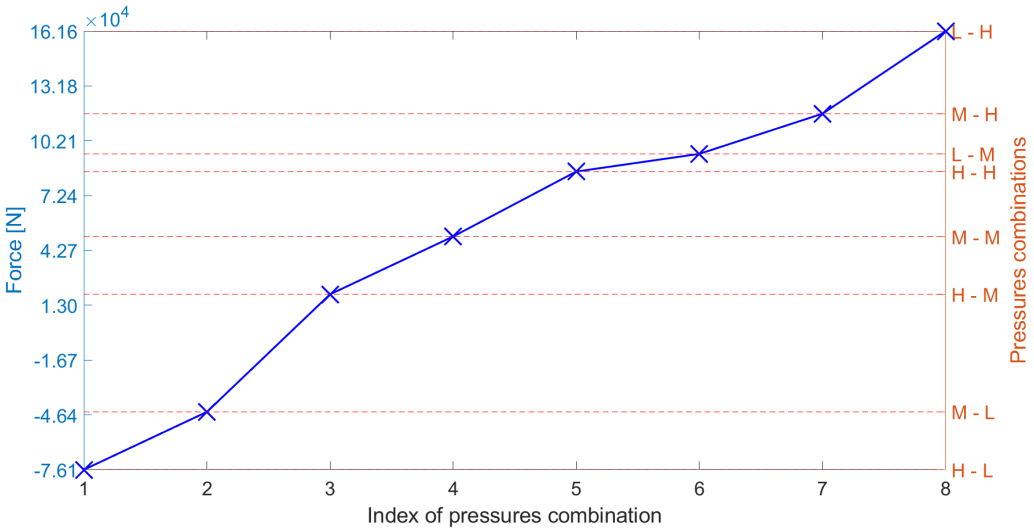

Figure 5.3: Ideal Operating Modes of Boom in DCPR architecture

As mentioned in the previous chapter, these operating modes are considered ideal and cannot be fully realized in practice due to inevitable pressure losses. However, they serve as reference points for the accumulator recharging control system, which, even in the double configuration, employs the same logic discussed earlier.

In the following figure 5.4, we can observe two instances of flow regeneration that facilitate energy recovery through kinetic energy during the turret's deceleration phase. This process enables high pressure to be supplied using medium pressure in conjunction with external inertia. For further clarification on the control strategies of the actuators and the hydraulic motor, it is recommended to consult the thesis [18].

5.2.2 Arm+Bucket Power Supply System Sizing

Regarding the second pair of combined actuators, specifically the arm and bucket, the parameters chosen for sizing the accumulators are presented in the table 5.4. The logic used is consistent with that explained in the previous chapter, where the aim was to identify lower pressure values that align with the external loads from the Dig and Dump cycle, specifically values ranging between 10 and 80 bar. Simultaneously, using the algorithm provided in the appendix 6.3, ideal operating

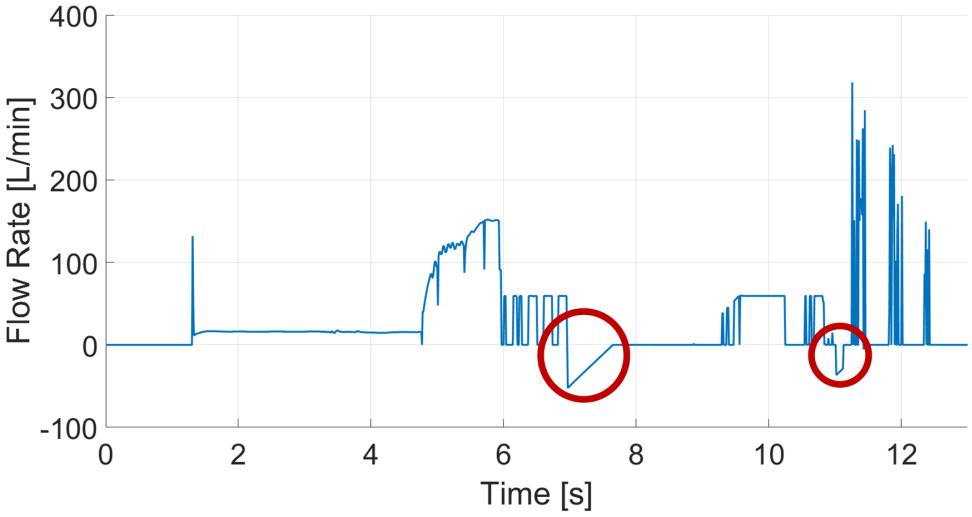

Figure 5.4: Flow Rate Regeneration to HP accumulator Boom/Swing

modes were identified to yield eight values that are as equidistant from one another as possible.

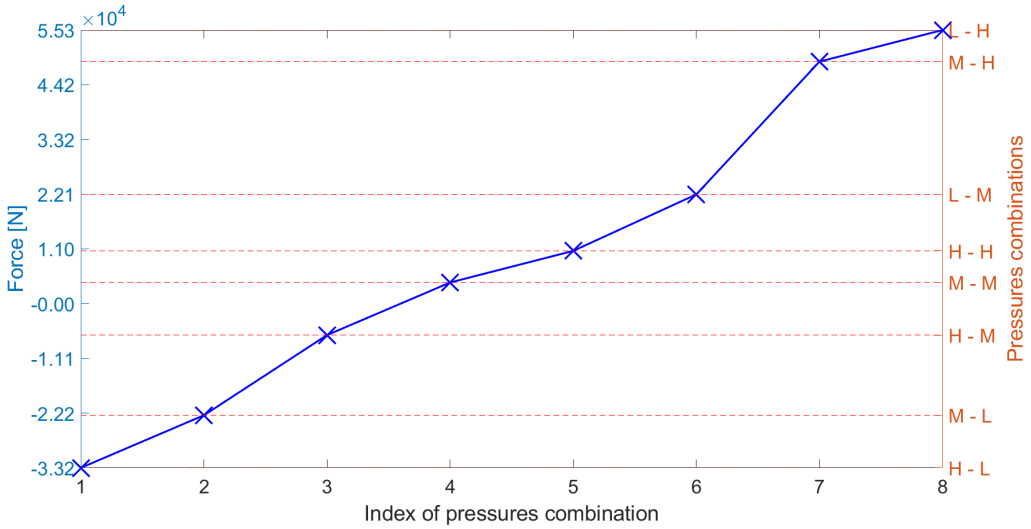

Figure 5.5: Ideal Operating Modes of Arm in DCPR architecture

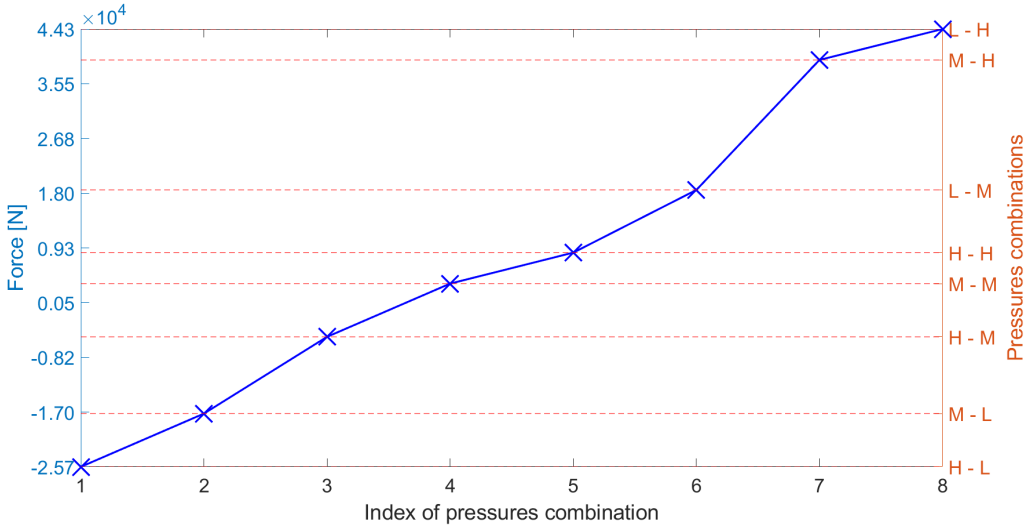

Figure 5.6: Ideal Operating Modes of Bucket in DCPR architecture

5.3 Single and Double CPR Analysis Comparison for Dig and Dump

It is crucial to compare the two architectures based on the common pressure rail to determine whether the dual configuration can serve as a viable alternative to the single architecture. As discussed in the previous chapters, the single architecture has already been studied and developed in prototype form [7], demonstrating significant benefits in terms of efficiency and fuel consumption. The most comprehensive working cycle represented by Dig and Dump will be taken as a reference for analyzing both models.

A preliminary examination of the final fuel consumption produced by both architectures during the established cycle reveals that the dual configuration exhibits a slight improvement of approximately 7% compared to the single configuration (see Figure 5.7). However, a thorough analysis of the energy contributions within the accumulators is necessary to gain a more complete and realistic understanding of actual consumption.

To facilitate this, an algorithm, shown in the Appendix 6.3, has been developed that converts the remaining energy quantity in the accumulators into fuel consumption. If, at the end of the cycle, the accumulators are more discharged compared to their initial volume and pressure, it indicates that the consumption contribution should be added to the output consumption derived from the engine map interpolation table. Conversely, if the accumulator values show an increase from the starting point, the contribution in terms of fuel consumption should be

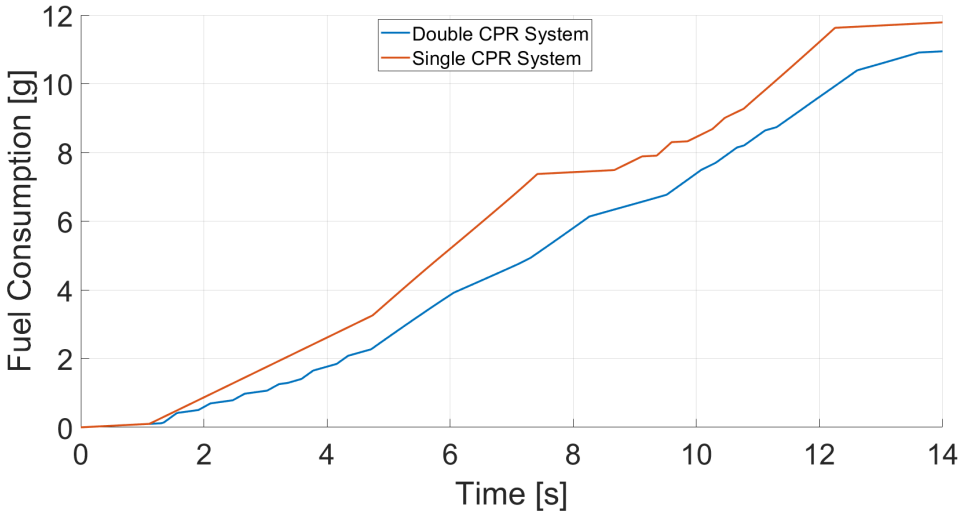

Figure 5.7: Fuel Consumption Comparison during Dig and Dump

subtracted. Considering these additional contributions, it becomes evident that the energy and fuel savings are actually much less significant, settling around 4%.

From this analysis, it is evident that there could be an improvement in fuel savings with the double configuration if the external loads on the actuators are reduced. To test this hypothesis, the external forces acting on the arm and bucket actuators were halved (see Figures 5.8 and 5.9), and the analyses of the Dig and Dump duty cycle were conducted again under these reduced loads.

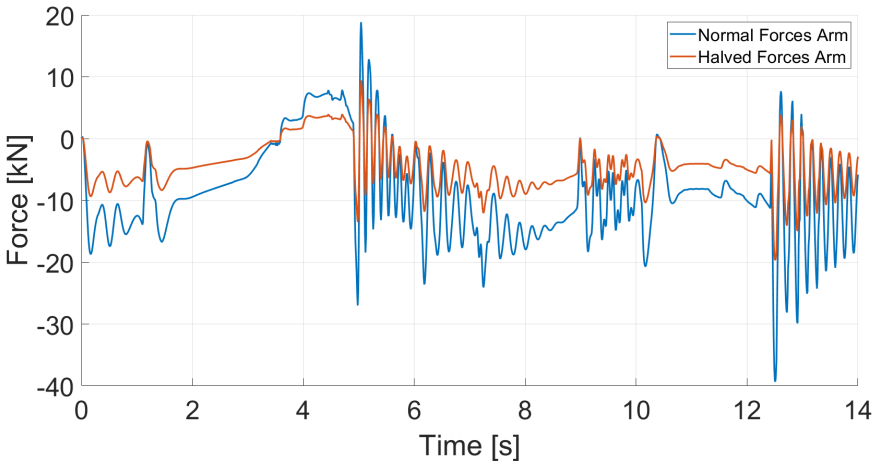

Figure 5.8: Comparison Between Normal and Halved Forces acting on Arm in Dig and Dump Cycle

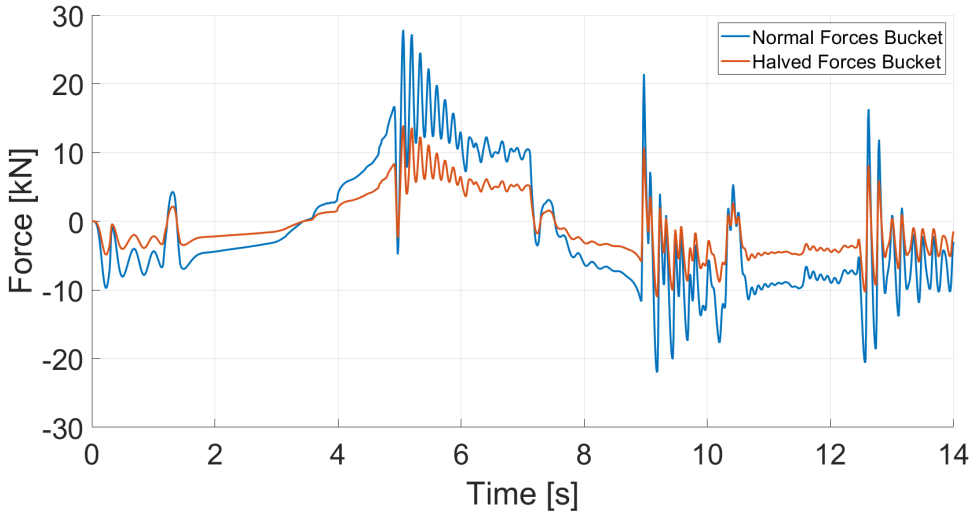

Figure 5.9: Comparison Between Normal and Halved Forces acting on Bucket in Dig and Dump Cycle

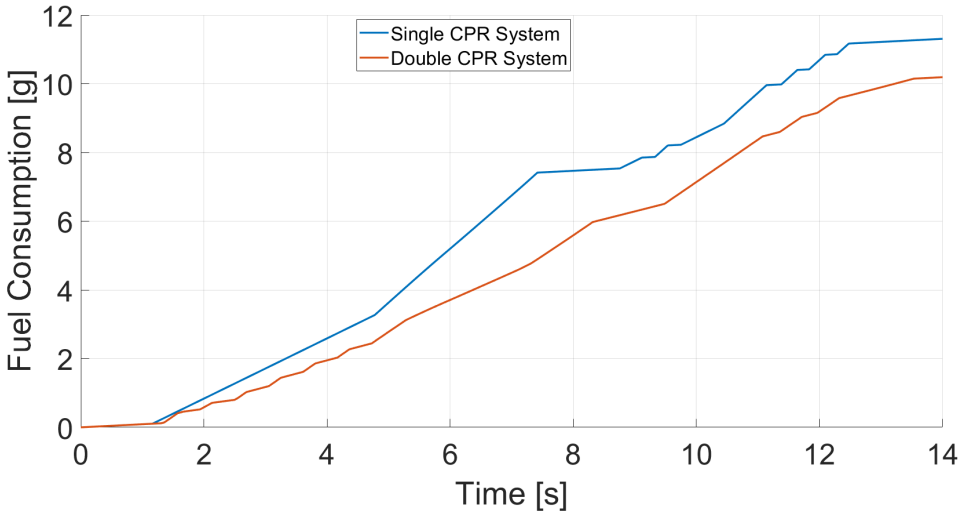

Figure 5.10: Halved Forces Dig and Dump Fuel Consumption Comparison

This adjustment provided a clearer understanding of how lower external forces affect the efficiency and performance of the double architecture. By examining the results under these new conditions, it becomes possible to assess whether the dual configuration can yield significant fuel savings when operating under lighter loads, ultimately contributing to enhanced operational efficiency and reduced fuel consumption in practical application.

In the figure 5.10, it can be observed that by reducing the external loads on the arm and bucket actuators, the total fuel consumption for both configurations decreases. However, this time, the gap between the two configurations widens. Specifically, the double configuration exhibits approximately a 10% lower fuel consumption, a difference that remains relatively unchanged when considering the contributions from within the accumulators.

HP Parameter	**Value**
Max Pressure (p_2)	65 bar
Min Pressure (p_1)	50 bar
Pre-Charge pressure (p_0)	45 bar
Nominal Volume (V_0)	15 l

MP Parameter	**Value**
Max Pressure (p_2)	15 bar
Min Pressure (p_1)	10 bar
Pre-Charge pressure (p_0)	9 bar
Nominal Volume (V_0)	15 l

Table 5.4: DCPR: Arm/Bucket Accumulators Sizing Values after Halving Forces

Lower consumption results were achieved by adjusting the pressures within the high pressure accumulator of the coupled arm/bucket system, which allowed for further reductions in the ideal operating pressure values. This adjustment helps prevent unnecessary pressure losses caused by excessively high operating pressures.

In contrast, no such modification was made to the single common pressure rail system, as the loads on the other two actuators remain high. Since all the actuators are supplied by the same two accumulators and a single pump, it is not feasible to reduce the high pressure values. These pressures significantly impact consumption by increasing the power and torque demands on the internal combustion engine.

This underscores the importance of tailoring pressure settings in each configuration to optimize efficiency and minimize energy consumption in different operational scenarios.

Chapter 6

CPR Problems and Possible Solutions

The study thus far has demonstrated the significant advantages of implementing the CPR architecture on a 9-ton hydraulic excavator across two different excavation cycles, namely dig-and-dump and air grading (see Section 1.3). These advantages are primarily reflected in substantial fuel efficiency improvements when compared to traditional Load Sensing architecture [17], all while maintaining strong operational performance and precise execution of the cycles.

A key finding, discussed in Chapter 4, shows that the system's operational pressures consistently remain well below the standard maximum limits expected for machinery of this size. Typically, a 9-ton excavator can handle peak pressures between 290 and 320 bar. However, in its current configuration, the system's maximum pressure output is limited by the high-pressure rail, capped at 175 bar under current settings. While this is sufficient for standard excavation tasks like dig-and-dump or air grading, these pressure levels may be inadequate when facing more demanding conditions, such as excavating through rock or challenging substrates.

To ensure the excavator remains operational even in challenging conditions, where high external loads demand significantly higher pressures for the actuators, it was necessary to redesign the bladder accumulators to meet the maximum pressure requirements of a real machine. Operating pressures in the common lines close to the critical threshold result in a considerable increase in energy consumption, negating many of the advancements outlined in Section 4 and in the referenced theses [17] and [18].

One potential solution, detailed in this chapter, is the introduction of a pressure intensifier in the high-pressure line, which makes it possible to use the model with the same characteristics described in the previous chapters.

To simulate and assess the excavator's performance under extreme conditions, a new operating cycle, termed the heavy-duty cycle, was developed and will be explained in the following section.

It is important to note that all these analyses were conducted exclusively on the Single CPR architecture.

6.1 Heavy Duty Cycle

Tasks like moving heavy materials or clearing large roots require additional testing beyond the standard Dig and dump and Air Grading cycles (see Section 1.3). For this reason, an extra cycle was introduced, specifically designed to assess the excavator's performance in challenging situations such as these. This cycle is crucial for evaluating the single CPR architecture's effectiveness, which must demonstrate reliable handling also in extreme conditions to be considered a viable alternative to conventional, well-established systems.

This newly defined cycle, named the "heavy duty work cycle", focuses on assessing the excavator's capabilities during demanding operations. To maintain consistency, the cycle starts with the same initial configuration as the air grading and dig and dump cycles. From this point, the excavation phase begins, followed by a simulation where the excavator encounters a substantial obstacle that blocks the bucket. The cycle does not include a return to the initial position, as the primary objective is to evaluate the excavator's ability to endure high actuator pressure when managing heavy loads. Once this goal is met, the cycle concludes to optimize the use of simulation time.

In the AMESim simulation environment, the cycle duration was set to 9 seconds. Starting from the initial reference position, the excavator was programmed to digging until it encountered an obstacle in the ground. Removing this virtual obstacle required the maximum pressures achievable within the original excavator hydraulic system, which is around 290 bar. Figures 6.1 and 6.2 illustrate the key stages of the cycle, depicting the start and end points.

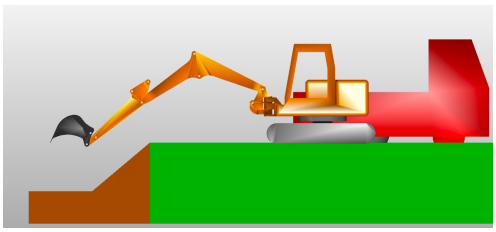

Figure 6.1: Heavy Duty Cycle - Start

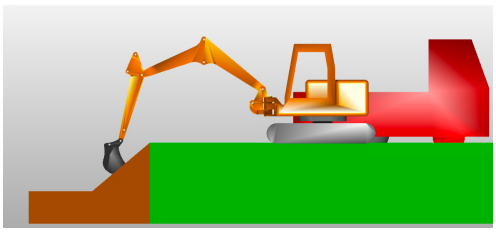

Figure 6.2: Heavy Duty Cycle - End

As outlined earlier, the primary goal of this cycle is to assess the excavator's capability to handle more demanding tasks. To achieve this, not only were reference speeds for the actuators defined to guide the movement, but reference forces were also specified and integrated into the model. This approach was designed to evaluate the system's ability to effectively sustain these forces. The reference velocities, displayed in Figures 6.3 to 6.5, were derived by aligning the initial velocities of the actuators with those observed during the dig-and-dump cycle (refer to the Chapter 3). Following this, a sharp reduction in velocity occurs as soon as the critical forces come into play.

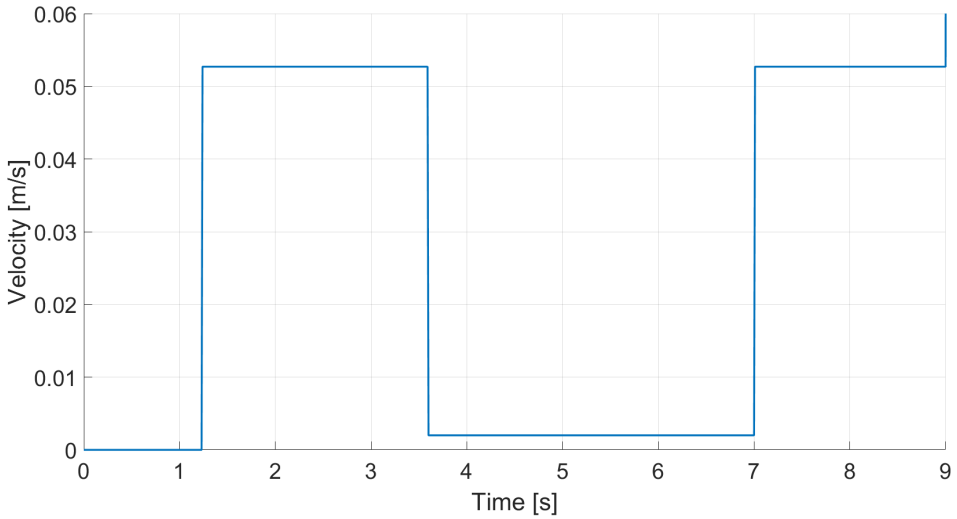

Figure 6.3: Heavy Duty Cycle - Boom Reference Velocity

To achieve the required pressures in the hydraulic circuit, the forces applied to the actuators were derived based on each actuator's specific characteristics. Since the force exerted by an actuator is proportional to the pressure within its chambers and the surface areas involved, the actuators' geometric properties were used to calculate the necessary force to attain the desired maximum pressure in the system. Figures 6.6, 6.7, and 6.8 display the input forces sent to the actuators. Just like the actuator velocity inputs, the forces initially mimic the external loads from the Dig and Dump cycle. They then sharply rise to simulate the presence of a significant obstacle, such as rocks or roots. As the cycle approaches its conclusion, the forces return to the predefined Dig and Dump values, representing the successful removal of the obstacle.

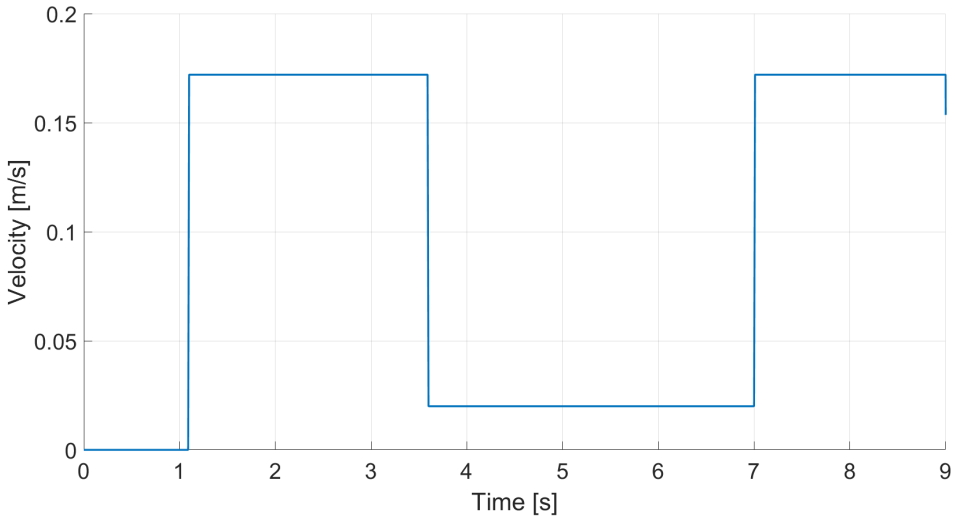

Figure 6.4: Heavy Duty Cycle - Arm Reference Velocity

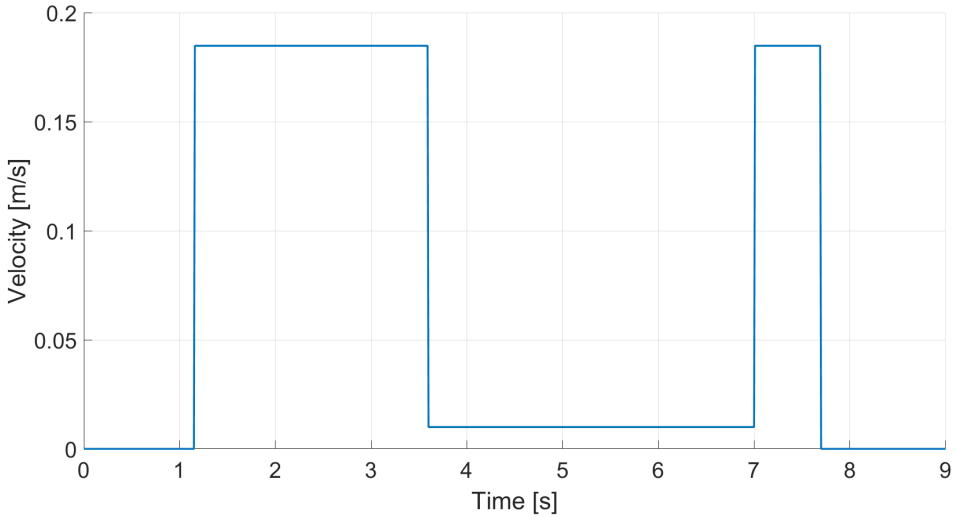

Figure 6.5: Heavy Duty Cycle - Bucket Reference Velocity

6.2 Accumulators Pressure Increment

As previously mentioned, a systematic approach was employed to calculate the maximum forces the excavator must withstand during its operational cycle. Actuators, which are the main components that transform hydraulic power into mechanical movement, produce forces that are directly influenced by their surface area and the pressure applied. Given a maximum operating pressure of around 290 bar, the

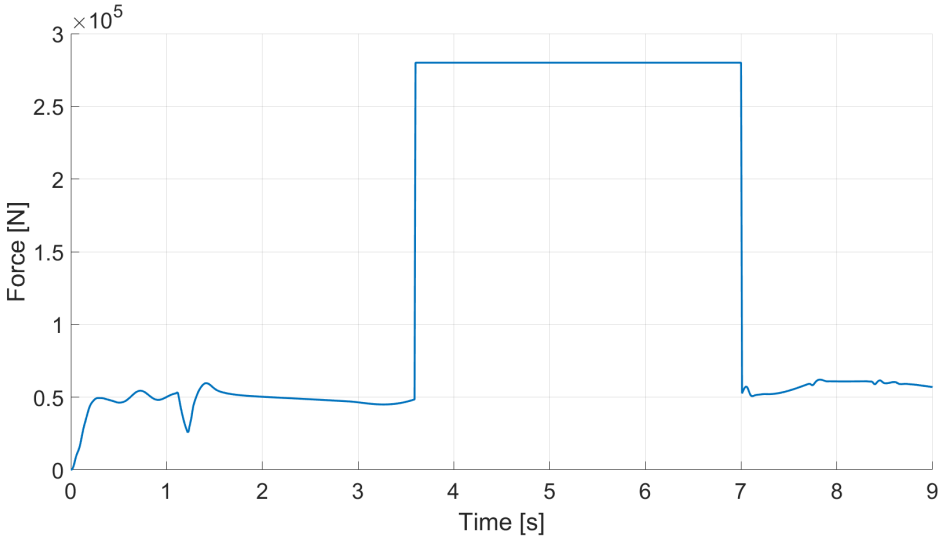

Figure 6.6: Heavy Duty Cycle - Boom Critical Forces

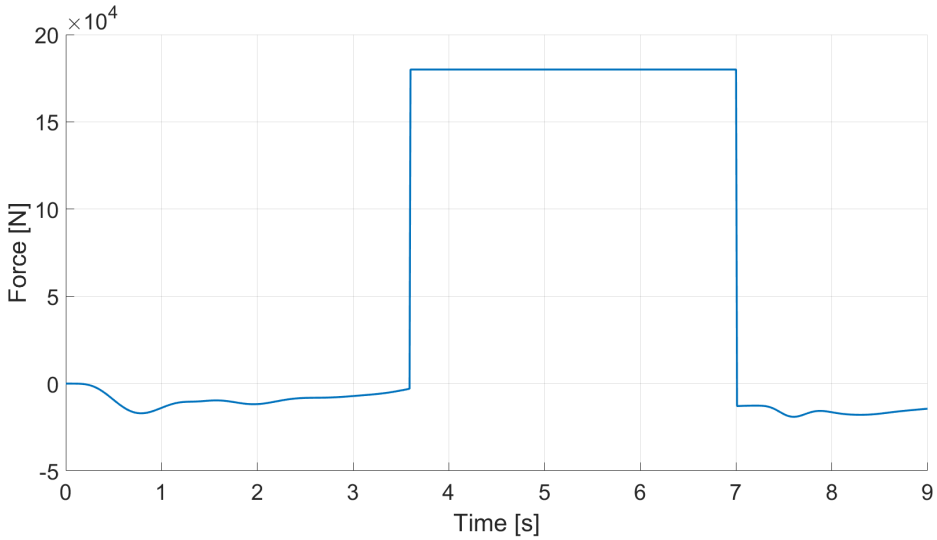

Figure 6.7: Heavy Duty Cycle - Arm Critical Forces

surface areas of the actuator chambers were evaluated. By multiplying the pressure by the chamber areas, the maximum forces that each actuator can endure were established.

To guarantee the excavator's functionality under these critical conditions, it was essential to substantially increase the pressures within the accumulators in the single CPR architecture. The adjustment focused solely on pressure changes, while the volumes remained the same as those outlined in Chapter 4. Considering

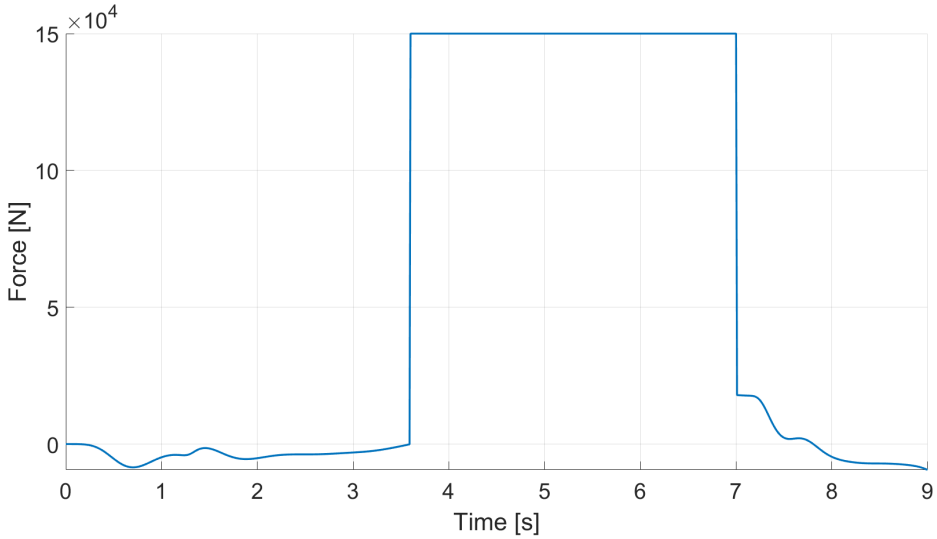

Figure 6.8: Heavy Duty Cycle - Buck Critical Forces

potential pressure drops, the final values used for the accumulators are summarized in the table 6.1.

HP Parameter	Value
Max Pressure (p_2)	310 bar
Min Pressure (p_1)	280 bar
Pre-Charge pressure (p_0)	200 bar
Nominal Volume (V_0)	30 l

MP Parameter	Value
Max Pressure (p_2)	150 bar
Min Pressure (p_1)	120 bar
Pre-Charge pressure (p_0)	80 bar
Nominal Volume (V_0)	30 l

Table 6.1: Heavy Duty Cycle - Single CPR Accumulators Sizing

While the strategy of increasing the pressure in the accumulators effectively ensures that the excavator can handle the maximum pressures expected in real operational conditions, it also presents significant drawbacks when the machine is used for standard cycles and loads. As analyzed in this thesis and illustrated in the Table 6.2, the single CPR architecture with accumulators resized for critical pressures demonstrates less advantage in terms of fuel savings during both the Dig and Dump and Air grading cycles.

In conclusion, while the Common Pressure Rail architecture consistently demonstrates advantages over Load Sensing machines, the feasibility of implementing CPR with high pressure accumulators must be carefully evaluated, taking into account the specific dimensions and operational requirements of the excavator.

Architecture	Duty Cycle	Fuel [g]
Load Sensing	Dig and Dump	25.59
Single CPR_Heavy	Dig and Dump	24.54
Load Sensing	Air grading	17.58
Single CPR_Heavy	Air grading	11.22

Table 6.2: Fuel Consumption Comparison between LS and Single CPR_Heavy during different duty cycles

6.3 Pressure Intensifier

A solution proposed by CNHi to integrate the advantages of common pressure rail architectures with challenging and critical scenarios, such as that encountered in the heavy duty cycle, is the introduction in the hydraulic circuit of a pressure intensifier.

A hydraulic pressure intensifier is a vital device in hydraulic systems, designed to increase the pressure of hydraulic fluid. Its primary function is to convert low pressure hydraulic fluid into high pressure fluid, enabling the operation of machinery and equipment that require substantial high force. Typically, this device consists of two chambers separated by a piston, like the Parker pressure Intensifier shown in the Figure 6.9, which hydraulic diagram has been implemented in AMESim for the integration with the Single CPR model.

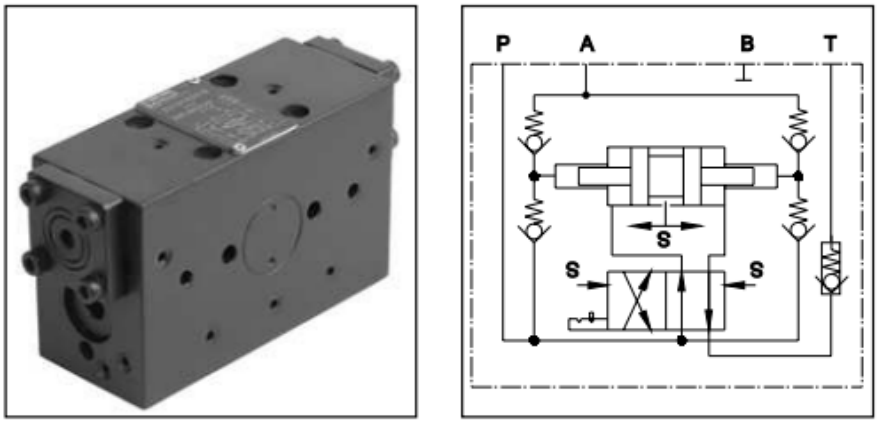

Figure 6.9: Parker Pressure Intensifier

Pressure intensifiers are utilized in scenarios where a particular component of a hydraulic system requires a pressure significantly higher than what the available primary pressure can deliver, especially for clamping functions [19]. Moreover, a

pilot-operated check valve can be installed below the pressure intensifier to enable the rapid filling and decompression of the high pressure section.

When low-pressure fluid enters the input chamber, it exerts force on the piston, causing it to move. As the piston shifts, it compresses the fluid in the output chamber. Since the input side has a larger area than the output side, the pressure in the output chamber becomes significantly greater than in the input chamber. This mechanism enables the hydraulic intensifier to generate high pressure from a low-pressure source.

The main functional components of the pressure intensifier consist of the intensifier piston, the rocker mechanism, and the slide valve with a locking feature. Additionally, there are four check valves that separate the high-pressure section from the low-pressure section, along with a check valve positioned at the tank port to isolate the tank section from the primary pressure [19]. Pressure gauges monitor the pressures in both chambers, ensuring safe and efficient operation.

As noted at the beginning of this section, the schematic of the Parker pressure intensifier, illustrated in the figure 6.9, has been replicated in AMESim (see Figure 6.10) by adjusting the actuator areas to achieve an area ratio, referred to as the intensification ratio, of 1:2 between the input and output. This indicates that the output pressure is twice the inlet pressure of the fluid. Given the assumptions made and the heavy-duty cycle discussed in the beginning of this chapter, it is sufficient to double the nominal pressure of the high-pressure rails in the standard CPR architecture outlined in Chapter 2 to attain pressures capable of overcoming critical external loads.

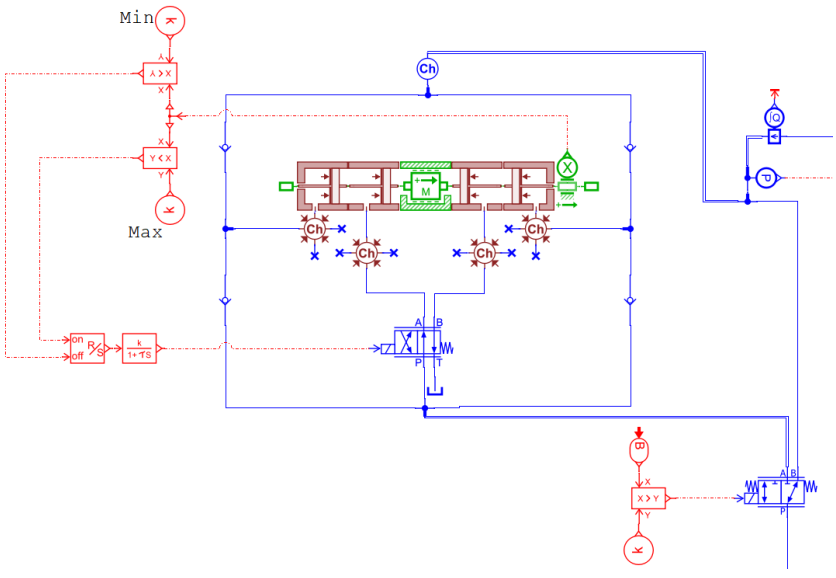

Figure 6.10: Pressure Intensifier Detail on AMESim

In fact, it is sufficient to adjust the high-pressure line by utilizing the pressure intensifier as needed, increasing the pressure from 175 bar in standard conditions to 350 bar in critical situations. This approach enables optimal utilization of the benefits of the CPR architecture without substantially affecting efficiency and fuel consumption. The figure 6.11 illustrates the implementation of the intensifier model in AMESim, on the HP rail of the model.

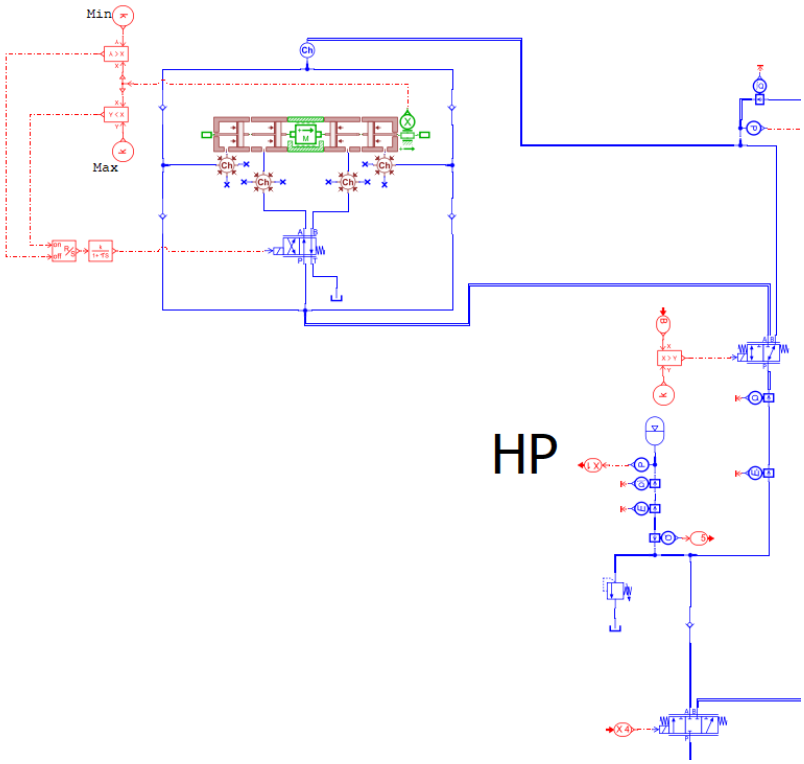

Figure 6.11: Pressure Intensifier Integration on AMESim

The valve shown in the figure 6.12 was specifically designed using the Valve Builder tool in AMESim to create a switch that permits fluid flow through the intensifier only when needed and under specific conditions, set to activate upon exceeding a maximum force threshold.

Once the high-pressure section is filled with oil (for example, during the extension of a clamping cylinder), the pressure intensifier begins its operation. The low pressure causes the intensifier piston to move due to the surface area ratio, compressing the oil column in the high-pressure section.

At the end of the piston stroke, the rocker mechanism activates, switching the directional slide valve to the crossed position. This action allows the intensifier piston to pump oil from the piston rod area into the high-pressure section. The

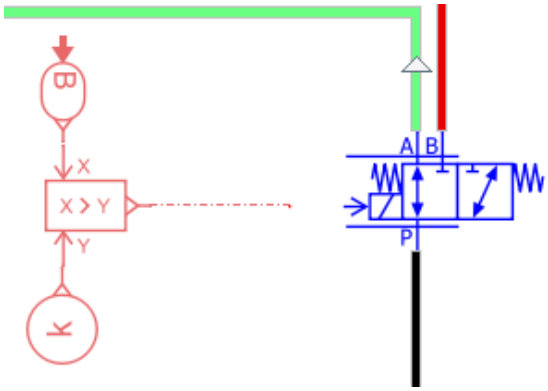

Figure 6.12: Switch Valve to Intensifier

switching speed of the slide valve is influenced by the operating speed of the intensifier piston.

The movement of the slide valve (see Figure 6.13) is illustrated in the Figure 6.14 and is restricted to a maximum stroke of 25 cm on each side. It is essential to highlight that the smaller areas of the actuator, from which the boosted pressure values are released, have a diameter of 35 mm, while the larger areas, through which the fluid at lower pressure enters, have a diameter of 50 mm. Consequently, the ratio between these two areas is 1:2, which, as mentioned earlier, leads to a doubling of the final pressure (see Figure 6.15).

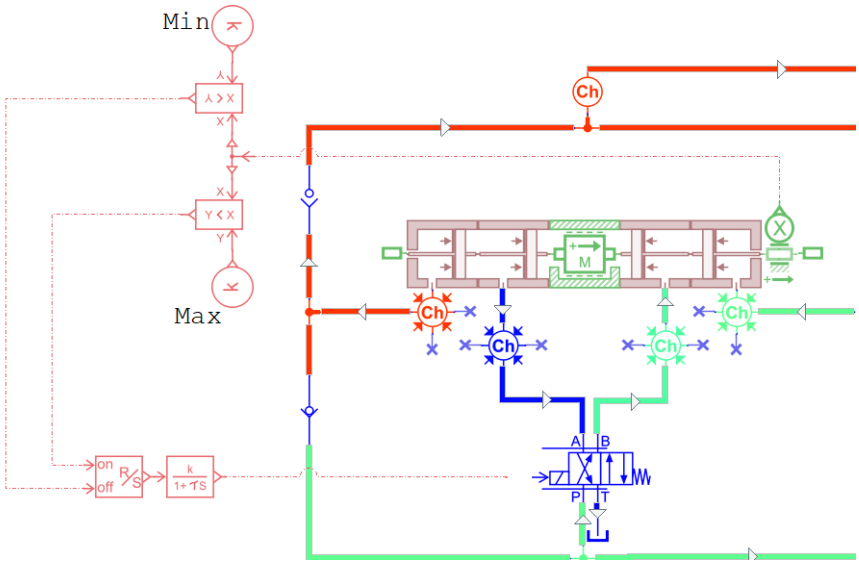

Figure 6.13: Slide Valve Detail

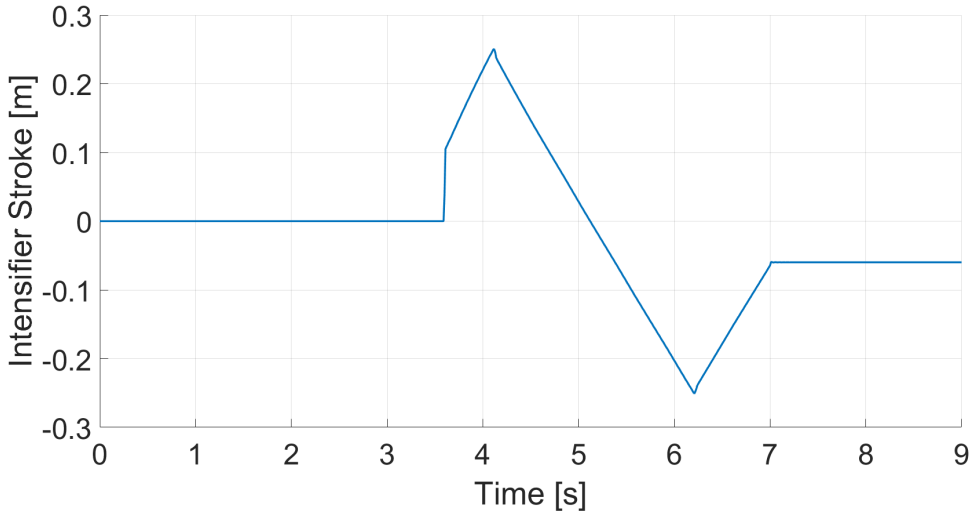

Figure 6.14: Pressure Intensifier Stroke during Heavy Duty Cycle

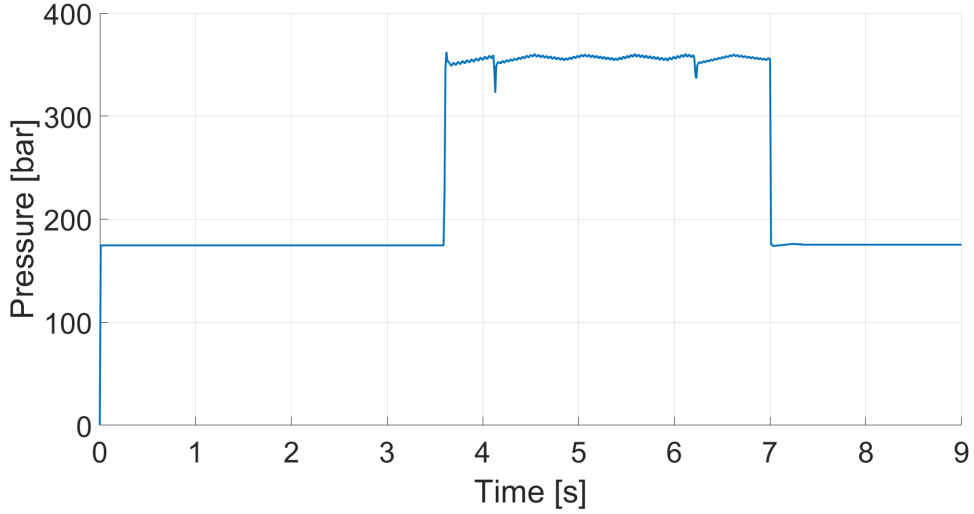

Figure 6.15: Pressure from Intensifier during Heavy Duty Cycle

One significant advantage of hydraulic pressure intensifiers is their space efficiency. They enable high pressure without necessitating large, heavy pumps, making them a practical solution in confined spaces. Additionally, by utilizing lower-pressure systems to achieve high pressures, they can result in energy cost savings. Their versatility makes them suitable for a wide range of applications, from industrial machinery to specialized testing equipment, while also allowing for precise control over pressure levels in hydraulic systems.

In conclusion, hydraulic pressure intensifiers are crucial components of hydraulic systems, providing an effective means of generating high pressures for various applications. Their ability to transform low-pressure fluid into high-pressure output enhances operational efficiency and performance across numerous industries.

Conclusion

This thesis has successfully demonstrated the transformative potential of the Common Pressure Rail (CPR) architecture as an innovative solution for hybrid hydraulic excavators. Through meticulous analysis and optimization of the power supply system, it has been established that CPR systems can significantly enhance energy efficiency by reducing fuel consumption and minimizing the energy losses commonly associated with traditional hydraulic circuits. The integration of bladder accumulators and the development of a robust control system designed to maintain quasi-constant pressure levels not only validate the advantages of this innovative architecture but also highlight its practical applicability in real-world scenarios.

Extensive testing across various operational conditions, including dig and dump cycles, air grading, and heavy-duty tasks, revealed a remarkable enhancement in energy efficiency, exceeding 50% compared to conventional Load Sensing architectures. These results indicate that the CPR system effectively optimizes hydraulic flow and reduces throttling losses, thereby maximizing the useful work done by the hydraulic actuators. Such improvements are crucial in promoting sustainability in construction operations, where fuel consumption and operational costs are significant concerns.

Moreover, the exploration of a dual power supply system within this research has underscored the effectiveness of circuit segmentation in achieving even greater fuel efficiency. By analyzing the performance of separate hydraulic circuits, this thesis has illustrated how targeted enhancements can lead to superior energy management and operational flexibility. Addressing the challenges posed by operating pressures that approach the system's maximum operating pressure, the strategies of resizing accumulators and introducing pressure intensifiers have emerged as viable solutions to mitigate potential performance limitations, thereby enhancing the overall robustness of the CPR architecture.

Overall, the findings of this study underscore the viability of well-designed CPR architectures as sustainable alternatives to conventional hydraulic systems. By maximizing energy recovery and enhancing operational efficiency, these systems not only contribute to significant reductions in CO_2 emissions but also pave the way for a more environmentally friendly approach to construction machinery. The

potential for widespread adoption of CPR technology could lead to a paradigm shift in how hydraulic systems are designed and implemented, promoting a greener future for the construction industry.

Looking ahead, future work may focus on further refining these systems, investigating advanced materials and technologies that could further enhance performance. Additionally, exploring the implementation of CPR architectures across various applications and machinery types will be crucial in demonstrating their versatility and broader impact. Such efforts will not only advance the field of hydraulic engineering but also support global initiatives aimed at reducing the carbon footprint of the construction sector, aligning with contemporary environmental goals and the pursuit of sustainable development.

Appendix

MATLAB CODE FOR FINDING THE BEST COMBINATION PRESSURE CHOICE FOR EACH ACTUATOR

```
big_chamber_area=pi*piston_diameter^2/4*10^-6;
small_chamber_area=pi*(piston_diameter^2-rod_diameter^2)
/4*10^-6;
l_pressure=0;
m_pressure=linspace(60*10^5,90*10^5,1000);
h_pressure=linspace(160*10^5,190*10^5,1000);

vettore_errori = zeros(size(m_pressure,1000));
i=1;
z=1;
g=1;
errore = zeros(1,6);
force=zeros(9,1);
vettore_minimi = zeros(size(m_pressure,2),1000);
intervallo = zeros(1,7);

for w=1:size(h_pressure,2)
    Force_H_L = big_chamber_area*h_pressure(g);
    Force_L_H = - small_chamber_area*h_pressure(g);
    m_boom = (Force_H_L - Force_L_H)/8;
    for t=1:size(m_pressure,2)
        matrix1=[l_pressure, m_pressure(z), h_pressure(g)];
        matrix2=matrix1;
        for k=1:3
            for j=1:3
            force(i,:)=matrix1(k)*big_chamber_area-
            matrix2(j)*small_chamber_area;
            i=i+1;
            end
```

```
30          end
31          forza_ = sort(force);
32          forza = zeros(8,1);
33          i=1;
34          u = 1;
35          for f=1:size(forza_)
36              if forza_(f,1) ~= 0
37                  forza(u) = forza_(f,1);
38                  u = u+1;
39              end
40          end
41          e = 0;
42          for r=1:7
43              intervallo(1,r)= forza(8-e,1)-forza(7-e,1);
44              e=e+1;
45          end
46          t=0;
47          for o=1:6
48              errore(1,o)=abs(intervallo(1,7-t))-
49              abs(intervallo(1,6-t));
50              t=t+1;
51          end
52      vettore_errori(g,z) = rms(errore);
53      z=z+1;
54      end
55      z=1;
56      g=g+1;
57  end
58
59  for k=1:size(h_pressure,2)
60
61          [M,I] = min(vettore_errori(k,:));
62
63          vettore_minimi(k,1) = M;
64          vettore_minimi(k,2) = I;
65  end
66
67  [Min, Index]=min(vettore_minimi(:,1));
68  HP = h_pressure(Index)
69  vettore_minimi(Index,2)
70  MP = m_pressure(vettore_minimi(Index,2))
```

MATLAB CODE FOR FINDING THE FUEL CONSUMPTION FROM THE ACCUMULATOR CONTRIBUTION

```
function fc_accumulator = algo_fc_acc_ale(pump_disp,
q_pump,
volume_start, volume_final, pressure_start,
pressure_final, eff_hydro_mech)
    load('N67_rescaled_to_55kW.mat');
    if volume_start > volume_final
        volume_diff = volume_start - volume_final; % L
        time_to_charge = 60*volume_diff/q_pump; %s
        time_vector = linspace(0, time_to_charge, 10);
        pressures = linspace(pressure_start*10^5,
        pressure_final*10^5, 10);
        torque = pressures * pump_disp
        *10^-6/(2*pi)/eff_hydro_mech;
        omega = 1200*ones(1,10)*2*pi/60;
        fc_ = fuelFlwRate(omega,torque)*1000;
        fc_accumulator = -trapz(time_vector,fc_);
    else
        volume_diff = volume_final - volume_start; % L
        time_to_charge = 60*volume_diff/q_pump; %s
        time_vector = linspace(0, time_to_charge, 10);
        pressures = linspace(pressure_final*10^5,
        pressure_start*10^5, 10);
        torque = pressures * pump_disp
        *10^-6/(2*pi)/eff_hydro_mech;
        omega = 1200*ones(1,10)*2*pi/60;
        fc_ = fuelFlwRate(omega,torque)*1000;
        fc_accumulator = trapz(time_vector,fc_);
    end
end
```

Bibliography

[1] Toshiharu Abekawa, Yuuichirou Tanikawa, and Atsuhiko Hirosawa. *Introduction of Products Introduction of Komatsu genuine hydraulic oil KOMHYDRO HE*. 2010 (cit. on p. 1).

[2] Mateus Bertolin and Andrea Vacca. «A Parametric Study on Architectures Using Common-Pressure Rail Systems and Multi-Chamber Cylinders». In: *Proceedings of the IEEE Global Fluid Power Society PhD Symposium*. 2022, pp. 1–8 (cit. on p. 1).

[3] J Lumkes and J Andruch. «Hydraulic circuit for reconfigurable and efficient fluid power systems». In: *The 12th scandinavian international conference on fluid power*. Vol. 1. 2011, pp. 83–98 (cit. on p. 1).

[4] Milos Vukovic, Roland Leifeld, and Hubertus Murrenhoff. «Reducing Fuel Consumption in Hydraulic Excavators—A Comprehensive Analysis». In: *Energies 2017, Vol. 10, Page 687* 10 (5 May 2017), p. 687. ISSN: 19961073. DOI: 10.3390/EN10050687. URL: https://www.mdpi.com/1996-1073/10/5/687/htm%20https://www.mdpi.com/1996-1073/10/5/687 (cit. on pp. 1, 4).

[5] «A coupled hydraulic and mechanical system simulation for hydraulic excavators». In: *Proceedings of the Institution of Mechanical Engineers. Part I: Journal of Systems and Control Engineering* 234 (4 Apr. 2020), pp. 527–549. ISSN: 20413041. DOI: 10.1177/0959651819861612 (cit. on p. 4).

[6] Kwangman An, Hyehyun Kang, Youngkuk An, Jinil Park, and Jonghwa Lee. «Methodology of excavator system energy flow-down». In: *Energies* 13 (4 2020). ISSN: 19961073. DOI: 10.3390/en13040951 (cit. on p. 5).

[7] Milos Vukovic. *Hydraulic hybrid systems for excavators*. 2017. ISBN: 9783844053128 (cit. on pp. 7, 8, 16, 20, 21, 43–46, 49, 53, 66, 73).

[8] Dipl.-Ing Milos Vukovic and Roland Leifeld. «STEAM-a hydraulic hybrid architecture for excavators». In: *10th International Fluid Power Conference*. 2016, pp. 151–162 (cit. on pp. 7, 8, 16).

[9] Damiano Padovani, Massimo Rundo, and Gabriele Altare. «The working hydraulics of valve-controlled mobile machines: Classification and review». In: *Journal of Dynamic Systems, Measurement and Control, Transactions of the ASME* 142 (7 July 2020). ISSN: 15289028. DOI: 10.1115/1.4046334/1074597 (cit. on pp. 10–13, 22).

[10] Perry Y. Li, Jacob Siefert, and David Bigelow. «A hybrid hydraulic-electric architecture (HHEA) for high power off-road mobile machines». In: *ASME/-BATH 2019 Symposium on Fluid Power and Motion Control, FPMC 2019* (2020), pp. 1–8. DOI: 10.1115/FPMC2019-1628 (cit. on p. 14).

[11] Husnain Ahmed. *ENERGY EFFICIENCY ANALYSIS OF MULTI-PRESSURE HYDRAULIC SYS-TEM*. 2019 (cit. on p. 15).

[12] Milos Vukovic, Sebastian Sgro, and Hubertus Murrenhoff. «Steam - A mobile hydraulic system with engine integration». In: *ASME/BATH 2013 Symposium on Fluid Power and Motion Control, FPMC 2013*. American Society of Mechanical Engineers, 2013. DOI: 10.1115/FPMC2013-4408 (cit. on pp. 17, 19).

[13] Tri Cuong Do, Tri Dung Dang, Truong Quang Dinh, and Kyoung Kwan Ahn. «Developments in energy regeneration technologies for hydraulic excavators: A review». In: *Renewable and Sustainable Energy Reviews* 145 (June 2020 2021), p. 111076. ISSN: 18790690. DOI: 10.1016/j.rser.2021.111076. URL: https://doi.org/10.1016/j.rser.2021.111076 (cit. on p. 19).

[14] Thiebes P. and Geimer M. *Energy storage devices for industrial vehicles with hybrid drive trains*. URL: www.kit.edu (cit. on p. 20).

[15] G. Altare and Politecnico di Torino. Dipartimento energia. *Analisi e simulazione di circuiti idraulici per macchine movimento terra: tesi di dottorato*. 2013. URL: https://books.google.it/books?id=0wpyAQAACAAJ (cit. on pp. 22, 23, 34).

[16] Gabriele Altare, Damiano Padovani, and Nicola Nervegna. «A commercial excavator: Analysis, modelling and simulation of the hydraulic circuit». In: *SAE Technical Papers*. Vol. 8. SAE International, 2012. DOI: 10.4271/2012-01-2040 (cit. on pp. 23, 31).

[17] Gargiani Giulia. *Comparative Analysis of Load Sensing and Common Pressure Rail Architectures in Hydraulic Excavators: Energy Flow Path and Fuel Economy - MSc Thesis* (cit. on pp. 34, 37, 66, 77).

[18] Moffa Gabriele. *Development of Control Logic for Common Pressure Rail Architecture in Hybrid Excavators - MSc Thesis* (cit. on pp. 43, 53, 58, 71, 77).

[19] «Parker Pressure Intensifier - Series SD500». In: () (cit. on pp. 83, 84).